Rigas Georgiou

Daytime radiative cooling

A new passive cooling method for dwellings in the Mediterranean island of Cyprus

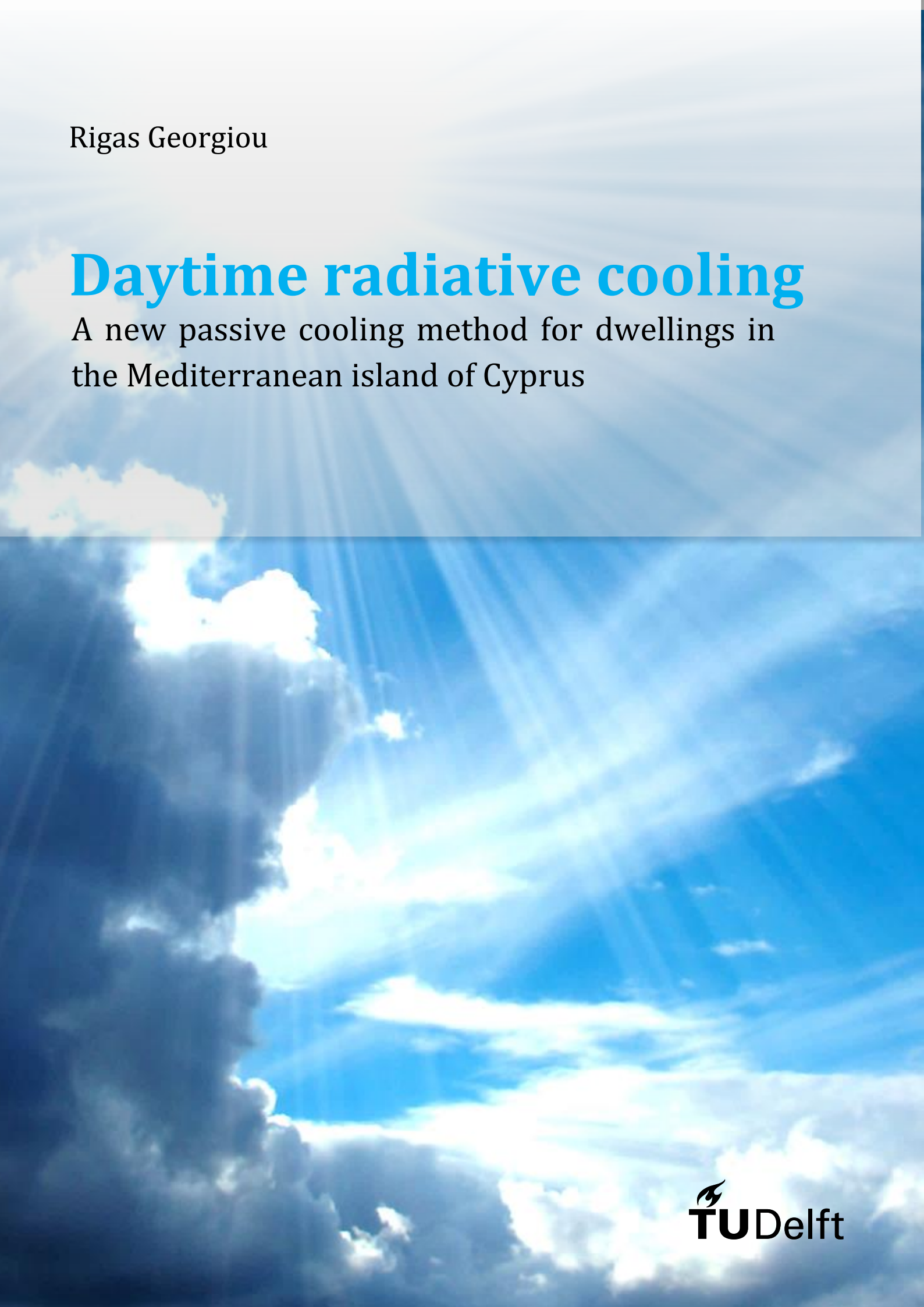

TU Delft

Daytime radiative cooling

A new passive cooling method for buildings in the Mediterranean island of Cyprus

By

Rigas Georgiou

in partial fulfilment of the requirements for the degree of

Master of Science
in Civil Engineering

at the Delft University of Technology,
to be defended publicly on Friday June 21, 2019 at 12:30 PM.

Thesis committee:
Prof. ir. R. Nijsse (Chair)
Faculty of Civil Engineering and Geosciences

Dr. ir. W. H. Van der Spoel (Daily supervisor)
Faculty of Architecture and the Built Environment

Dr. ir. H. R. Schipper
Faculty of Civil Engineering and Geosciences

This thesis is confidential and cannot be made public until June 20, 2019.

An electronic version of this thesis is available at http://repository.tudelft.nl/.

TU Delft

Preface

This thesis report is the final step of my studies at the Delft University of Technology and completes my Master's degree in the Building Engineering track of Civil Engineering.

For his continuous support during the period I worked on this project, I would like to sincerely thank Dr. Willem van der Spoel who was always ready to offer his very valuable assistance without which, the completion of this project would be impossible. To Dr. Roel Schipper I express my gratitude for his useful remarks in the process of finalising this report, and to Professor Rob Nijsse I would like to say that he has been a very helpful chair of my graduation committee.

This report also concludes my three-year circle in the Netherlands. They have been years full of personal and academic struggles but also years of amazing experiences. For their endless support, I express my gratefulness to my family who had never stopped believing in me. To my friends, distant and nearby, old and new, I say a big 'thank you' for always being here for me, always back me up and always be ready to live a new adventure.

Delft, June 2019

Contents

Table of figures

Abstract

Daytime radiative cooling (DRC) is a very novel passive cooling method for buildings that utilises the recent technological advance in wavelength selective-emittance material research and takes advantage of a transparency window that exists in the atmosphere between 8 and 13 μm. Application of DRC in locations where warm weather prevails for most of the year and cooling requirements of dwellings outweigh the respective heating ones could result in saving significant amounts of energy. Such a location is the small Mediterranean island of Cyprus. Designing an ideal radiative cooler is a challenging task and so it is to design an appropriate system that exploits the benefits of DRC. In such a design, a stratified thermal storage water tank can have a detrimental role. To identify whether it is possible to apply such a system in Cyprus, this project exploits the use of Matlab Simulink which has been used to run more than 6000 simulations, for a sensitivity and a varied analysis, taking into consideration different parameters with particular emphasis on the physical properties of the radiative cooling apparatus According to the data obtained, for the efficiency of a daytime radiative system to be maximized, the longwave transmission and emissivity coefficients of the cooler should be maximal while the shortwave transmission coefficient and the effective heat transfer coefficient to the environment should be minimal. Additionally, larger volumes of storage tanks achieve better results.

1

Introduction

Daytime radiative cooling is a very new passive cooling method for buildings. As a result, many questions relevant to it must be first answered in order to be successfully applied. Those questions relate to the realisation possibilities of the method and to its potential capabilities. Also unknown it is for which climates it is ideal and what physical parameters are detrimental for its efficiency.

For a number of these questions to be answered, a research approach should be followed. Such an approach consists of, firstly, a literature review, secondly, a model design and thirdly, a simulation process. Only then reliable conclusions can be made.

1.1. General

This report is the final outcome of a Master graduation project for the Building Engineering track of the Civil Engineering Master at the Delft University of Technology. The topic of this research is the application of daytime radiative cooling, which is a very novel passive cooling method, at a dwelling in the Mediterranean island of Cyprus, the home country of the author. The selection of this topic is a result of, first, the author's desire to carry out research relevant to passive cooling techniques for buildings and investigate their applicability in Mediterranean climate locations and, second, the recent technological advance on research relevant to wavelength selective-emittance materials.

This document includes all the work done during the last months, from the literature reviewed at the very beginning of this project to the final conclusions that follow an extensive set of simulations.

1.2. Research questions

A number of research questions have identified at the start of the project to be answered at its end. During the process, more specific research questions have evolved while the main question has remained the same. This question is:

1. *How can the recent technological advance in wavelength selective-emittance material research be applied in order to passively cool buildings located in a Mediterranean climate, even during daytime?*

In addition, there are three sub-questions to be answered which are:

2. *Can daytime radiative cooling be successfully applied without the need of any active cooling technique?*
3. *Which physical parameters influence the efficiency of such a system and to what extent?*
4. *Is the Mediterranean climate the right climate to apply daytime radiative cooling?*

1.3. Research approach

For the research questions to be answered, a research approach that includes several steps is followed. The approach is mostly theoretical, which means that practical matters, such as feasibility of installations, are not taken into account. Instead, what is principally investigated is the physical properties of elements that are used in the cooling system proposed and how they influence the overall efficiency of the system. The research approach adopted is illustrated in the flow diagram of figure 1-1, where the steps followed are grouped into six phases.

The first phase consists of the scientific research conducted in order for the problem to become better understood. A review on literature relevant to radiative passive cooling and to methods by which the gains of such cooling can be utilized in buildings is made. The former is presented in Chapter 2 while the latter in Chapter 3. Research was also carried out in order to obtain useful information about the

situation in Cyprus, which is the geographical field of application of this project. This is presented in Chapter 4.

In the next process phase, an appropriate cooling system is selected based on the information gained during the previous phase. In addition, a dwelling considered representative, for Cypriot standards, is selected as the case study. These are included in Chapter 5.

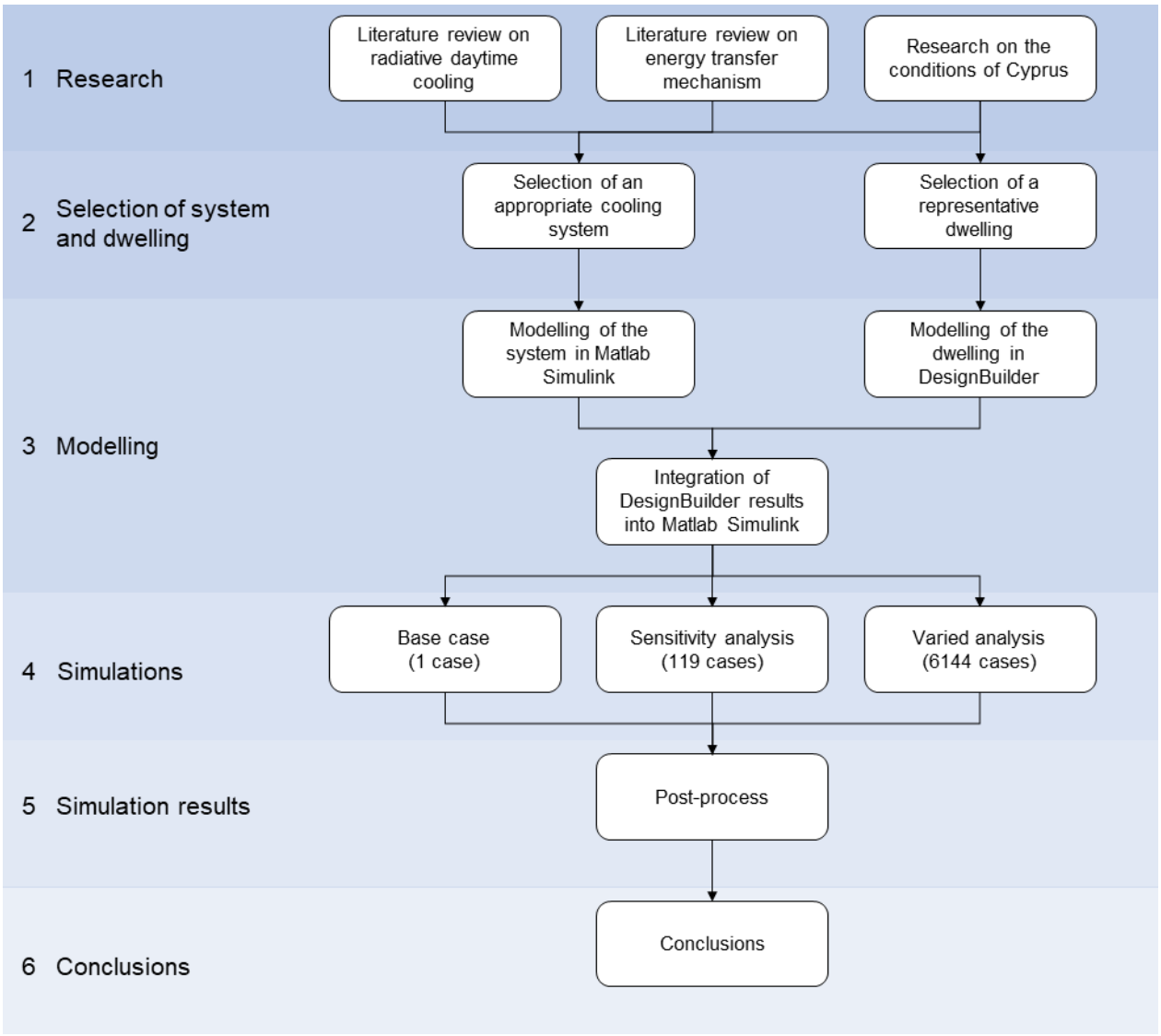

Figure 1-1. Research approach - process steps followed.

Phase 3 is the most time-consuming phase as during it, the model of the cooling system was completed. That includes the creation of the several-component model in Matlab and Simulink and the modelling of the dwelling selected, in the previous phase, in DesignBuilder. Then the Matlab Simulink model is finalized by using as input some of the data obtained from DesignBuilder. The process followed is explained in Chapter 6 with additional information in Appendices A and B.

Phase 4 and 5 consist of the simulations per se and the post-processing of their results. In particular, a base case is simulated initially to obtain some information about the behaviour of the system. Then, a sensitivity analysis is conducted to investigate the significance of each parameter of the system

individually. Last, a varied analysis is made in which all combinations of the values of parameters selected to be investigated further are simulated. The simulations made and their results are presented in Chapter 7.

Finally, the last process phase is included in Chapter 8 of this thesis report. There, the conclusions regarding the answering of research questions as well as recommendations are given.

2

Daytime radiative cooling and the ideal cooler concept

Radiative heat transport is one of the three heat transfer mechanisms. An emission coefficient is required for its calculation as well as the Steffan-Boltzmann constant. What differentiates it from the other means of heat transfer is that through it, heat can be transferred to extremely long distances and that its transferred amount is proportional to the fourth power of the absolute temperature of the heat source.

Daytime radiative cooling is the natural phenomenon during which a surface of higher temperature radiates its heat to a lower temperature surface. Taking advantage of this physical process and of an infrared window existing in the atmosphere between 8 and 13 μm could result in the birth of a passive cooling method for buildings; a method in which buildings radiate their excess heat to the much-lower-temperature sky.

Making this a reality requires utilising the recent technological advance in selective-emittance material research in order to design an ideal cooler able to operate during daytime despite being exposed to direct sunlight. In the past years, many researchers have tried to design, experimentally or theoretically, such strong and selective emitters using mostly metallic mirrors and polymeric materials.

2.1. Radiative heat transfer

Radiative heat transfer is, along with convection and conduction, one of the three heat transfer mechanisms. Any body or surface radiates heat as long as it has a temperature higher than absolute zero, that is equal to 0 K or around -273 °C.

In order for the radiated amount of heat emitted by a surface to be calculated, an idealised black body is considered. Such a body is a hypothetical body which absorbs all the radiation that falls on its surface regardless of its frequency or angle of incidence. Any black body heated to a given temperature emits thermal radiation with the emission spectrum being first fully described by Max Planck in 1900.

The quantity of heat given off via radiation by a surface is, in contrast to convection and conduction, directly proportional to the *fourth power* of its absolute temperature, as shown in figure 2-1. This quantity can be calculated (Van der Linden *et al*, 2017) using the Stefan-Boltzmann law which for a black body is:

$$q = \sigma \cdot T^4 \qquad (1)$$

Where: q_s = the heat flow density of the radiation, W/m^2

σ = the Steffan-Boltzmann constant which equals $5.67\ 10^{-8}\ W/m^2\ K^4$

T = the absolute temperature, K

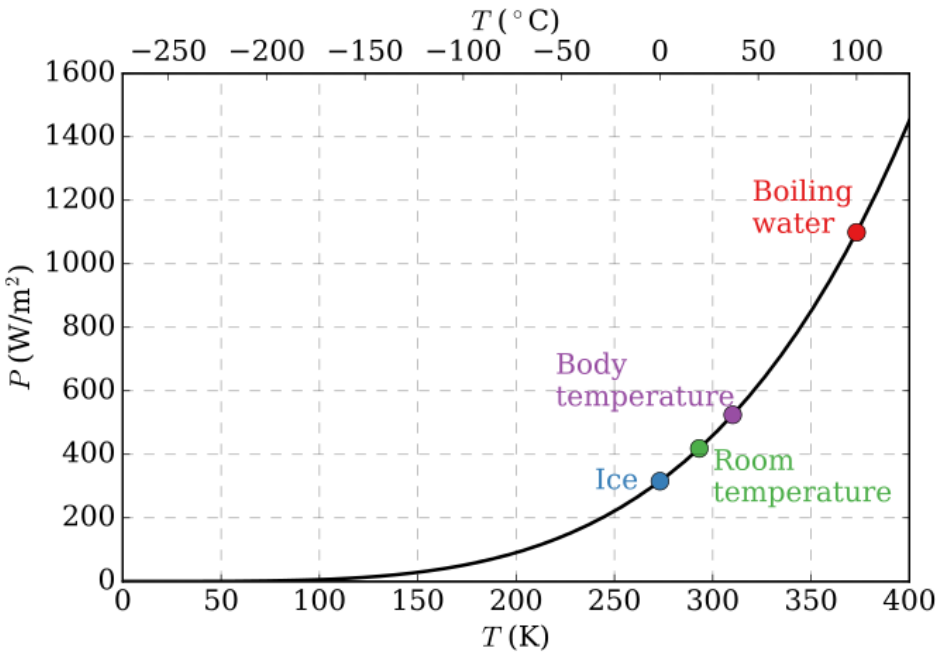

Figure 2-1. The radiative power emitted by a black body plotted against its temperature according to Steffan Boltzmann's law (Wikimedia Commons, 2016).

As mentioned before a black body is an idealistic concept and such a body does not exist in nature. For real existing objects, or grey objects, an emission coefficient is introduced which transforms the Stefan-Boltzmann law as follows:

$$q = \varepsilon \cdot \sigma \cdot T^4 \qquad (2)$$

Where: q_s = the heat flow density of the radiation, W/m^2

ε = the emission coefficient of the surface of the material

σ = the Steffan-Boltzmann constant which equals $5.67\ 10^{-8}\ W/m^2\ K^4$

T = the absolute temperature, K

The emission coefficient of the ideal black body in thermal equilibrium is equal to 1.0, as implied by equations 1 and 2; for any other body it is between 0.0 and 1.0.

In reality when two objects or two surfaces of different temperatures face each other, they both emit thermal radiation and at the same time absorb or reflect a part of each other's heat radiation. Some of the reflected radiation is re-absorbed by the original surface that emitted it and so on. This continuous exchange of heat results, on balance, on a heat flow from the higher temperature surface to the one with the lower temperature. This radiative heat transfer between two parallel and infinitely long surfaces can be determined (Van der Linden et al, 2013) using the following equation:

$$q = \frac{\varepsilon_1 \cdot \varepsilon_2}{\varepsilon_1 - \varepsilon_1 \cdot \varepsilon_2 + \varepsilon_2} \sigma \cdot (T_1^{\,4} - T_2^{\,4}) \qquad (3)$$

Where: q_s = the net radiation transfer, W/m^2

ε_1, ε_2 = the emission coefficient of surfaces 1 and 2 respectively

T_1, T_2 = the temperature of surfaces 1 and 2 respectively, K

In practice the aforementioned formula for radiative heat transfer between two surfaces can be simplified with the introduction of a heat transfer coefficient as follows:

$$q_s = \alpha_s \cdot (T_1 - T_2) \qquad (4)$$

Where: q_s = the net radiation transfer, W/m^2

α_s = the heat transfer coefficient, $W/m^2\ K$

T_1-T_2 = the temperature difference between the two surfaces, °C or K

It should be noted that the simplification of the formula is wrong in principle but the error it gives when used, especially in normal building practice, is insignificant.

2.2. Daytime radiative cooling

Radiative cooling is the physical process during which a body or a surface of higher temperature radiates heat to body or a surface of lower temperature. Daytime radiative cooling refers to a state-of-the-art passive cooling method for buildings that is based on the heat loss emitted via long wave thermal radiation from a terrestrial body, which is the building, towards the sky, which is the largest known heat sink in our universe and, of course, has a much lower temperature than any terrestrial object.

This novel passive cooling method takes advantage of the infrared atmospheric window that exists between the frequency of 8 and 13 μm of the spectrum of electromagnetic radiation. That window is, in fact, an overall dynamic property of the earth's atmosphere that allows an amount of infrared radiation, from terrestrial and oceanic surface and from the cloud tops, pass through the atmosphere without being absorbed or re-emitted and thus, without increasing the atmosphere's temperature. It is called infrared as it has a wavelength range just greater than that of the red of the visible light, between 8 and 13 μm, as shown in figure 2-2. A second, but weaker, atmospheric window exists between 16 and 25 μm. According to Suichi *et al*. (2018), the average transmittance of the first window is 0.89 while for the second window it is much lower at 0.43.

The spectral composition of the infrared atmospheric window varies significantly in relevance to the local environmental conditions such as the percentage of water vapour in the atmosphere and the land or sea surface temperature. In fact, the presence of a large gap in water vapour's absorption spectrum is the main reason this window exists (Wilson *et al*., 2012). As can be seen in figure 2-3, water vapour is the main greenhouse gas and is responsible for the absorption and scattering by the atmosphere of a significant amount of radiation in many bands of the electromagnetic spectrum. But, as figure 2-3 shows, between 8 and 13 μm water vapour absorbs and scatters much less radiation; other greenhouse gases, such as carbon dioxide, oxygen and ozone, are responsible for the small amount of radiation absorbed and scattered in this band.

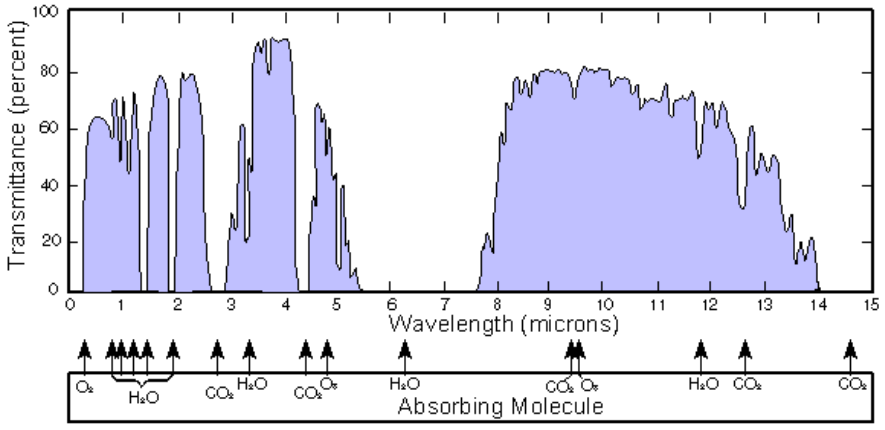

Figure 2-2. Transmittance of the atmosphere between 0 and 15 μm. The atmospheric window can be seen between 8 and 13 μm (Wikimedia Commons, 2014).

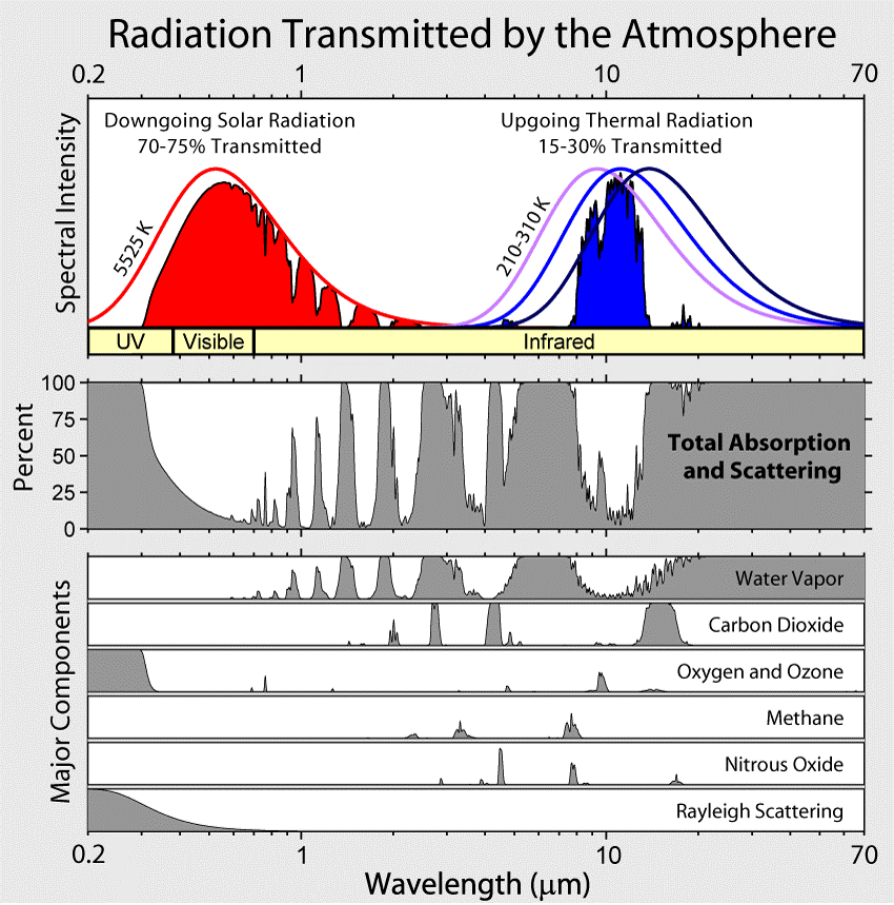

Figure 2-3. The amount of thermal radiation absorbed or scattered by the several gasses of the atmosphere between 0.2 and 70 μm. The infrared window exists between 8 and 13 μm (Wilson *et al*., 2012).

The application of daytime radiative cooling has not yet been fully realized but the same is not true for *nighttime* radiative cooling. Several efficient nocturnal radiative cooling systems that use radiative coolers on the roofs of buildings have been studied and applied in the past with favourable emissivity over infrared wavelengths (Zhai *et al*., 2017). However, application of such systems during daytime, when the cooling demands peak, is a task much more challenging as the solar absorbance due to direct sky access causes the radiative cooler to heat.

2.3. Theory and physics

A surface becomes a daytime radiative cooler only if it has a net positive power outflow when its temperature (T) equals ambient air temperature (T_{amb}) under direct sunlight, as underlined by Raman *et al*. (2014). In such a scenario, the amount of heat radiated to the sky is more than the amount gained through absorption of atmospheric thermal radiation and sunlight.

The gains and losses of a radiative cooler of area A at temperature T, with a spectral and angular emissivity $\epsilon(\lambda,\theta)$, are shown in figure 2-4 and are summarized in the following power balance equation:

$$P_{cool}(T) = P_{rad}(T) - P_{atm}(T_{amb}) - P_{sun} - P_{cond+conv}(T, T_{amb}) \quad (5)$$

Where:

$P_{cool}(T)$	=	the net cooling power of the radiative cooler
$P_{rad}(T)$	=	the power radiated out by the structure
$P_{atm}(T_{amb})$	=	the absorbed power due to incident atmospheric thermal radiation
P_{sun}	=	the incident solar power absorbed by the structure
$P_{cond+conv}$	=	the power lost due to convection and conduction

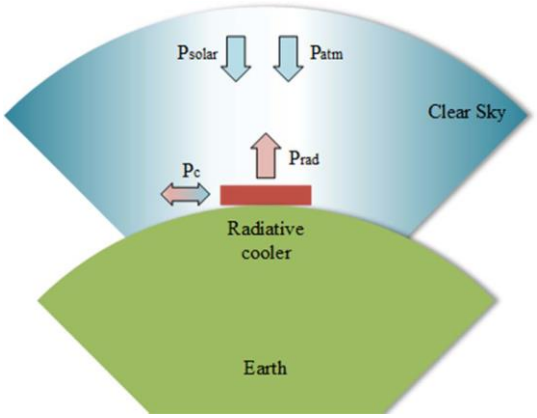

Figure 2-4. Gains and losses of a daytime radiative cooler (Zeyghami *et al.*, 2018).

The power radiated out by the structure $P_{rad}(T)$ is depended to the angular integral over a hemisphere and to the spectral radiance of a blackbody and can be calculated using the following equations:

$$P_{rad}(T) = A \cdot \int d\Omega \cos\theta \int_0^{\infty} d\lambda I_{BB}(T,\lambda)\epsilon(\lambda,\theta) \quad (6)$$

$$\int d\Omega = 2\pi \int_0^{\pi/2} d\theta \sin\theta \quad (7)$$

$$I_{BB}(T,\lambda) = \frac{2hc^2}{\lambda^5} \frac{1}{e^{hc/(\lambda k_B T)} - 1} \quad (8)$$

Where:

$\int d\Omega$	=	the angular integral over a hemisphere
$I_{BB}(T,\lambda)$	=	the spectral radiance of a blackbody at temperature T
h	=	the Planck's constant
k_B	=	the Boltzmann constant
c	=	the speed of light
λ	=	the wavelength
$\epsilon(\lambda,\theta)$	=	the structure's emissivity

The power absorbed as a result of incident atmospheric thermal radiation $P_{atm}(T_{amb})$ is depended on the angle-depended emissivity of the atmosphere and can be calculated using the formulas:

$$P_{atm}(T_{amb}) = A \int d\Omega \cos\theta \int_0^{\infty} d\lambda I_{BB}(T_{amb}, \lambda)\epsilon(\lambda, \theta)\epsilon_{atm}(\lambda, \theta) \quad (9)$$

$$\epsilon_{atm}(\lambda, \theta) = 1 - t(\lambda)^{1/\cos\theta} \quad (10)$$

Where: $\epsilon_{atm}(\lambda, \theta)$ = the angle-depended emissivity of the atmosphere

$t(\lambda)$ = the atmospheric transmittance in the zenith direction

The absorbed incident solar power P_{sun} is calculated using the formula:

$$P_{Sun} = A \int_0^{\infty} d(\lambda\epsilon(\lambda, \theta_{sun})I_{AM1.5}(\lambda) \quad (11)$$

Where: $I_{AM1.5}(\lambda)$ = the AM1.5 spectrum representing the solar illumination

Equations 9 and 11 are formed by replacing the structure absorptivity with its emissivity, using the Kirchhoff's law.

The convective and conductive power loss $P_{cond+conv}(T,T_{amb})$ is calculated using the following equation:

$$P_{cond+conv}(T, T_{amb}) = Ah_c(T_{amb} - T) \quad (12)$$

Where: h_c = a coefficient that represents the combined effect of conductive and convective heating of the radiative cooler because of tis contact with external surfaces and the air

Equation 5 imposes three very strict constraints that should be satisfied by the cooler for daytime radiative cooling to be achieved:

1. It must strongly reflect sunlight to minimize incident solar power (P_{sun}). More specifically, it needs to have strong reflecting properties over visible and near-infrared wavelengths.
2. It must emit thermal radiation (P_{rad}) strongly while diminishing its incident atmospheric thermal radiation (P_{atm}). These can be achieved by reducing to zero its emission at wavelengths where the atmosphere is opaque and ensure that it emits strongly and selectively at wavelengths where the atmosphere is transparent (between 8 and 13 μm).
3. It must be very well sealed from its environment (adjacent surfaces and air) in order for the coefficient (h_c) and, in turn, the power lost due to convection and conduction ($P_{cond+conv}$) to be minimized.

The two first constraints dictate that all wavelengths outside of the atmospheric window should be reflected while at the same time, strong and selective emission within the atmospheric window should be taking place. In practice this means that more than 94% of sunlight should be reflected for worthwhile daytime radiative cooling to be achieved.

The third constraint prompts a design challenge as the surfaces on the immediate environment of the radiative device will heat up because of their exposure to sunlight and this excess heat will be transferred to the device.

2.4. Ideal cooler

The demanding physical requirements for the radiative cooler cannot be satisfied by elements already existing in nature. It is for that reason that several metamaterials have been proposed to achieve the absorbing and reflecting requirements, mentioned above. Those metamaterials are materials specifically engineered in order to achieve properties not existing in nature and are, in general, assemblies of multiple elements. The materials used are frequently in layers on a scale smaller than the wavelength of the several phenomena influenced by them.

The conventional concept for designing and constructing a daytime radiative cooler is based on the concept of a simultaneous solar reflector and a strong and selective infrared emitter, consisting of metallic mirrors and polymeric materials (Wu et al., 2018) and usually sealed from its environment. The metallic mirror reflects the unfavorable irradiation while the polymer acts as the emitter that dissipates the thermal energy to the outer space emitting only in the atmospheric window (Zeyghami *et al*., 2018). Common materials used as base materials of the metamaterials are aluminium, silver and silica. As Vall and Castell (2017) state:

> *« The performance of the radiative cooling technology is affected by the physical properties of the device and also by the surrounding conditions. Therefore, special attention must be paid at materials and environmental conditions. »*

One of the first researches relevant to the design of an ideal daytime radiative cooler was the one published by Raman *et al*. (2014). Their experiment focuses on demonstrating a radiative cooling device able to maintain a steady-state temperature lower than the ambient temperature during daytime and to measure the cooling power of it as a function of its net cooling power outflow under direct sunlight and relevant to the daytime peak conditions. In order to do so, they introduced and numerically optimized a design based on photonic films that are one-dimensional and thus more compliant with large scale manufacturing.

The photonic solar reflector of Raman *et al*. (2014), shown in figure 2-5, consists of seven alternating layers of hafnium dioxide (HfO_2) and silicon dioxide (SiO_2) on top of a silver (Ag) layer which is in turn placed on a silicon (Si) wafer. The top three thick layers of HfO_2 and SiO_2 are mainly responsible for thermal radiation from the cooler while the bottom four thin layers assist in the optimization of solar reflection. Combining those layers results in a 'microscopically planar and integrated structure' capable of achieving strong thermal emission and high solar reflectance. The cooler is designed on top of an apparatus and suspended in an innovative relatively well sealed air pocked that decreases both convection and conduction phenomena between the cooler and the roof surface. The solar cooler designed has been experimentally proven to be capable of reflecting 97% of the incident sunlight, emitting strongly and selectively within the transparency window, cooling to 4.9 °C below ambient temperature under direct sunlight and having a cooling power of 40.1 W/m^2.

The design of Raman et al. (2014) was used as a basis and altered in the research of Kecebas et al. (2017). In detail, three layers of alumium oxide (Al_2O_3) where added to the stack, while keeping the same overall thickness by decreasing the thickness of the bottom thin layers. This particular oxide was chosen because it has a stronger absorption in the 8-13 μm spectrum, specifically beyond 10 μm, and a non-absorbing behavior in the visible and near-infrared spectrum. Adding the Al_2O_3 resulted in increasing the emissivity within the transparency window.

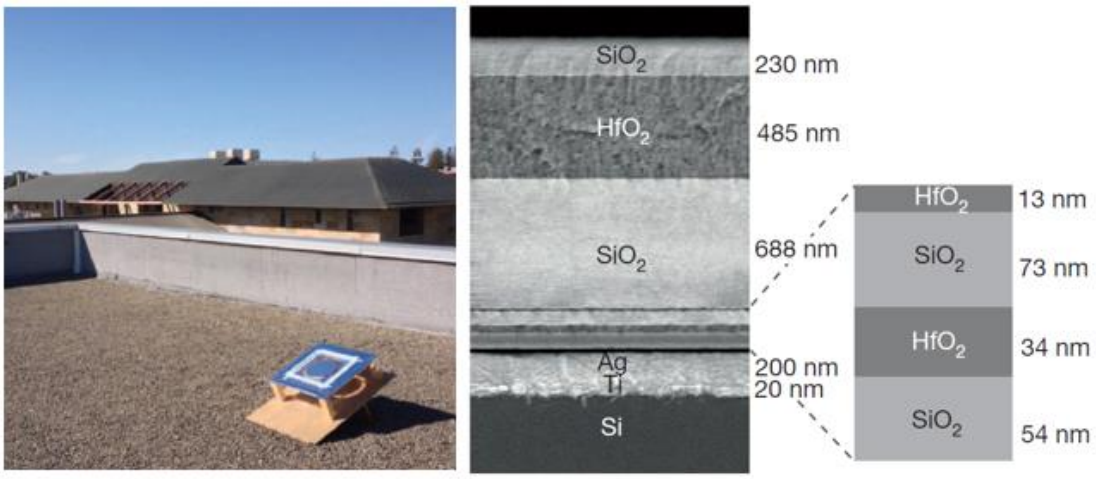

Figure 2-5. (Left) The radiative cooling structure designed by Raman *et al*. (2014); (Right) the layers of the solar reflector.

The research of Rephaeli *et al*. (2013) preceded the one of Raman *et al*. (2014) for a few months and demonstrated, for the first time, an integrated thermally selective emitter on top of a broadband mirror capable of implementing radiative cooling during daytime. In particular, the authors presented a metal-dielectic photonic structure, with a net cooling power of 100 W/m^2 at ambient temperature, consisting of two thermally emitting photonic crystal layers of silicon carbide (SiC) and quartz on top of a solar reflector made of magnesium fluoride (MgF_2) and titanium dioxide (TiO_2) which lies on silver (Ag) substrate, as shown in figure 2-6.

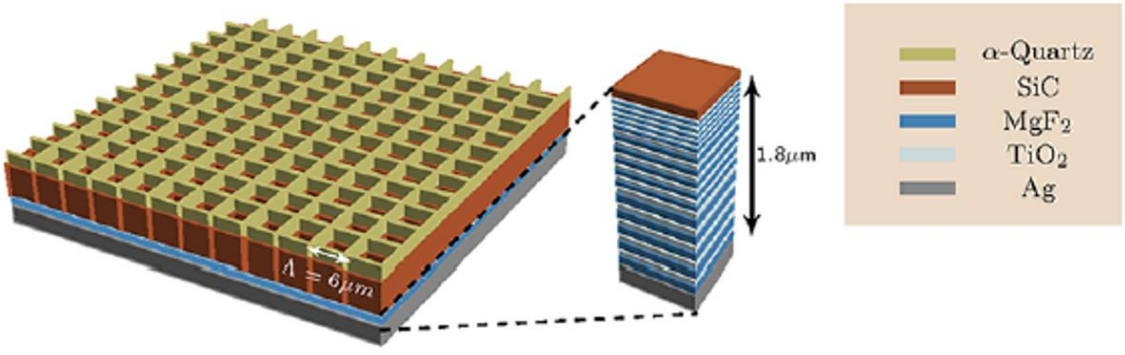

Figure 2-6. The metal-dielectic photonic structure presented by *Rephaeli et al*. (2013).

A similar emitter-reflector approach was followed in the research of Wu *et al.* (2018) where a novel 'moth-eye-like'[1] two dimensional anti-reflecting all-dielectric micropyramid structure has been proposed. It consists of alternating layers of aluminum oxide (Al_2O_3) and silica (SiO_2), with a thickness of 2 μm and 1 μm respectively, placed on top of a silver (Ag) layer, as can be seen in figure 2-7. Aluminum oxide and silica are the chosen materials as they exhibit exceptionally low loss in the solar spectrum and significant high loss in the mid-infrared range. This pyramidal radiative cooler has been demonstrated to have a net cooling power of 122 W/m^2 at ambient temperature.

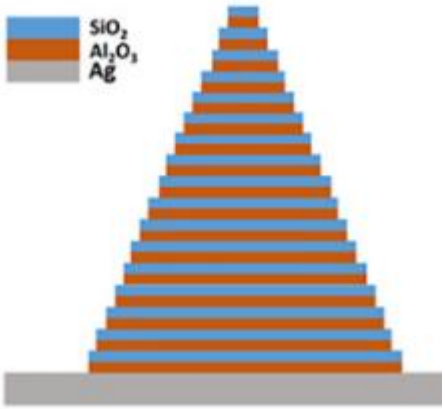

Figure 2-7. The all-dielectric micropyramid structure Introduced by Wu *et al.* (2018).

Alternating layers were also used in the study of Hossain *et al*. (2015) where a multilayer metal-dielectric anisotropic microstructure, consisting of an array of symmetrically shaped conical metamaterial pillars as shown in in figure 2-8, was proposed and experimentally demonstrated. Each pillar is made of alternating layers of 30-nm-thick aluminium (Al) and 150-nm-thick germanium (Ge) while the substrate of the structure is an 150-nm-thick aluminium layer that is thick optically enough to minimize any infrared transmission through it. The experimental results indicate that this microstructure has the ability to provide a cooling power of 116.6 W/m^2 and to cool down 12.2 and 9 °C below ambient temperature during night and day respectively.

In Yang *et al.* (2018) research, focus has been on the realization of the highest possible solar reflectance. In particular, the authors designed a dual-layer structure that achieves an integrated reflectance of 0.991 over the wavelength range from 0.28 to 4.0 μm, which is the highest ever recorded for any material, artificial or natural. The two layers of the structure are a submillimetre (0.24 mm) thick polytetrafluoroethylene (PTFE) sheet, shown in figure 2-9, and a back silver (Ag) reflector which are coated on a glass substrate. PFTE is a white material with immensely high diffuse reflectance in the wavelength range between 0.2 and 2.5 μm (ultraviolet to near-infrared).

[1] The eyes of the moths are equipped with a rare nanostructured film able to eliminate reflections which allows them to see well in the dark without reflections and, thus, without their location being exposed to predators. This antireflective coating works because it consists of a hexagonal pattern of bumps that have dimensions smaller than the wavelength of visible light. Application of biomimicry has led to moth-eye structures that are good anti-reflectors in the optical regions (Wu *et al*., 2018).

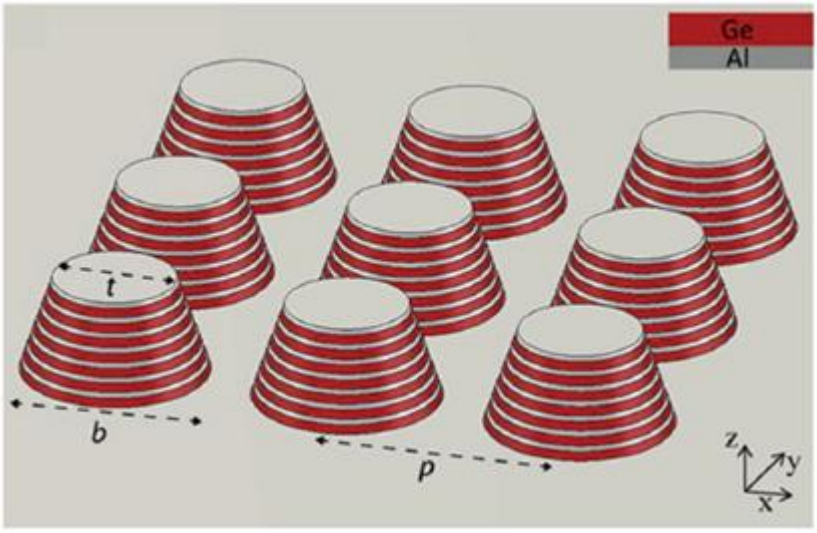

Figure 2-8. The multilayer metal-dielectric anisotropic microstructure introduced by Hossain *et al*. (2015).

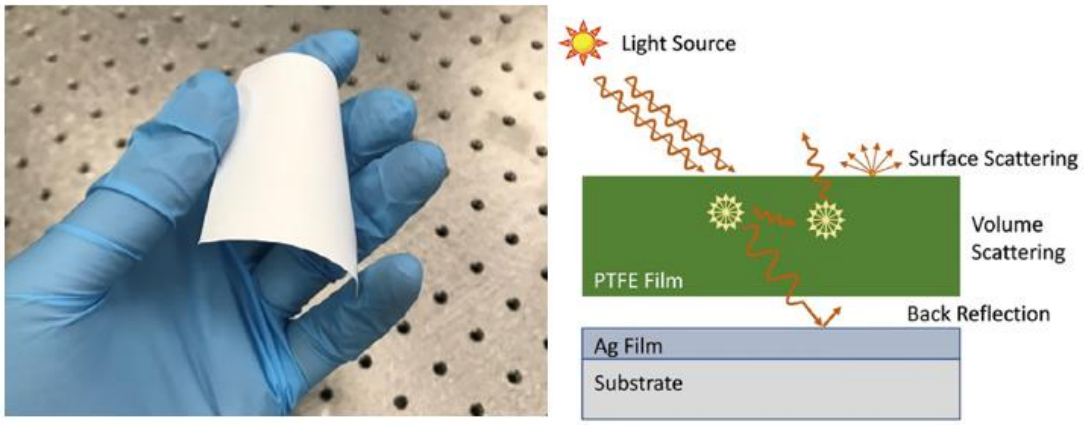

Figure 2-9. (Left) The PFTE sheet designed by Yang *et al*. (2018), without the sliver; (Right) Schematic representation of reflecting and scattering of the dual-layer structure.

The harmfulness of emitting and absorbing outside of the infrared transparency window was investigated in the research of Kou *et al*. (2017) where not expensive and abundant materials were used that achieve daytime radiative cooling without the need for complicated photonic devices. This was possible by designing a device that emits and absorbs in a broad range of wavelengths which can be seen in figure 2-10. More specifically, it consists of a fused silica wafer coated with a polydimethylsiloxane (PDMS) as a top layer and a silver film as a back reflector. The device sits on top of an aerogel blanket attached to the bottom surface of a Petri dish which is covered by a polyethylene film that shields it from convective phenomena.

This polymer-coated fused silica mirror structure appears to have some very promising capabilities. It is able to cool 8.2 and 8.4 °C below ambient temperature under direct sunlight and at night respectively and it is estimated that it can provide an average cooling power of about 127 W/m^2

during daytime. It is efficient, though, only when there are not high cooling requirements or as the authors (Kou *et al*., 2018) conclude:

> *« For applications in which the desired temperature is not substantially different from ambient temperature, a radiative cooler with near unity emissivity over a broad infrared spectrum will achieve better performance than one that emits only in the atmospheric window. »*

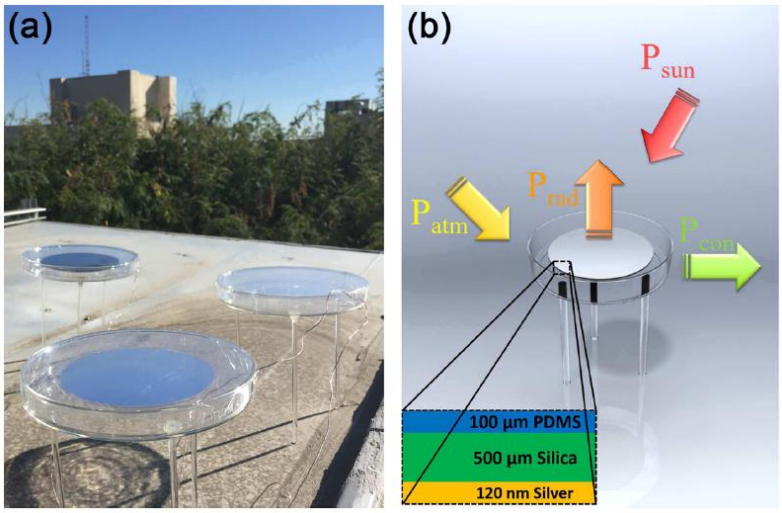

Figure 2-10. (Left) The radiative cooling samples designed by Kou *et al*. (2017); (Right) Schematic of the experiment setup.

The radiative cooling performance of metal-dielectric-metal (MDM) spectral selective emitters, whose radiation characteristics can be controlled, was investigated by Lee *et al*. (2017). In particular, a metal and dielectric thermal plasmonic structure consisting of gold (Au) with a zinc sulphide (ZnS) dielectric was designed. A 200 nm layer of ZnS was deposited on top of a 100 nm layer of Au which was in turn deposited on a cleaned silicon substrate. Then a square Au disc array was patterned on top of the dielectric with the use of photolithography. The experimental and numerical results of the study showed that an MDM spectral selective emitter can have a surface temperature 38 °C lower than the ambient temperature.

Zhai *et al*. (2017) aimed in designing an economical roll-to-roll metamaterial that could be viable for extensive application and use. They demonstrated combined daytime and nighttime radiative cooling using a 50-nm-thick randomized glass-polymer hybrid metamaterial, shown in figure 2-11, consisting of randomly distributed silicon dioxide (SiO_2) microspheres in a polymeric matrix (polymethylpentene, PMP) backed with a 200-nm-thick silver (Ag) coating. The structure is able to achieve 0.93 infrared emissivity, 96% solar irradiance reflectance and a radiative cooling power of 93 W/m^2 under direct sunshine. The material was produced in 300-mm-wide sheets with the impressive rate of five meters per minute.

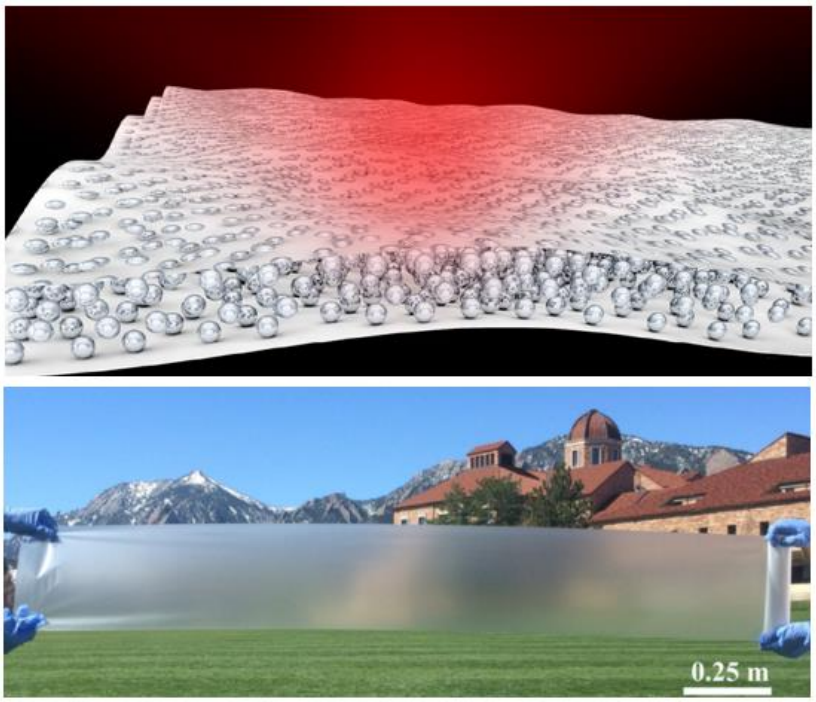

Figure 2-11. (Top) Schematic of the glass-polymer hybrid metamaterial as proposed by Zhai *et al*. (2017); (Bottom) A photo showing the metamaterial film, before being coated with silver.

The application of an ideal radiative cooler in a dry and humid environment, such as the one in Okinawa, Japan, was studied by Suichi *et al*. (2018). After experimental and numerical investigation, they concluded that in such an environment a radiative device should have minimized emissivity also within the second atmospheric transparency window, between 16 and 25 μm. In particular, the device designed consisting of layers of silicon dioxide (SiO2) and poly (methyl methacrylate, PMMA) on top of an aluminium (Al) mirror appeared to have a temperature 2.8°C higher than the ambient temperature of 35°C because it was also emitting in the second atmospheric window which was almost closed because of the infrared absorption of water vapour as a result of high precipitable water vapour (PWV).

In table 2-1, a summary of several proposals for the ideal composition of a radiative cooler is presented. The materials and type of device used in each proposal as well as cooling power and reflectivity and/or emissivity achieved, when available, are listed.

Reference	Radiative cooler	Reflectivity/Emissivity	Cooling power
Rephaeli *et al*. (2013)	A photonic structure consisting of two crystal layers of silicon carbide (SiC) and quartz on top of a solar reflector made of magnesium fluoride (MgF_2) and titanium dioxide (TiO_2).	N/A	Has a net cooling power of 100 W/m^2.
Raman *et al*. (2014)	An integrated photonic solar reflector and thermal emitter consisting of seven	Reflects 97% of incident sunlight, emits strongly and selectively in the	Cools to 4.9 °C and has cooling power of 40.1 W/m^2

Reference	Radiative cooler	Reflectivity/Emissivity	Cooling power
	alternating layers of HfO_2 and SiO_2 on top of a layer Ag on top of a silicon wafer.	atmospheric transparency window.	
Hossain *et al*. (2015)	A metal-dielectic anisotropic microstructure consisting of conical metamaterial pillars made of aluminum (Al) and germanium (Ge).	N/A	Provides cooling power of 116.6 W/m^2 and to cool down 12.2 and 9°C below ambient temperature during night and day respectively.
Kou *et al.* (2017)	A polymer-silica-mirror consisting of a fused silica wafer coated with a polydimethylsiloxane (PDMS) as a top layer and a silver film as a back reflector.	N/A	Cools 8.2°C (under direct sunlight) and 8.4°C (at night) below ambient temperature. Has an average net cooling power of about 127 W/m^2
Lee *et al*. (2017)	A metal and dielectic thermal plasmonic structure consisting of gold (Au) with a zinc sulphide (ZnS) dielectric.	N/A	Can reach a surface temperature 38 °C lower than ambient.
Zhai *et al*. (2017)	Micrometre-sized SiO2 spheres randomly distributed in the matrix material of polymethylpentene (PMP) (randomized glass-polymer hybrid metamaterial) backed with a sliver coating	Achieves infrared emissivity greater than 0.93 across the atmospheric window. Reflects approximately 96% of solar irradiance.	Reaches noon-time radiative cooling power of 93 W/m^2 under direct sunshine.
Wu *et al*. (2018)	A pyramidal nanostructure consisting of alternative layers of Al_2O_3 and SiO_2 multilayer films on top of a silver layer.	N/A	Achieves a net cooling power of 122 W/m^2
Yang *et al.* (2018)	A dual-layer structure consisting of a polytetrafluoroethylene (PTFE) sheet on top of a silver film.	Has a total solar reflectance of approximately 0.99.	N/A

Table 2-1. A review of several radiative coolers proposed or constructed as mentioned in several scientific papers. The reflectivity and emissivity properties of each cooler as well as its cooling power are listed, when available.

3

Energy transfer mechanism

While, in recent years, research regarding the materials composing the daytime radiative cooling has been extensive, the same cannot be said for the research related to the transfer mechanism of energy collected via daytime radiative cooling. Several publications exist that present the mechanisms behind cooling down buildings using nocturnal radiative cooling but only a limited amount of them is related to daytime radiative cooling.

Focus on daytime radiative cooling research has been in designing hybrid systems, that is by designing systems in which this passive cooling technique works in parallel with conventional active systems, such as split air-conditioning units. The two sub-systems work complementary to each other and the energy produced by the passive one is stored into an energy storage thermal tank.

Such tanks usually use water as storage medium and, due to the ability of water to have lower densities in higher temperatures, are stratified. Stratification keeps masses of water of different densities and temperatures separated in different layers and has significant advantages related to the storage of thermal energy. A stratified water tank should be designed following principles relevant to, amongst other aspects, its geometry and insulation characteristics.

3.1. Nocturnal radiative cooling

There are numerous strategies for utilizing nighttime radiative heat gains in buildings, according to Zhang *et al*. (2018). They include passive systems in which selective emitting materials are applied directly on roofs and active selective systems, illustrated in figure 3-1, that can be categorized as follows:

a. Water based (open loop): Systems that consist of a shallow rooftop pond in which heat can be transferred from the roof through the water in the pond to the surrounding atmosphere by radiation, convection and evaporation.

b. Water based (closed loop): Systems where water is used as a fluid transferring heat and heat is dissipated by a cooling radiator.

c. Air based: System where air provides instantaneous cooling to indoor spaces with the use of a fan or by taking advantage of the buoyancy force. It is considered simpler and cheaper but can't be easily integrated with buildings.

d. Hybrid radiative/non radiative: Integrated systems consisting of a nighttime radiative cooling mechanism and another energy-related system, such as split air-conditioning

e. Hybrid water/air based: Integrated systems formed by a combination of an air and a water based system

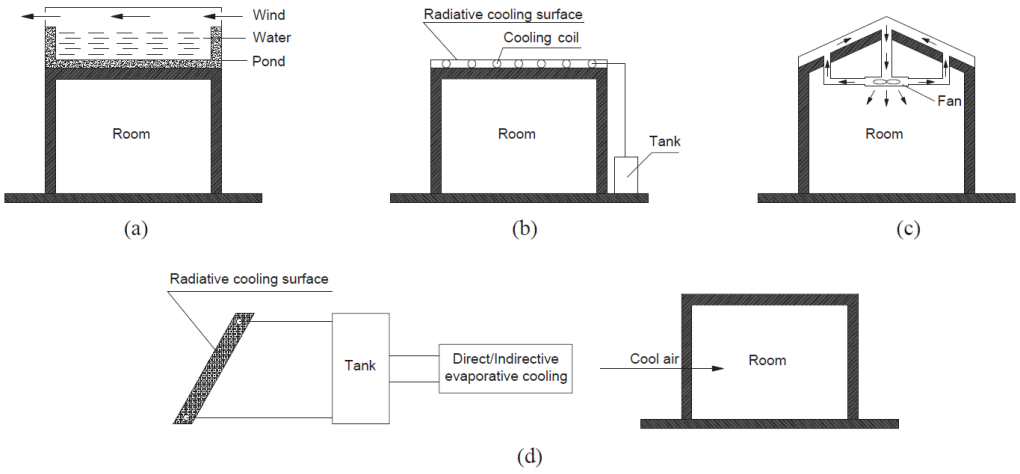

Figure 3-1. Active systems utilizing the heat gains of nocturnal radiative cooling: (a) Open loop water based system; (b) Closed loop water based system; (c) Air based system; (d) Hybrid system.

In their study, Zeyghami *et al*. (2018) report that it is possible to supply a residential building with 80% of its cooling demands using nighttime radiative cooling in favourable climates. The authors introduce two common options, described in the following paragraphs, which utilize the heat gains of nocturnal radiative cooling.

The first one involves cooling down the thermal mass of the building which usually corresponds to a horizontal roof or a roof water pool; similar to the open loop water based system mentioned above. The thermal mass is cooled directly during the night and then during the day it is sealed and insulated

using a movable insulation. Summer cooling demand can be satisfied without the need of any other energy source only if the dew point temperature is low enough.

The second method mentioned includes the use of a transfer medium that can be either air or water between the radiator and the envelope of the building. An example of this method, in its most basic form, is a system consisting of a near black emitter, an array of heat pipe elements and a thermal storage tank, as shown in figure 3-2 in the system designed by Ezekwe (1990). This system has a cooling capacity of 628 kJ/m^2 per night under clear sky conditions and the ability to cool to around 7 degrees below ambient temperature. It is a closed loop water system as presented above.

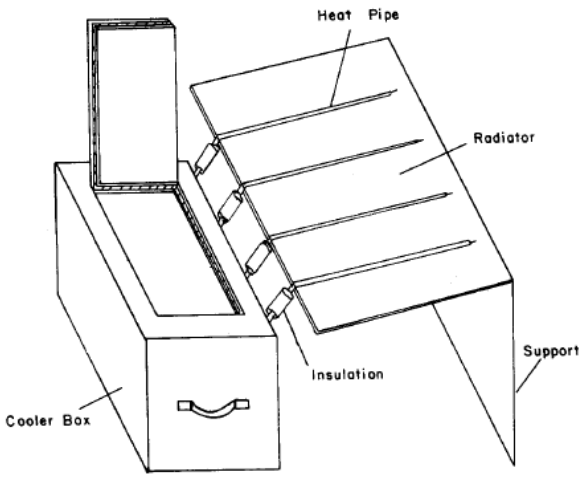

Figure 3-2. The closed loop water based system designed by Ezekwe (1990).

3.2. Utilization of daytime radiative cooling

As stated earlier, scientific research has been concentrated in designing and optimizing the ideal radiative cooler without further investigating systems that are able to transform the roof radiative gains into actual cooling input in the indoor building environment. Raman *et al* (2014), for example, only assume that there is a mechanism able to transfer a percentage of the heat load to the radiative heat surface while other cooling demands are handled by a conventional HVAC system.

As part of their research, Zhang *et al* (2018) developed a comprehensive 'hybrid diurnal radiative cooled-cold storage cooling system' applied in single family houses in four cities, with different climates, in the United States to investigate whether such a cooling system can be a cost-effective solution for providing radiative cooling to residential buildings. That kind of houses is selected because they have a high ratio of roof area to floor area and a relatively low cooling energy load per unit floor. It is one of the few studies relevant to application of daytime radiative cooling since previous studies of similar systems were investigating only nocturnal application due to the increased solar heating of the radiative coolers during the day.

The research in simulated for houses in the United States where the most common cooling system used for this kind of houses is the split air conditioner (SAC) and this is the reason why the complete system introduced is one in which it is feasible to integrate an existing SAC.

The system proposed consists of two distinct subsystems and many individual elements shown in the sketch in figure 3-3, where the labels A to H represent the intersections of pipes and the labels VA to VF represent valves. The first subsystem is composed of cold energy collectors, branded as *RadiCold* modules, laminated with a radiative cooling metamaterial film and placed on top of water channels and a cold storage water tank connected with a network of pipes. The second subsystem is a reduced sized air conditioner (RSAC) that aims to provide complimentary cooling when the stored cold energy is not sufficient. Other significant elements within those subsystems are a module pump, an evaporator, a supply fan, a cooling coil, air diffusers, a tank pump and several valves. A significant advantage of this system is that it can be applied in new houses but also retrofitted into existing ones as the first subsystem is independent to the air conditioner.

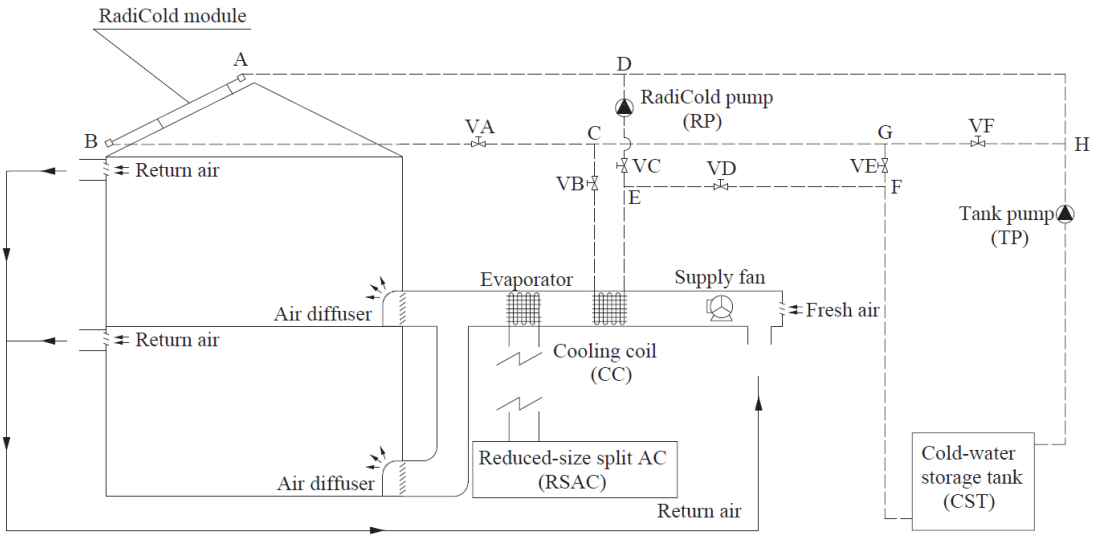

Figure 3-3. Sketch of the hybrid radiative cooling system designed by Zhang *et al.* (2018).

In addition, this system is also able to operate in three different modes according to the current cooling requirement conditions and to the energy stored in the tank. Those operating modes are: *Direct space cooling*, for when the cooling power of the radiative modules is equal or lower than the space cooling demand; *Combined spaced cooling and cold storage charging*, for when the cooling power of the radiative modules is higher than the space cooling demand; *Cold storage for space cooling*, for when the energy stored in the tank is cooled to cool the space.

In figures 3-4 to 3-6, the loops that the cooled water follows for each operating mode are illustrated. The loops are highlighted with red colour as are the labels of the valves that are open for each mode.

Figure 3-4 illustrates the direct space cooling mode where the passive cooler subsystem provides an amount of cooling energy that is the same or lower than the cooling demand of the house. This energy is used directly to cool the space through the cooling coil. No cooled energy is stored in the tank in this mode. In addition, the air conditioning unit operates in order to provide additional cooling if the cooling energy provided by the passive cooler is lower than the one needed.

Figure 3-5 illustrates the combined space cooling and cold storage charging mode in which the cooling energy provided by the passive cooler is higher than the cooling demand. Part of this energy

is used to cool directly the space while the rest of it is charged into the cold-water storage tank. The air-conditioning system does not operate in this mode.

Figure 3-6 illustrates the cold storage for space cooling mode where cooling energy from the passive cooler is unavailable for any purpose. This happens when there is no direct sky access; during the night and when the sky is not clear. In this mode the water stored in the tank is used to cool the space through the cooling coil.

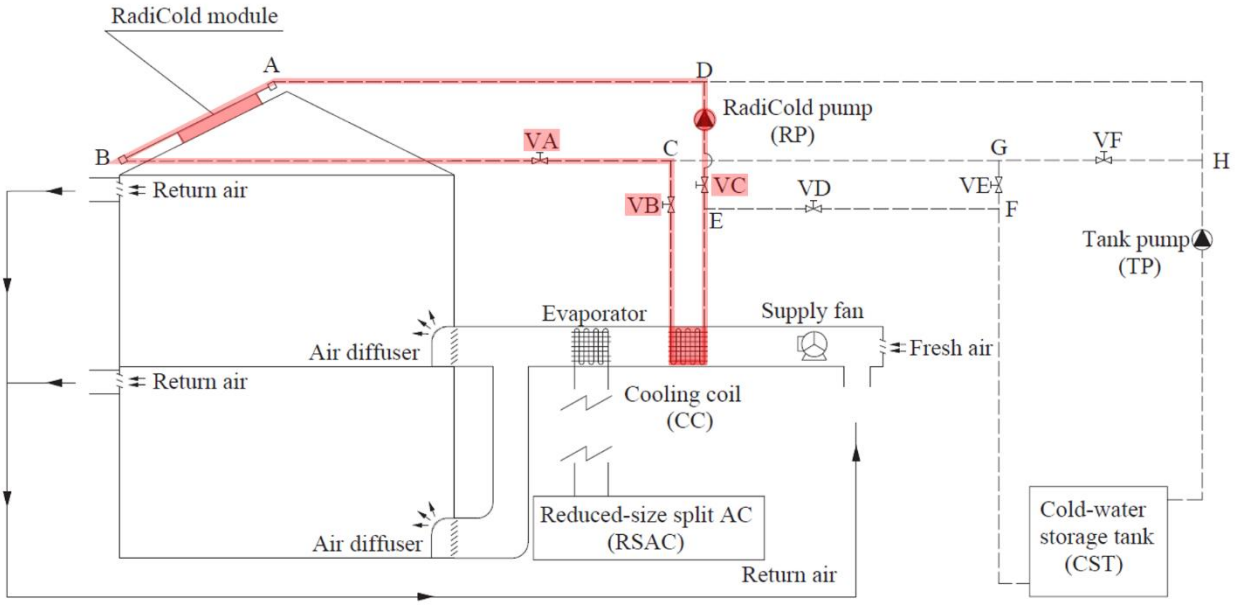

Figure 3-4. First operation mode (Direct space cooling) of the system of Zhang *et al.* (2018). Valves VA, VB and VC are open. In this mode the RSAC could be operating or not.

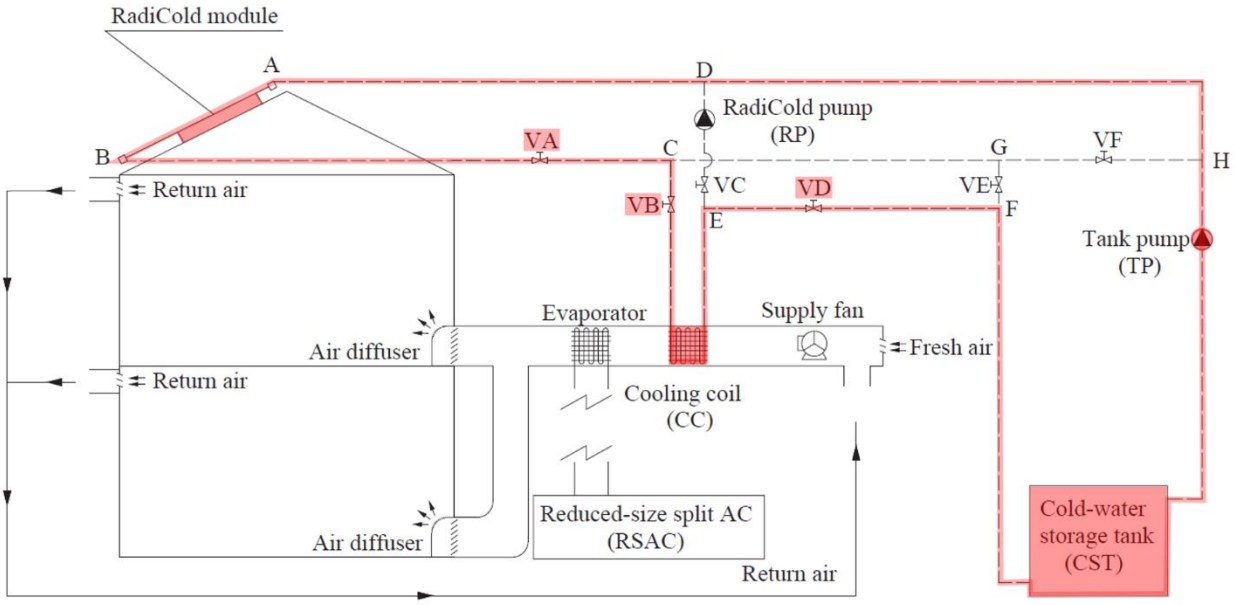

Figure 3-5. Second operation mode (Combined space cooling and cold storage charging) of the system of Zhang *et al.* (2018). Valves VA, VB and VD are open.

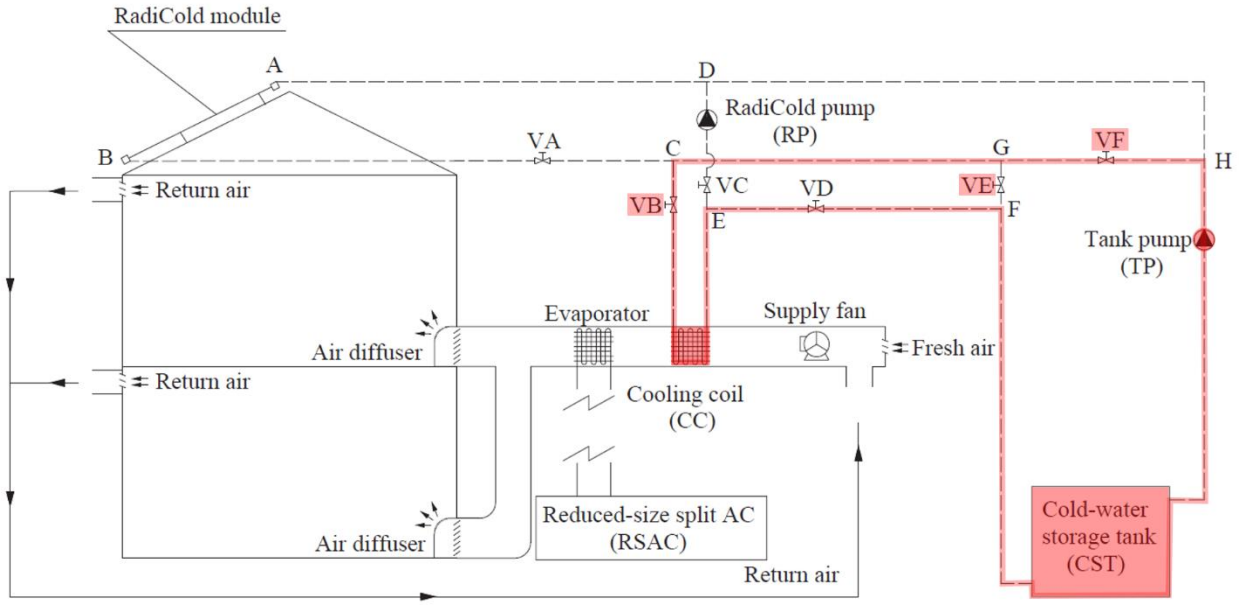

Figure 3-6. Third operation mode (Cold storage for space cooling) of the system of Zhang *et al.* (2018). Valves VB, VE and VF are open.

The authors followed an optimization process in order to determine the number of radiative modules used and the sizes for the elements of the system, considering also the financial prospect of applying such a technology. The four locations for which a simulation was made, along with their respective climates, and the calculated annual cooling electricity savings, electricity reduction compared to a split air conditioner lonely (SACL) and payback period are presented in table 3-1. Annual electricity savings ranging from 26 to 46% could be reached according to this research.

Location	Climate	Annual cooling electricity savings (kWh)	Reduction compared to SACL (%)	Payback period (years)
Orlando	Hot-humid	1355	25.7	8.0
San Diego	Hot-dry	779	38.5	4.8
San Francisco	Maritime	288	45.8	7.3
Denver	Cold	799	37.1	7.5

Table 3-1. Simulation results on electricity savings and payback periods from Zhang *et al.* (2018) research.

3.3. Thermal energy storage tanks

In the previous subsection a cooling system was presented that uses as a component a cold-water storage tank. Those tanks are usually stratified as explained below.

The term water stratification describes the situation in which a water column is divided into layers of different water masses (Cushman-Roisin *et al.*, 2011) that have different properties, such as density, salinity, oxygenation or temperature. The most common property responsible for the division into layers is density which is related to the ability of water to have higher densities in lower

temperatures, as depicted in figure 3-7. In simple words, stratified water consists of water parcels of various densities that, because of gravity, arrange themselves so that the lower densities are placed above higher densities. A varied water temperature column is formed by a number of layers that act as barriers not allowing the water to be mixed and has significant applications in energy storage systems, when designed properly.

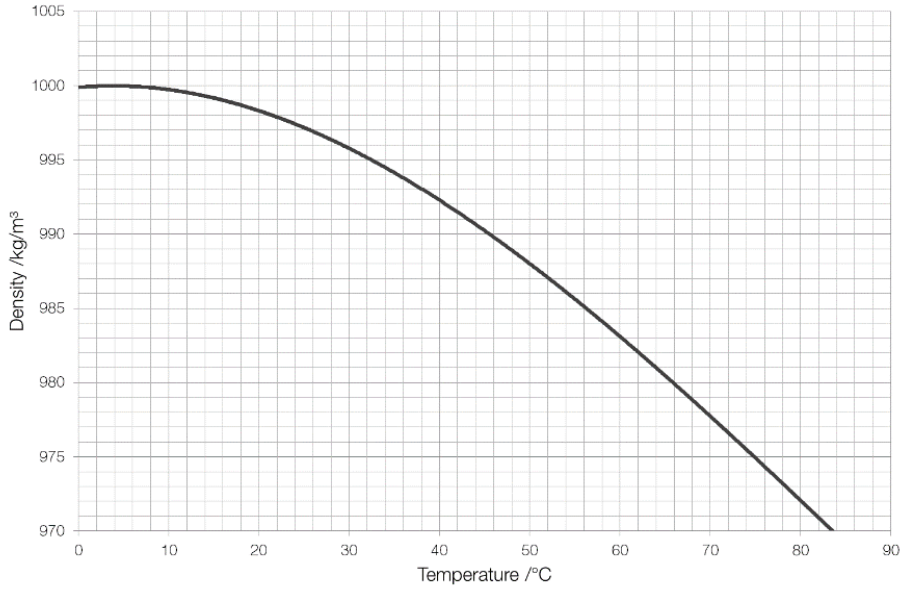

Figure 3-7. The density of water plotted against its temperature.

The use of energy storage as an energy management technology appears to have increased application as a result of the significant concerns related to the need for energy, or exergy, conservation. In most of the cases, energy demand and energy supply do not coincide, so the existence of an energy storage technology is detrimental for the peaks of energy demand and supply to be levelled according to Ekechukwu and Onyegegbu (2014). Such a technology is able to save excess produce energy and insert it in a system at instances when there is no supply or when supply rate is less than demand rate.

The mediums in which energy may be stored vary. It can be chemical energy; such as electrochemical batteries or biomass, mechanical energy; such as pumped storage hydroelectricity; and heat. When the latter is the case, the term thermal energy storage (TES) is used which can be then distinguished into sensible TES and latent TES. The first refers to the storage of latent heat that comes from the phase change of a material at a moderately constant temperature while the second refers to the storage of heat relevant to the change of temperature of a material. It is worth noting that the word 'thermal' is used to describe those systems instead of the word 'heat' as the latter implies that only heat can be stored while in reality both heat and cold can be stored, which makes the former term more appropriate.

Water is the most common material used in sensible TES systems because it is inexpensive, almost always, readily available and has a high heat capacity. In addition, Rahman *et al*. (2015) underlines that a stratified water tank is an economical storage medium which can be integrated without any difficulties into the energy producing system of a building and operate in conjunction with systems that produce heat or cold on-site.

According to Dincer and Rosen (2011), the design of a thermally stratified TES water tank should be proper for its use to be effective. One of the most important design aspects is the positions of the water inlet and outlet and two relevant poorly and properly designed cases are illustrated in figure 3-8. Also, in the figure one is able to see the thermally effective quantity of water that results from the placement of the inlet and the outlet. In addition, the tank should have a good thermal-retaining performance since, in most of the cases, it must store water for periods of several hours.

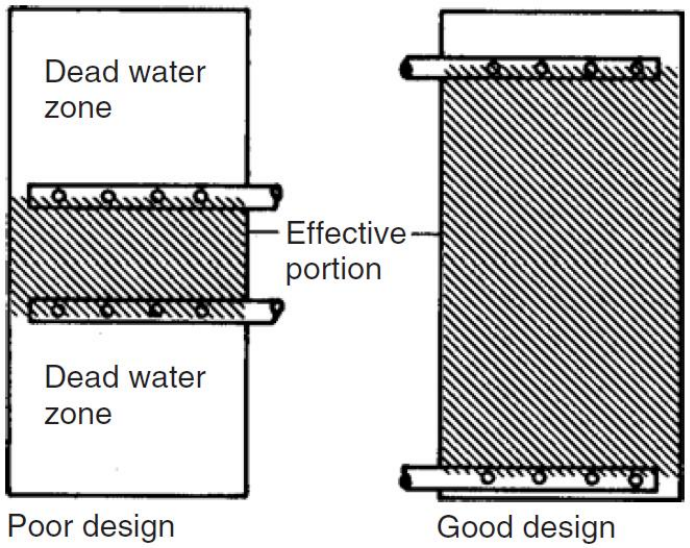

Figure 3-8. A poor and a good design of a water energy storage tank and the effective water portion in each case (Dincer and Rosen, 2011).

Summarizing, the requirements a well-designed thermal energy storage water tank should satisfy are the following:

1. It should be able to store separate masses of water at different temperatures, thus being stratified. Even during charging and discharging periods, mixing of water should be minimal.
2. The water inlet and outlet should be placed in such positions so that effective storage capacity is maximized, and the dead water zone is minimized.
3. The tank should be properly insulated for the heat loss and gains to be minimized.

Additionally to the requirements stated above, some other considerations should be taken into account when designing such a tank. When it comes to its geometrical features, it is desirable that the tank has a deep water-storage configuration which is achieved by locating the inlets and outlets as close as possible to the top and bottom of it, as already mentioned, and by making the tank having a shape significantly larger vertically than horizontally. Because of that and since the surface area which is in contact with the storage water should be minimized, it is common for cylindrical tanks to be preferred. Operating-wise the water temperature difference between the lower and the upper parts should be at least larger than 5 °C. To maintain this water temperature difference, controls can be used if required. Also, the mass flow rate of water getting in and out of the tank should not be high. Designing the tank so that it follows those design principles, along with satisfying insulating and

water-proofing requirements, lead to the establishment of a properly functioning stratified water tank that acts as a good thermal storage medium.

4

The case of Cyprus

Cyprus is an island nation in the eastern Mediterranean Sea located where Europe, Asia and Africa meet at 35°N latitude and 33°E longitude. It is a land with a long and tumultuous history and shares a predominantly hot Mediterranean climate with its maritime neighbours, a main characteristic of which is the great number of clear-sky days per year.

Capital Nicosia stands on the central lowland region of the island while the three other urban centres, namely Larnaca, Limassol, and Paphos, are situated along the south coast. The morphology of the island is dominated by a central mountain range.

Social, geographical, and climate conditions have shaped its citizens' housing habits while its energy isolation, as an island, has not led to the implementation of sustainable ways of energy production. The high demand for cooling energy and the absence of any passive cooling techniques result in high electricity consumption which could be reduced by implementing a way to produce cool passively.

4.1. Climate

Cyprus has a Mediterranean climate with long and dry summers from mid-May to mid-September and rainy but mild winters from mid-November to mid-March, according to the Department of Meteorology (2018). The morphology of the island is dominated by Troodos, a central massif peaking at Olympus at almost two thousand metres, while the second mountain range of the island is the northern long and narrow Kyrenia range, also called Pentadaktylos. A central plain, Mesaoria, lies between the two mountain ranges. The coastal plains and valleys are home to all the island's urban regions, besides the capital Nicosia, as shown in in figure 4-1. The length of the day deviates from 9.8 hours in December to 14.5 hours in June.

Figure 4-1. A map of Cyprus showing the central Troodos massif, the northern Kyrenia range, Mesaoria central plain between them and the location of the urban centres of the island.

The most characteristic element of Cyprus' climate is the clear skies and the high amount of sunshine. The central plain and the eastern lowlands enjoy a whole year average of 75% of bright sunshine for the hours when the sun is above the horizon. This translates to about 11.5 of bright sunshine hours per day for the six summer months and 5.5 bright sunshine hours for December and November.

As stated before, summers on the island are hot while winters are mild but it should be noted that coast vicinity and altitude modify temperatures significantly. It is for that reason that Cyprus is divided into four climatic zones, illustrated in figure 4-2. Marine influences result in cooler summer and warmer winters near the coastline and altitude lowers temperatures by about 5°C per 1000 metres. In addition, there is a remarkable seasonal difference between mid-summer and mid-winter temperatures varying from 18 °C inland to 14 °C on the coastal areas. Also, in the summer, the day maximum and night minimum temperature difference is quite large ranging from 16° C on the central

plain to 9 to 12 °C elsewhere. The mean daily, summer average maximum and winter average minimum temperatures for the four urban areas and higher parts of the Troodos mountain are presented in table 4-1. The average daily mean, maximum and minimum temperature for Larnaca, on the south-east coast are presented in figure 4-2. Larnaca is only location in Cyprus for which EnergyPlus provides weather data.

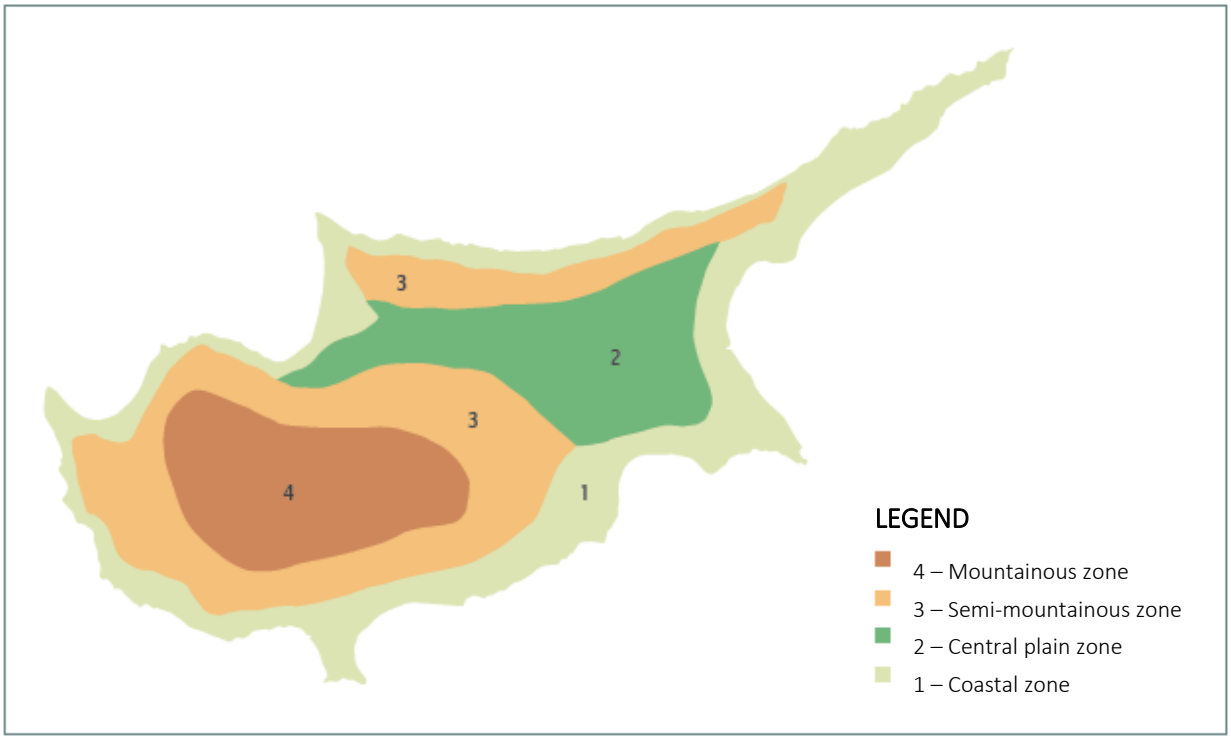

Figure 4-2. The four climatic zones of Cyprus (MCIT, 2015).

	July/August		**December/January**	
	Mean daily (°C)	Average maximum (°C)	Mean daily (°C)	Average minimum (°C)
Nicosia (Central plain)	29	36	10	5
Limassol (South coast)	28	33	13	8
Paphos (SW coast)	25	30	17	8
Larnaca (SE coast)	26	31	13	8
Troodos mountains	22	27	3	0

Table 4-1. The summer mean daily and average maximum temperatures and the winter mean daily and average minimum temperatures at several locations of Cyprus.

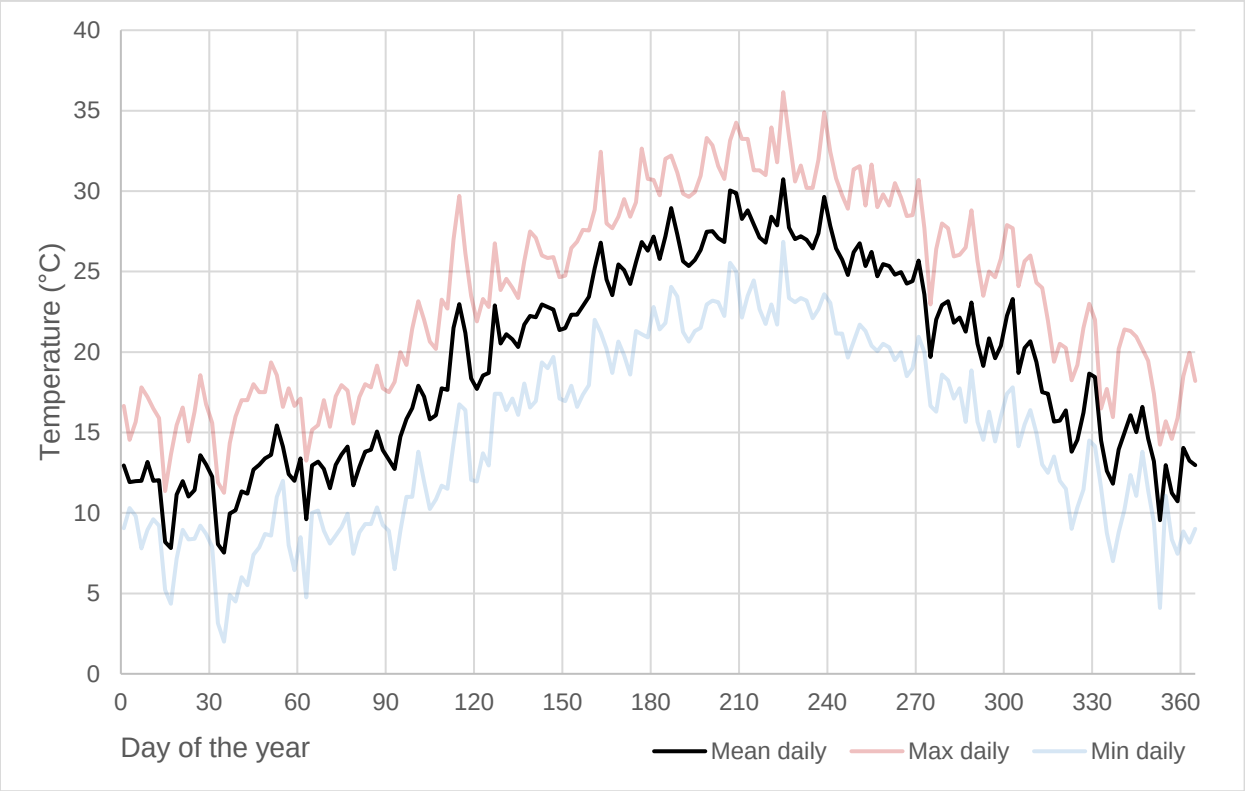

Figure 4-3. Average daily mean, maximum and minimum temperature in Larnaca, Cyprus (EnergyPlus weather data).

Relative humidity values are also influenced considerably by altitude and distance from the coast and are, to a large extent, a reflection of the air temperature differences because of the same reasons. During winter days and at nights through the whole year, relative humidity varies between 65 and 95%. Around midday in summer days it is significantly lower, reaching about 30% in the central pain while it can occasionally be as low as 15% (Department of Meteorology, 2018).

Figure 4-4 illustrates the evolution of average daily mean, maximum and minimum relative humidity (RH) through the year in Larnaca, which, as mentioned earlier, is a coastal city. From that graph one can conclude that, in reality there are is no significant seasonal fluctuation in average daily mean and maximum RH and the fluctuation is rather daily. The only seasonal trend that is clear is the increased average daily minimum RH in the summer months. Those values are, of course, average daily and do not illustrate the RH fluctuation within the day.

In order for the presence of RH within the course of a summer day to be presented, one can look at figure 4-5. There the hourly RH over a 10-day period in the middle of summer (10th to of July) is presented. It is obvious the RH has its peaks every twelve hours, around midnight, with values between 80 and 90%. The minimums also occur every twelve hours, around noun, with values between mainly 30 and 60 %.

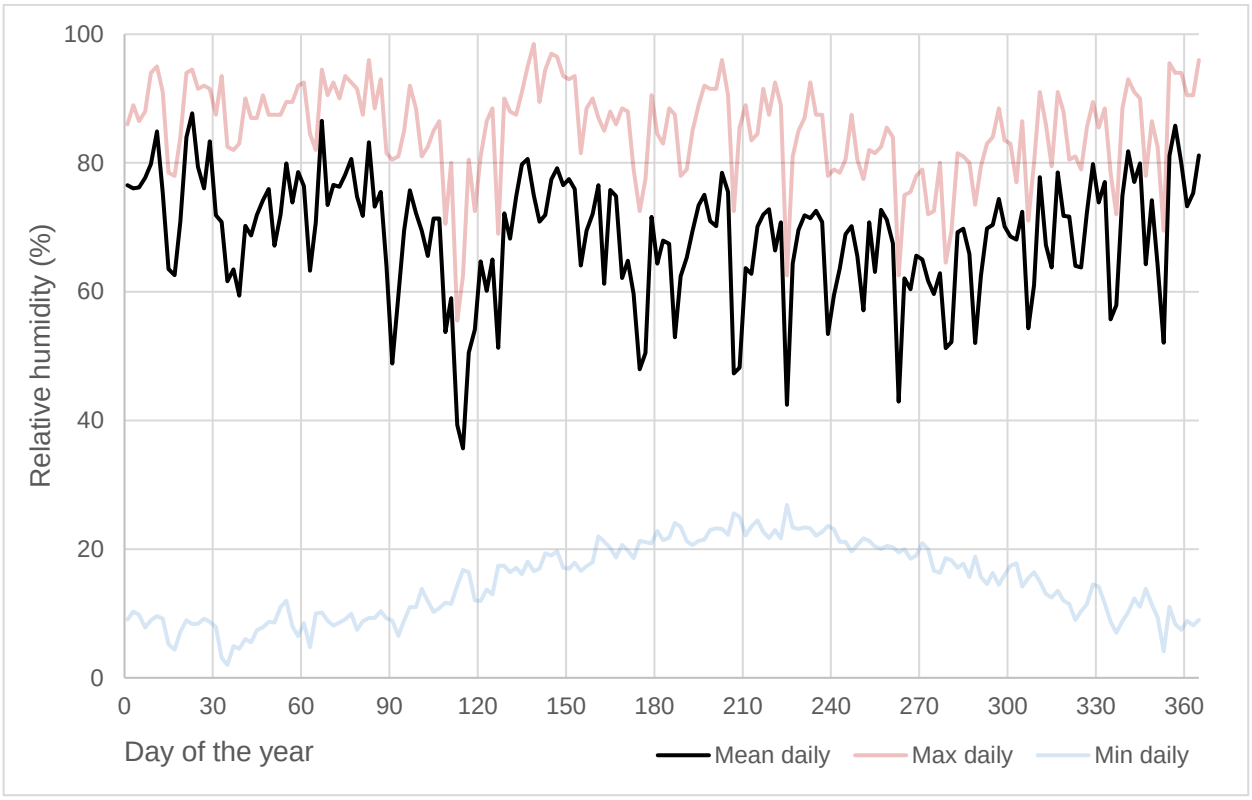

Figure 4-4. Average daily mean, maximum and minimum relative humidity in Larnaca, Cyprus (EnergyPlus weather data).

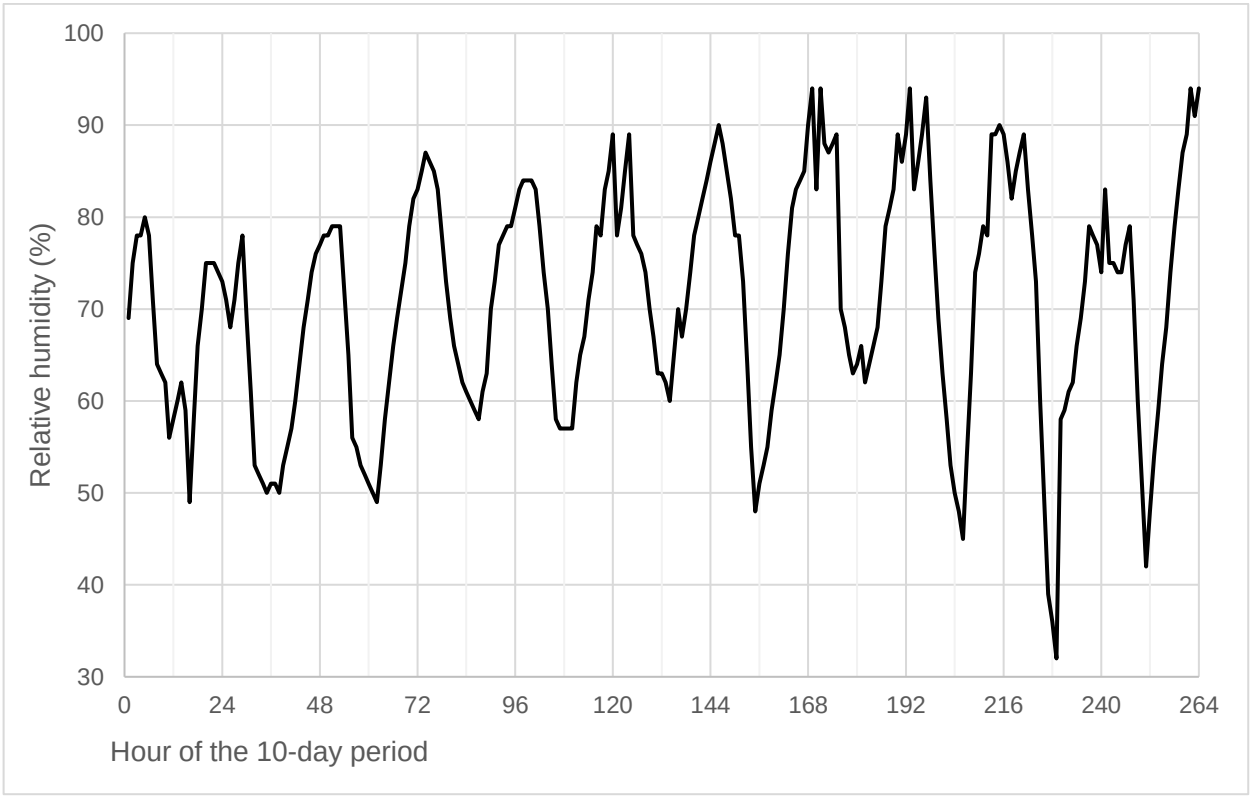

Figure 4-5. Hourly relative humidity for the period between 10 and 20 of June in Larnaca, Cyprus (EnergyPlus weather data).

4.2. Energy and dwellings

Cyprus, as an island, maintains a small isolated energy system which is heavily depended on imports to accommodate energy demand. In addition, before entering the European Union in 2004, Cyprus had no legislation nor regulations about the energy performance of buildings (Menicou *et al.,* 2015). Those factors highlight not only how important it is to initiate innovative energy saving methods, such as daytime radiative cooling, but also how high the energy saving potential is since the current building stock is 'energy-hungry'.

The total dwelling stock in Cyprus was, in 2011, around 420.000 residencies with the mean area per residency being approximately 153 m^2. Of them, 41% are detached houses, 14% are semi-detached houses, 8% are terraced houses, 29% are apartments and 8% are conventional dwellings in partly residential buildings as calculated by the Ministry of Energy, Commerce, Industry and Tourism (MCIT, 2013) and shown in table 4-2. Daytime radiative cooling could be a potential sustainable cooling method for detached, semi-detached and terraced houses as they have direct access to the sky. Those dwellings account together for 61% of the Cypriot dwelling stock.

Type	Amount	Percentage (%)
Detached	172 944	41.1
Semi-detached	59 050	14.0
Terraced	32 893	7.8
Apartments	123 557	29.4
Conventional dwellings in partly residential buildings	32 350	7.7

Table 4-2. Amount and percentage of each dwelling type within the total dwelling stock of Cyprus.

In the same MCIT report two reference existing residential buildings are identified. The first one is a three-bedroom detached house with only a ground floor and a building geometry of 16x15x2.8 m and the second one is three-bedroom detached house with a ground and a first floor and a geometry of 10x10x5.6 m.

Panayiotou *et al.* (2010) in their research about the Cyprus building energy performance methodology use three dwellings that are representative for the dwelling stock Cyprus and are in different climatic zones. The floorplans of them are shown in figures 4-6 to 4-8.

The Joint Research Centre of the European Commission in its 2017 report regarding the "Long-term strategy for mobilizing investments for renovating Cyprus national building stock" (Economidou et *al.,* 2017) states that in order to reduce the cooling demand which is significantly high in Cyprus due to its hot climate, passive cooling techniques and efficient cooling equipment should be used. In the same report it is mentioned that:

> *« While the extensive usage of solar thermal systems for the production of domestic hot water (DWH) makes Cyprus one of the worldwide leaders in the area, no other renewable energy technologies are widely diffused in the building stock in practice. »*

It should be noted that the absence of any passive cooling strategy in modern buildings comes in contrast with the extensive use of premature such strategies (e.g. natural ventilation and correct orientation) in vernacular architecture (Michael *et al,* 2017).

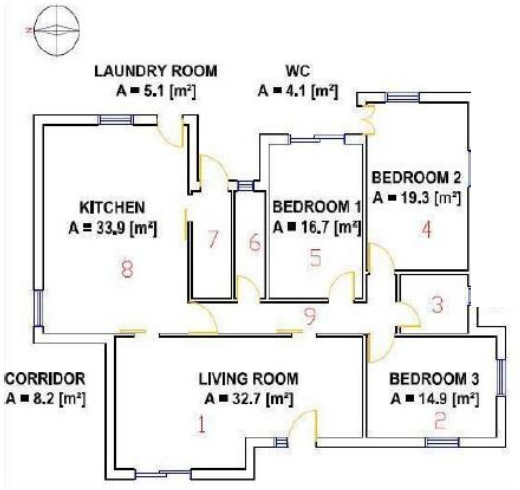

Figure 4-6. Floorplan of reference dwelling 1; detached building in Nicosia, low land zone (Panayiotou *et al,* 2010).

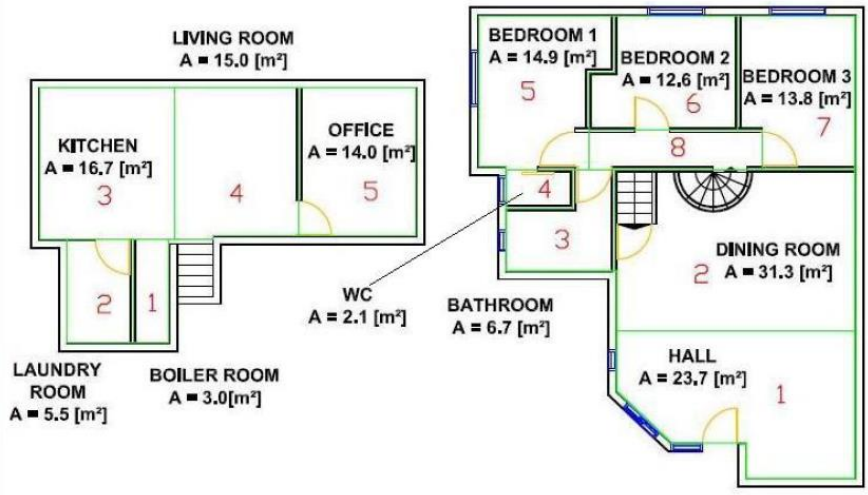

Figure 4-7. Floorplan of reference dwelling 2; detached building in Limassol, coastal zone (Panayiotou *et al.,* 2010). Ground floor is on left side and first floor on the ride side.

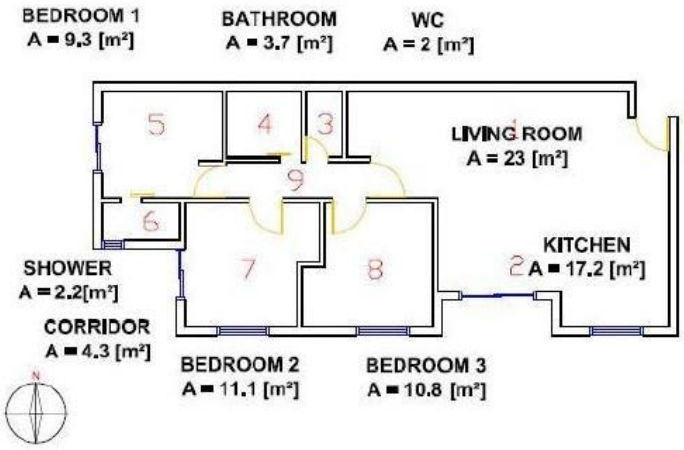

Figure 4-8. Floorplan of reference dwelling 3; apartment in Dali, semi-mountainous zone (Panayiotou *et al.,* 2010).

The climate characteristics of the island, mentioned in the previous subsection, lead to cooling energy demands for houses that are significantly higher than the respective ones for heating. It is estimated (MCIT, 2013) that energy required for cooling accounts for between 50% and 74% of the total energy requirements while energy required for heating accounts for 16.5% to 23.6%. Also interesting is that the average household chooses to cool, mainly by the use of air-conditioning systems, only less than a third of the mean area of its dwelling, that usually corresponds to the bedrooms and the living room.

According to the MCIT decree of 2009, the minimum energy performance requirements as they apply for new buildings and buildings with a surface larger than 1000 m^2 under major renovation are:

- Maximum U-value for roof: 0.75 W/m^2K
- Maximum U-value for wall: 0.5 W/m^2K
- Maximum U-value for floors in contact with external environment: 0.75 W/m^2K
- Maximum U-value for floors in contact with closed unheated space: 2.00 W/m^2K
- Maximum U-value for windows: 3.80 W/m^2K
- Average U-value (for residential buildings): 1.30 W/m^2K
- Average U-value (for non-residential buildings): 1.80 W/m^2K
- Energy performance certificate with at least B energy class
- Solar heater for hot water supply (only for residential buildings)
- Providence for installing a system that generates power from renewable energy systems (RES)

Existing dwellings, in general, to not meet those criteria and thus, tend to consume very high amounts of energy to satisfy their main electricity need, which is cooling. The implementation of a passive cooling method that can also utilise their existing high consuming split air-conditioners could result in serious energy savings for a considerable percentage of the Cypriot dwelling stock.

5

Cooling system and case-study dwelling

A scientific approach is followed in this research in order to investigate the applicability of daytime radiative cooling to a conventional dwelling in Cyprus. To do so several properties of a radiative cooling device are investigated, and not specific coolers as proposed in recent academic papers.

The system which utilises the radiative cooling gains is one able to operate in multiple modes, depending on the current demand and supply, and uses a stratified water tank in order to store thermal energy. Also, is able to integrate existing active cooling installations and satisfies the specific needs of a dwelling in Cyprus.

The dwelling which is used as a case study is one identified as a conventional Cypriot dwelling. The selected case study follows not only the geometrical trends of the dwelling stock but also assumes that the trends relevant to cooling habits of people are followed; that is the zones of the building that they choose to cool.

5.1. Radiative device

Since this research has a mostly scientific approach and not a practical one, not a specific radiative cooler from the ones presented in Chapter 2 is selected in order to be the apparatus producing cooled energy. Instead, several properties of the cooler are assumed and later altered so that their significance is investigated.

Initially it seems that the most important property of the cooler is the solar reflectance of it as the higher it is, the maximized the cooling output becomes. Another important property is the thermal resistance between the energy transfer medium and the outside environment. In this project no cost analysis is made, and research is focused to the characteristics of the cooler and the efficiency of it and the overall system proposed.

5.2. The proposed multi-modal system

The cooling system proposed is one able to satisfy the specific needs of the residencies in Cyprus and be integrated within the type of cooling systems generally used in the dwellings. This system is inspired by and is similar to the one proposed by Zhang *et al.* (2018), described in Chapter 3. The main advantage of this system that makes it suitable for the case of Cyprus is that it can integrate existing split air conditioning units that are already found in the vast majority of Cyprus' residencies.

Various similarities exist between the proposed system and the one designed by Zhang *et al.* (2018). In both cases, water is used as an energy transfer liquid as an energy transfer liquid while a water tank is used as a storage facility for the cooled water. Also, both the systems use an active cooling method to supply the space with cooled energy when there is not a sufficient amount of energy produced by the passive cooler.

The proposed system consists of four main components that are illustrated in their most simple form in figure 5-1, where all components are operating. Those components are:

1. A passive cooler
2. An active cooler
3. A water buffer tank
4. A heat exchanger of the room or space cooled

As can be seen in the illustration, the water in the tank doesn't have a uniform temperature. The cold water tends to sink in the bottom while the hot water tends to ascent in the top. This is the process of water stratification in thermal energy storage (TES) tanks as described in Chapter 3. The passive and active coolers exchange water, thus heat with the tank. They both send cooled water to the bottom of the tank while they receive hot water from the top of the tank. The heat exchanger of the room receives cooled water from the bottom of the tank while it sends back hot water to the top of the tank.

Important differences exist between the proposed system and the one of that it was inspired from. The main one is that in the former the cooled water from the passive cooler is send first to the water tank and then to the heat exchanger. In contrast, in the latter the water is provided directly to the cooling coil without passing through the water tank. A second fact that differentiates the two systems

is that the system of Zhang *et al.* (2018) the active cooling equipment doesn't exchange any water with the storage tank while in the proposed system active cooling provides the storage tank with cooled energy to be further transferred to the heat exchanger of the cooled space. Is worth noting that the active cooler is never used to only charge the water tank.

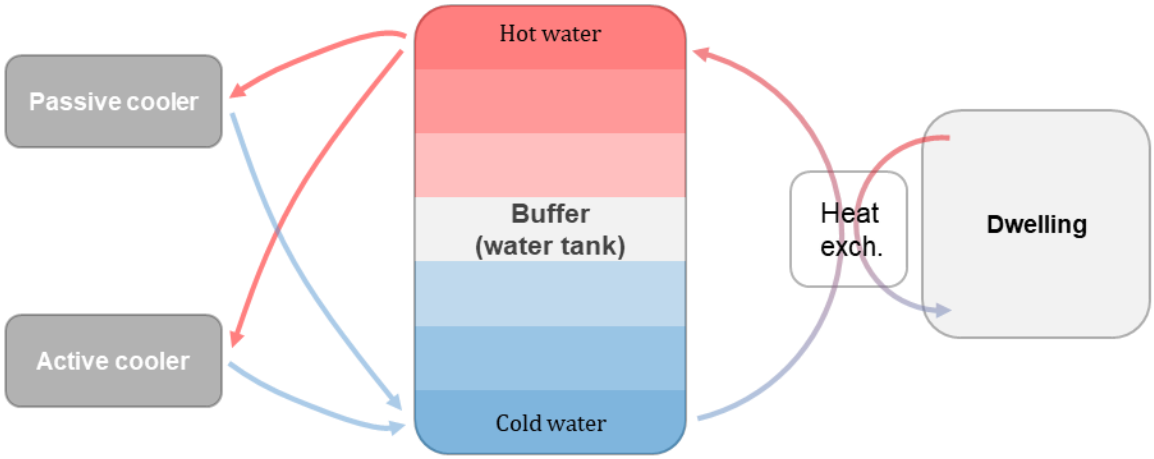

Figure 5-1. A simplified diagram of the proposed hybrid cooling system (Mode 1).

5.3. Operation modes

The proposed system operates in a number of modes depending on the capability of the passive cooler and on the cooling load of the dwelling at any instance.

The system is on operational mode 1, which is already illustrated in figure 5-1, when all elements of the system are operating. That is the case when the passive cooler and active cooler operate simultaneously to provide the dwelling with cooled energy. This happens when the dwelling has a cooling load that is not covered by the supply of the passive cooler.

The proposed system is on mode 2, shown in figure 5-2, when the passive cooler provides the dwelling with cooled energy that is enough to cover its cooling needs. In this mode, the excess energy produced by the radiative cooler is saved on the storage tank while the active cooler is not operating.

When there is demand by the dwelling but energy from the passive cooler is totally unavailable, for example during the night or on a cloudy day, and the energy already stored in the tank is not sufficient, the active cooler operates to send cooled water to the heat exchanger. This is operational mode 3 and is illustrated in figure 5-3.

It is possible that there is cooling demand from the dwelling and the energy from the passive cooler is not available, but the energy already stored in the water tank is enough to cover the demand. Then both the passive and active coolers are not operational, and the only exchange of water takes place between the water tank and the heat exchanger. This is mode 4 and can be seen in figure 5-4.

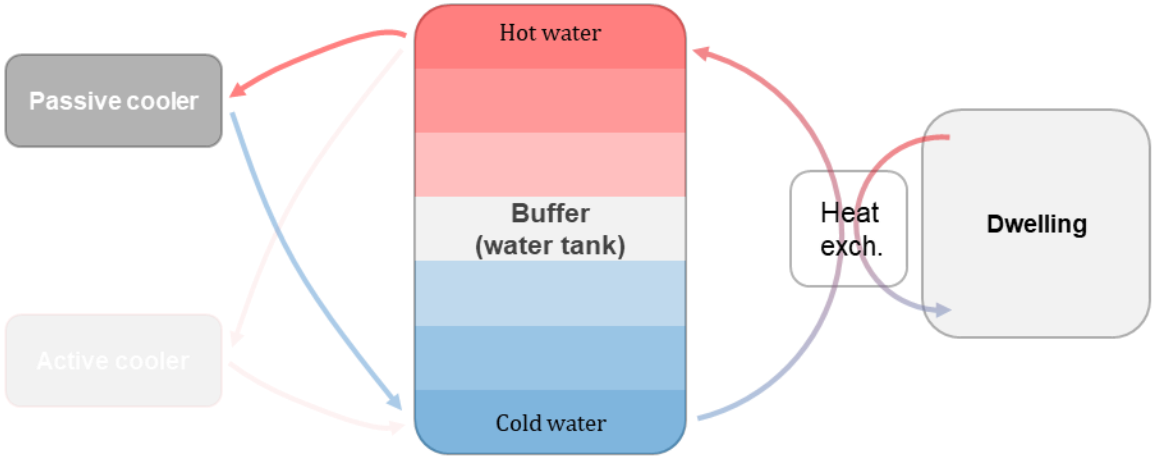

Figure 5-2. Mode 2 of the proposed system; when only the passive cooler provides cooled energy.

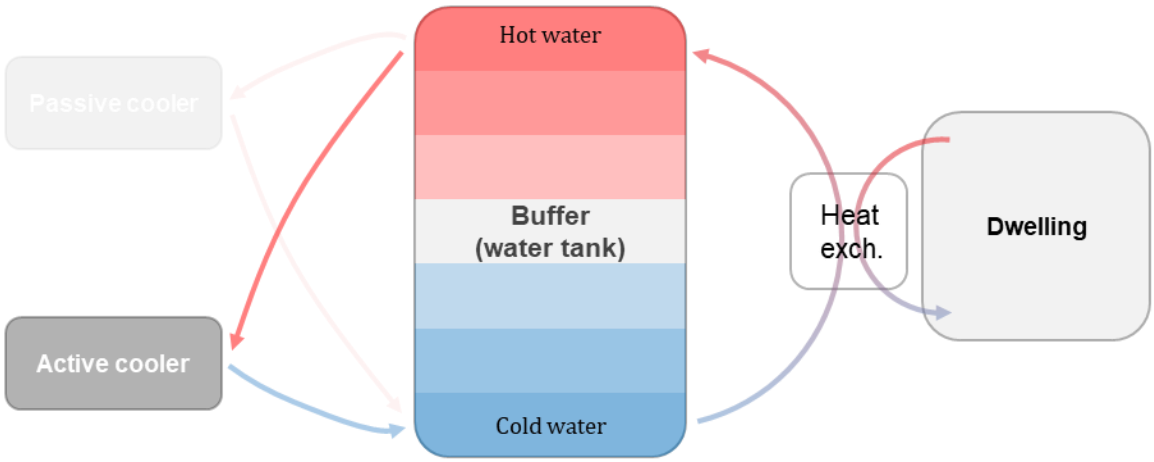

Figure 5-3. Mode 3 of the proposed system; when the active cooler covers the cooling demand.

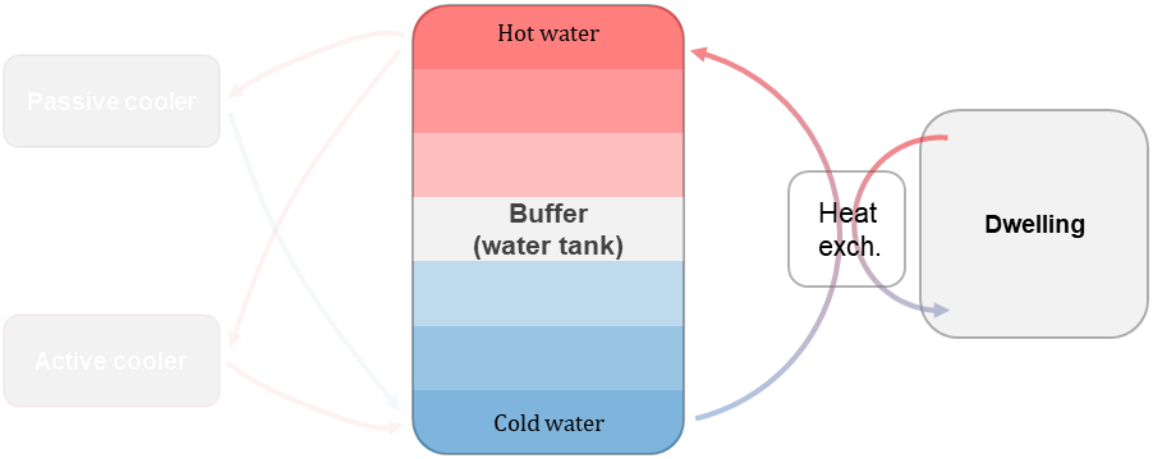

Figure 5-4. Mode 4 of the proposed system; when the energy stored in the water tank is enough to cover the dwelling cooling demand.

In mode 5 of the proposed system, cooling supply from the passive cooler is available but the dwelling has no cooling demand. In that case, illustrated in figure 5-5, the energy from the passive cooler is used to only charge the water tank.

Last is mode 6 in which there is no supply from the passive cooler and no demand from the dwelling. In that case, no component of the system is operating, as illustrated in figure 5-6.

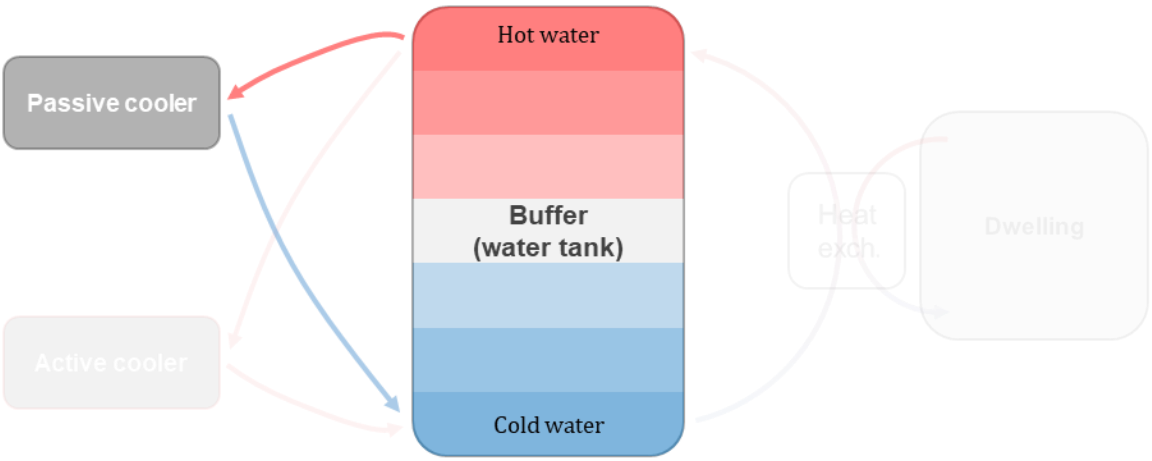

Figure 5-5. Mode 5 of the proposed system; when the energy supply from the passive cooler is used to only charge the water tank.

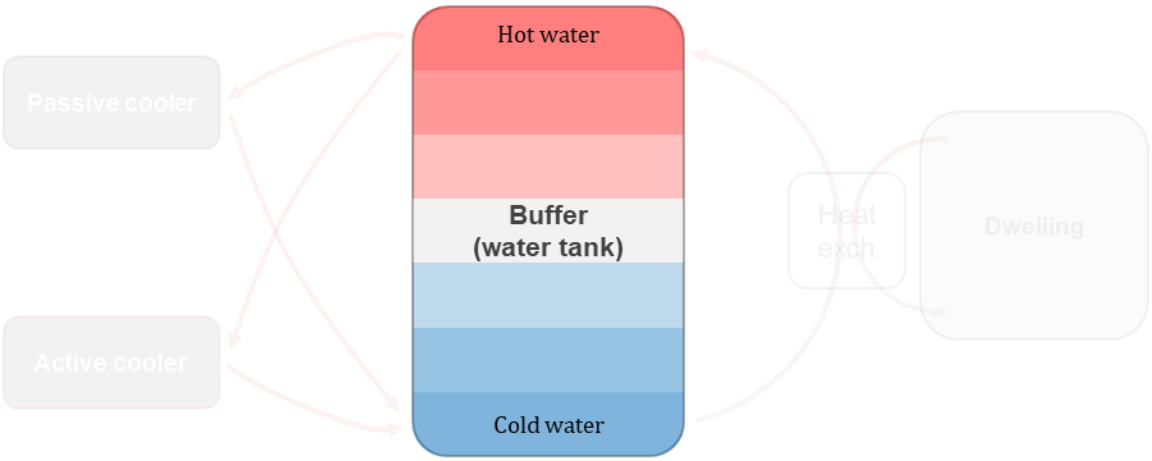

Figure 5-6. Mode 5 of the proposed system; when no component is operating.

5.4. Case study dwelling

As mentioned in previous parts of this document, the capabilities of the proposed passive cooling system are examined for a dwelling in Cyprus whose Mediterranean climate results in dwellings having very high cooling demands. For this reason, a dwelling that is considered conventional for Cypriot standards has been selected.

The dwelling chosen consists of only one floor and is the first of the dwellings considered representative for the Cypriot dwelling stock according to Panayiotou *et al.* (2010), also presented in Chapter 4 (figure 4-6). The main reason this dwelling is chosen is because its area almost equal to the average mean area of Cypriot dwellings; 153 m^2 (MCIT, 2013). The floor plan of the dwelling is presented in figure 5-7. Table 5-1 lists the gross floor area of each room and the length of its façade and the window-to-wall ratio in each direction. In addition, it is indicated whether each room is considered to be cooled or no. The rooms in which cooling takes place, for simulation purposes, are the kitchen, the three bedrooms and the living room.

The typology, structure and heating and cooling equipment of the case study dwelling follow the trends of the average dwelling in Cyprus. The floor height is 3 m while there are windows of two sizes. Larger windows in bedrooms, living room and kitchen have a length of 1.85 m and height of 1.2 m. Smaller windows in the WC and the bathroom have a length of 0.5 m and a height of 0.6 m. The doors have a height of 2.2 m, with the main external one having a length of 1.05 m in contrast to the internal ones whose length is 0.9 m. The balcony doors in the living room and in bedroom 1 have a length of 1.85 m. According to Panayiotou *et al*. (2010), the dwelling is a detached building built with conventional insulated brick walls (U-value=0.511 W/m^2 K) while its roof is not insulated (U-value=2.5 W/m^2 K). It is equipped with several split air conditioners to cover its cooling demands while it doesn't have a central heating system.

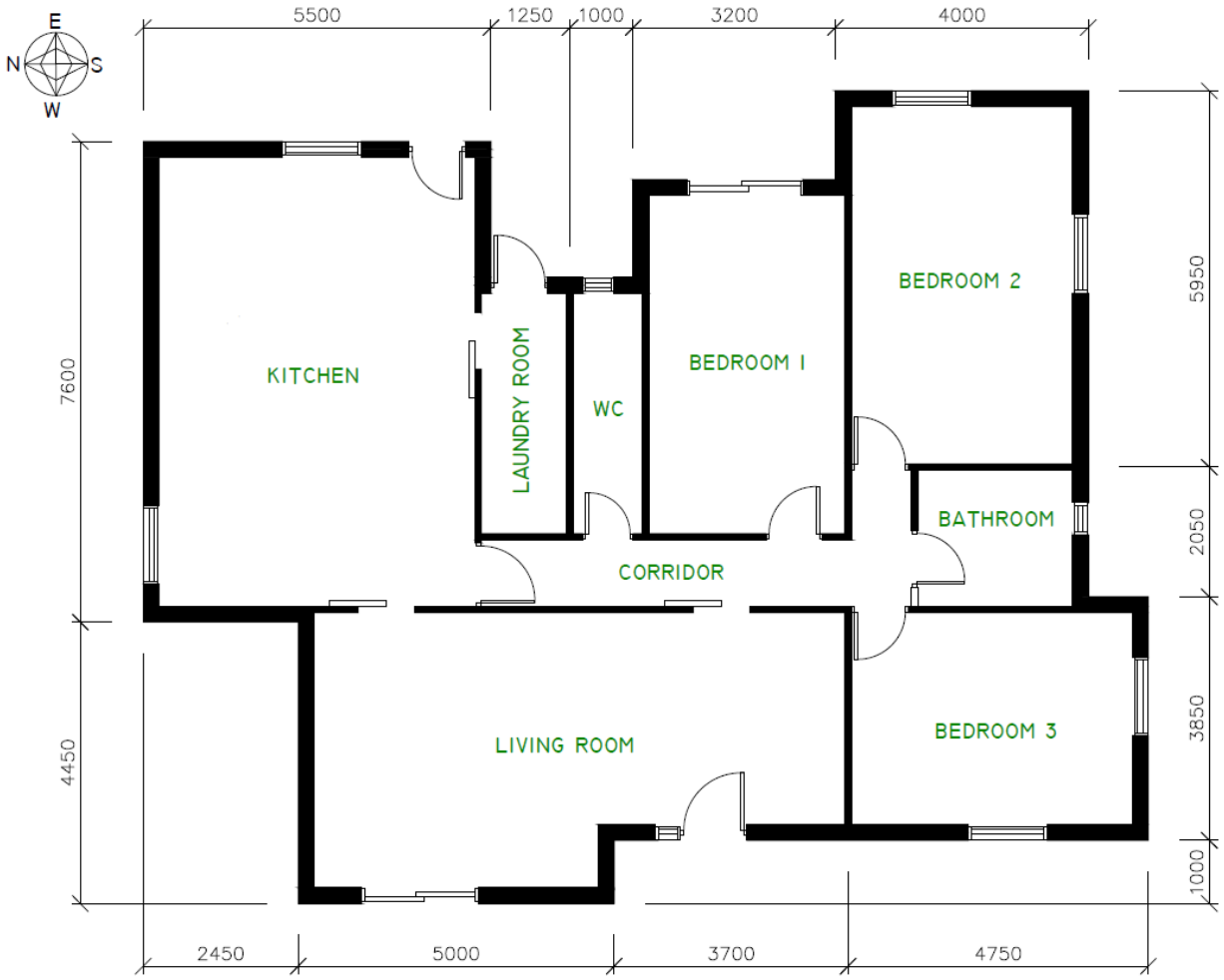

Figure 5-7. The conventional dwelling to be used as a case study (dimensions in mm).

Room	Area	Façade length (m)				Window-to- wall ratio				Cooled area
		North	East	South	West	North	East	South	West	
Kitchen	37.4	7.60	5.50			7%	27%			✓
Bedroom 1	17.4		3.20				74%			✓
Bedroom 2	21.6		4.00	5.95			14%	9%		✓
Bedroom 3	16.9			3.85	4.75			15%	12%	✓
Living room	35.2	4.45		1.00	8.70	0%		0%	39%	✓
WC	4.3		1.00				11%			
Laundry room	5.6	1.25					112%			
Bathroom	5.3			2.05				5%		
Corridor	8.8									

Table 5-1. The area, façade length and window-to-wall ratio of the rooms of the case study dwelling.

6

Simulation model

The model designed to test the capabilities of the proposed passive cooling system as well as its sensitivity to several parameters, is made using Matlab and Simulink. In addition, DesignBuilder is used to identify the cooling profile of the investigated case study dwelling and provide the other software with required data.

The modelling of the dwelling in DesignBuilder is based on three facts. The first is the geometrical characteristics obtained by the original source that referenced the dwelling as conventional for the Cypriot stock. The second is the limited characteristics provided by the same source relevant to the properties of the structure elements of the dwelling. The last relates to the habits followed for the majority of dwellings in Cyprus.

Matlab and Simulink work in parallel, with Simulink taking Matlab values as inputs. Matlab's environment is textual while Simulink's is schematic. The foundation of both the software's input is the equations that govern the physics of the several elements of the system; namely the passive cooler, the active cooler, the water storage tank and the heat exchanger.

6.1. DesignBuilder model

The first step of the simulation of the dwelling is to model it in the DesignBuilder software. This is done in order for the cooling profile of the dwelling, which is its cooling demand per time step, to be calculated and subsequently used in the simulations in Matlab and Simulink. A 3D visualised version of the model from DesignBuilder is shown in figure 6-1.

For conducting the simulation, the location template is set to be 'Larnaca Airport', the only available location templated for Cyprus. The coordinates of the location are: 34.88 N and 33.63 E.

Each room of the dwelling consists of a separate zone in the DesignBuilder model and, depending on the use of the room, has different activity characteristics. For each room, a DesignBuilder template was used, as can be seen in figure 6-2 and table 6-1. Each template has different values for activity parameters such us occupation density, schedule and office equipment. For every zone the cooling setpoint temperature is set to be 25 °C while the cooling operation schedule is set to be 'On 24/7'. In Matlab and Simulink the average operative temperature of all the cooled zones is used in the calculations.

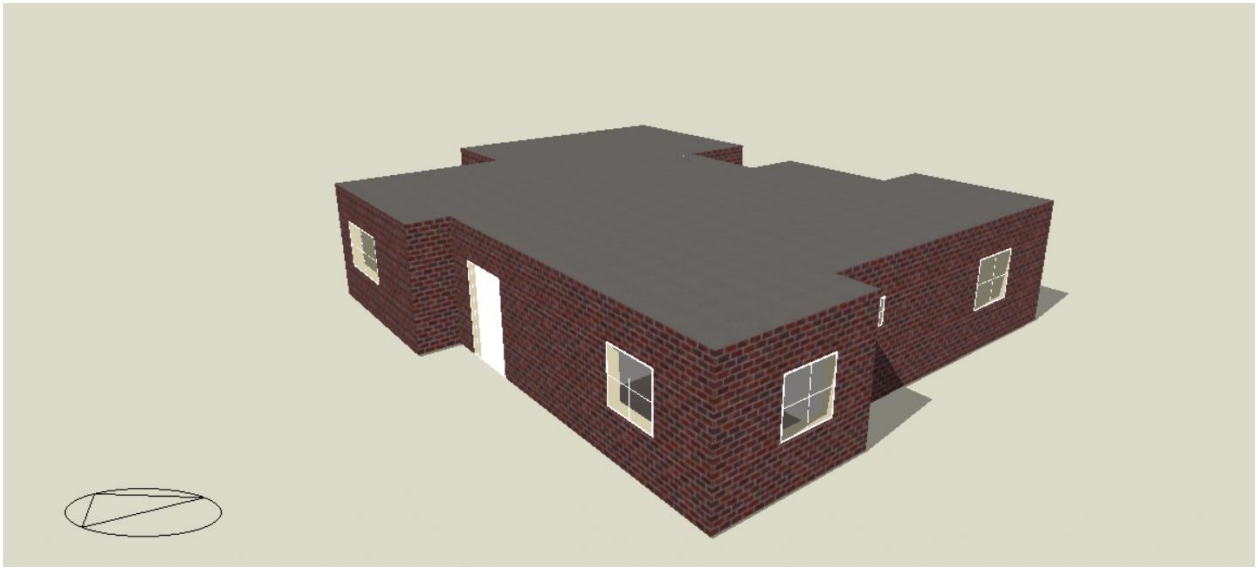

Figure 6-1. A 3D visualisation of the DesignBuilder model.

To be in line with the thermal transmittance characteristics of the external walls and the roof as defined for the specific dwelling by Panayiotou et al. (2010), specific materials are selected for these two construction elements. For the external walls, a four-layer construction consisting of outer brickwork, extruded polystyrene, inner brickwork and gypsum is selected. Using those layers, the U-value of the external walls equals 0.512 W/m^2K. the respective value for the roof, that is made of three layers of asphalt, concrete and gypsum, is 2.545 W/m^2K. Cross sections of both the structural elements are presented in figures 6-3 and 6-4. It is worth noting that while the outermost layer of the roof seems to be a dark colour asphalt, its solar absorptance has been changed to a lower value (0.600) in order to resemble the white flat roofs that is the norm amongst flat-roof buildings in Cyprus. In addition, since in the publication from which the conventional dwelling was taken there are no details about the thermal mass and the R-value of the walls there is no way to know whether

those construction elements correspond to the ones of the original dwelling. It is for that reason that no comparison is made between the results obtained in the simulation process and the ones provided in the research of Panayiotou *et al.* (2010).

Room	Activity template	Occupancy density (people/m²)
Kitchen	Domestic kitchen	0.0237
Bedroom 1	Domestic bedroom	0.0229
Bedroom 2	Domestic bedroom	0.0229
Bedroom 3	Domestic bedroom	0.0229
Living room	Domestic lounge	0.0188
WC	Domestic toilet	0.0243
Laundry room	Domestic circulation	0.0155
Bathroom	Domestic bathroom	0.0187

Table 6-1. Activity template and occupancy density used for each room in DesignBuilder model.

Figure 6-2. The several zones of the dwelling in the DesignBuilder model and the activity template used in each one.

Figure 6-3. Cross-section of the external walls structure, from DesignBuilder.

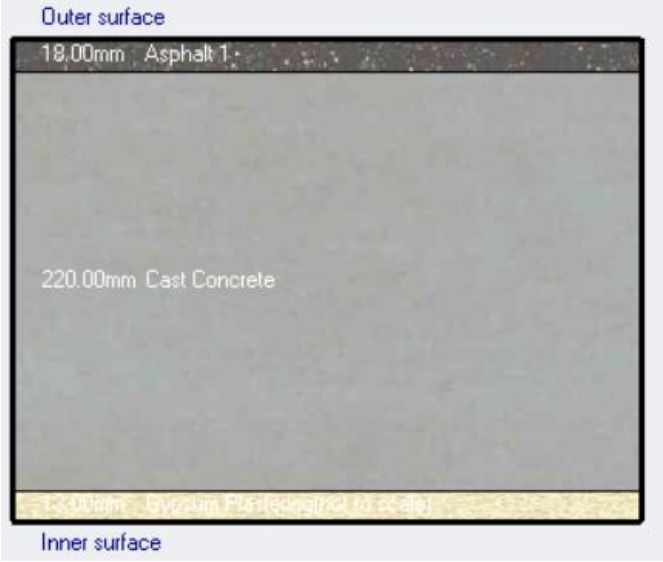

Figure 6-4. Cross-section of the flat roof structure, from DesignBuilder.

One last parameter that was altered in DesignBuilder is the one relevant to the shading of windows. In particular, blinds with high reflectivity are used which are located on the inside of the windows. This corresponds better to the situation in the majority of houses in Cyprus.

6.2. Physics

The system which, as said earlier, consists of a passive daytime radiative cooler, an active cooler, a water buffer tank and a heat exchanger, is governed by a set of equations. Those describe how each component works and what parameters are taken into account for each and also links the several components of the system with each other. This set of equations is given in the following paragraphs.

6.2.1. Daytime radiative cooler

The cooling transfer rate of the DTC is calculated using equation 13. This equation consists of four parts summed together and multiplied by the surface area of the cooler. Only one part is responsible for the production of cooling power while the remaining three reduce it.

The first part of the equation represents the absorbed shortwave solar power. The parameters that are used to calculate this size are the incoming shortwave radiation and the transmission coefficient for shortwave radiation of the DTC.

The second part of the represents the absorbed longwave solar power. The factors that influence the amount of this power are the incoming longwave solar radiation, the transmission coefficient for longwave radiation and the longwave emissivity coefficient.

The power radiated out by the cooler is the third part of the equation. For calculating the size of this power, the transmission coefficient for longwave radiation, the longwave emissivity coefficient and the average temperature of the water in the DTC, in degrees Kelvin, must be known.

The fourth, and final, part describes the combined convective and conductive heat losses of the cooler. The effective heat transfer coefficient is detrimental for the size of these losses. The other required values are the average temperature of the water in the DTC, in degrees Celsius, and the outside dry-bulb temperature of air.

The heat transfer rate has a negative sign when cooling power is transferred. This means that out of the four parts of the equation, the only one that contributes positively to the cooling rate is the third one which has a negative sign. In order to achieve the maximum possible efficiency of the DTC, this part should be maximised while the other three parts should be minimised.

$$P_{cool,dtc} = A_{dtc} \cdot [\ (P_{sw} \cdot \tau_{sw} + P_{lw} \cdot \tau_{lw} \cdot \varepsilon_{lw} - \tau_{lw} \cdot \varepsilon_{lw}\ \cdot \sigma \cdot\ T_{dtc,mean}{}^{4} + H_{dtc} \cdot (\theta_{air} - \theta_{dtc,mean})\ ] \quad (13)$$

Where:

$P_{cool,dtc}$	=	Cooling power of the daytime cooler, W
A_{dtc}	=	Surface area of the daytime cooler, m^2
P_{sw}	=	Incoming shortwave radiation, W/m^2
τ_{lw}	=	Transmission coefficient for shortwave radiation
P_{lw}	=	Incoming longwave radiation, W/m^2
τ_{lw}	=	Transmission coefficient for longwave radiation
ε_{lw}	=	Longwave emissivity coefficient
$T_{dtc,mean}$	=	Average temperature of the water in the cooler, K
H_{dtc}	=	Effective heat transfer coefficient, $W/m^2 K$
θ_{air}	=	Outside dry-bulb air temperature, °C
$\theta_{dtc,mean}$	=	Average temperature of the water in the cooler, °C

The average temperature of the water inside the DTC in degrees Celsius and in degrees Kelvin is calculated using the equations 14 and 15 respectively.

$$\theta_{dtc,mean} = \frac{\theta_{dtc,in} - \theta_{dtc,out}}{2} \quad (14)$$

Where: $\theta_{dtc,in}$ = Temperature of ingoing water to the cooler, °C

$\theta_{dtc,out}$ = Temperature of outgoing water from the cooler, °C

$$T_{dtc,mean} = \theta_{dtc,mean} + 273{,}15 \quad (15)$$

Equation 16 is a second equation for calculating the cooling rate of the DTC that associates the former with the specific mass flow rate of water through the cooler.

$$P_{cool,dtc} = A_{dtc} \cdot \dot{m}_{dtc,sp} \cdot c_w \cdot (\theta_{dtc,out} - \theta_{dtc,in}) \quad (16)$$

Where: $\dot{m}_{dtc,sp}$ = Specific mass flow of water through the cooler, kg/m^2/s

6.2.2. Heat exchanger

The heat exchanger provides cooling to the dwelling with a rate calculated using equation 17. The outgoing temperature of the exchanger, which equals the temperature of the incoming water from the exchanger at the top of the water buffer, is related to the efficiency of the exchanger and the existing temperature of the room it cools and is calculated with equation 18.

$$P_{cool,exch} = \dot{m}_{exch} \cdot c_w \cdot (\theta_{exch,in} - \theta_{exch,out}) \quad (17)$$

Where: $\dot{m}_{exch}$ = Mass flow of water through the heat exchanger, kg/s

c_w = Specific heat capacity of water, J/kg K

$\theta_{exch,in}$ = Temperature of ingoing water to the heat exchanger, °C

$\theta_{exch,out}$ = Temperature of outgoing water from the heat exchanger, °C

$$\theta_{exch,out} = \theta_{exch,in} + eff_{exch} \cdot (\theta_{room} - \theta_{exch,in}) \quad (18)$$

Where: eff_{exch} = Efficiency of the heat exchanger

θ_{room} = Air temperature of the room

6.2.3. Active cooler

The active cooler receives water from the top of the buffer tank at a temperature and sends water back to the bottom of the buffer tank at a temperature lowered by a certain amount of degrees as shown in equation 19. The cooling rate of the cooler is calculated using equation 20 that takes into consideration the mass flow rate of water through it and its ingoing and outgoing temperatures.

$$\theta_{act,out} = \theta_{act,in} - \Delta T_{act} \quad (19)$$

Where: $\theta_{act,out}$ = Temperature of outgoing water to the active cooler, °C
$\theta_{act,in}$ = Temperature of ingoing water to the active cooler, °C
ΔT_{act} = Water temperature drop in the active cooler, °C

$$P_{cool,act} = \dot{m}_{act} \cdot c_w \cdot (\theta_{act,out} - \theta_{act,in}) \quad (20)$$

Where: $P_{cool,act}$ = Cooling power of the active cooler, W
$\dot{m}_{act}$ = Mass flow of water through the cooler, kg/s

6.2.4. Water tank

The water buffer tank is modelized as a stratified water tank as explained in section 3.3. The water is divided into a number of layers, for which a node number is given. In addition, there are three nodes for the environmental temperature, and the temperature of the two incoming flows, from the coolers and the heat exchanger. Initially the thermal mass of each node is calculated using the equation 21.:

$$M = \frac{\rho_w \cdot c_w \cdot V_{tank}}{h_{node}} \quad (21)$$

Where: M = Thermal mass, J/K
ρ_w = Density of water, kg/m^3
V_{tank} = Volume of water tank, m^3
h_{node} = Haight of water layer, m

The conductivity values between q node and its adjacent note below is calculated using equation 22. The conductivity values between the bottom and the top nodes with the environment are given by equation 23while for the intermediate nodes, equation 24 is applied.

$$C = \frac{\lambda_w \cdot A_{tank}}{h_{node}} \quad (22)$$

Where: C = Conductivity, W/K
λ_w = Heat conduction coefficient of water, W/m K
A_{tank} = Surface area of the horizontal cross section of the tank, m^2

$$C = U_{tank} \cdot A_{tank} + U_{tank} \cdot 2\pi \cdot r_{tank} \cdot h_{node} \quad (23)$$

$$C = U_{tank} \cdot 2\pi \cdot r_{tank} \cdot h_{node} \quad (24)$$

Where:
- C = Conductivity, W/K
- U_{tank} = U-value of the water tank, W/m² K
- r_{tank} = Radius of the water tank, m

When the temperature of a node is lower than the temperature of the adjacent below node, the conduction equation 22 is altered into the equation 25. There an effective conductive coefficient for free convective mix is used instead of the normal heat conduction coefficient. This is so that the temperature differences between the two nodes are levelled out.

$$C = \frac{\lambda_{w,mix} \cdot A_{tank}}{h_{node}} \quad (25)$$

Where:
- C = Conductivity, W/K
- $\lambda_{w,mix}$ = Effective conductive coefficient for free convective mixing, W/m K

6.3. Matlab script

The script of the Matlab model is presented in Appendix A. There, the script for the elements of the model, which are the water tank, the daytime radiative cooler, the active cooler and the heat exchanger, is explained individually. In addition, there are small parts of the script related to the dwelling investigated and to the simulation time. The Matlab model works in parallel to the Simulink model.

In table 6-2, the main quantities entered in the script as input are given, along with some brief description for each one. It is worth mentioning that for some quantities variable values are used, as explained later.

Symbol	Value	Description
ρ_w	1000 kg/m³	Density of water
c_w	4280 J/kgK	Specific heat capacity of water
λ_w	0.6 W/mK	Heat conduction coefficient of water
r_{tank}	0.5 m	Radius of water tank
h_{tank}	1.50m	Height of water tank
U_{tank}	0.285 W/m²K	U-value of the water tank insulation
$\lambda_{w,mix}$	1000 W/mK	Effective conduction coefficient for free convective mixing of water
n_{tank}	10	Number of water layers in the tank

Symbol	Value	Description
A_{room}	110.2 m^2	Cooled area of the dwelling
A_{roof}	152.6 m^2	Area of the roof
$A_{dtc,per}$	40 %	Surface area of daytime cooler as a percentage of the roof area
H_{dtc}	0.05 W/m^2K	Effective heat transfer coefficient of the DTC
τ_{sw}	0.05	Transmission coefficient for shortwave radiation of DTC
τ_{lw}	0.95	Transmission coefficient for longwave radiation of DTC
ε_{lw}	1.00	Longwave emissivity coefficient for the cooled surface of the DTC
$\dot{m}_{dtc,sp}$	0.003 $kg/m^2/s$	Specific mass flow rate of water through the DTC
ΔT_{dtc}	2 °C	Minimum required temperature between the temperature at the top of the buffer tank and the DTC
ΔT_{act}	8 °C	Water temperature drop in the active cooler
eff_{exch}	0.75	Efficiency of the heat exchanger

Table 6-2. the reference values for the quantities entered as input in the Matlab script.

For practical reasons, the simulations take place only for the summer months of the year during which the cooling demand occurs. For that reason, the simulation start time is set to be 10.368e6 seconds and the simulation end time is set to be 26.265e6 seconds. These numbers correspond respectively to the start of April and to the end of October.

6.4. Simulink model

The textual scrip explained in Appendix A is the first part of the simulation model with the second one being the Simulink model. This model works in parallel with the Matlab script by which it takes several values as inputs. Data are also imported to Simulink from an Excel file that includes the weather data for the investigated location and the DesignBuilder simulation data for the dwelling under investigation. The Simulink model created consists of nine set of blocks that represent input of data, define the temperature and the volumetric rate of water flows in and out of the components of the system and describe the several processes that take place in relevance to the four components of the system. For the latter, a separate subsystem for each one is created.

Two very important aspects of the Simulink model are the control mechanisms for the passive and active coolers which dictate when each of the coolers operates.

Regarding the daytime passive cooler, it provides water to the tank only if its outgoing temperature of water is lower by a certain amount of degrees from the temperature at the top of the water tank. That is to ensure that the cooler always provides cold energy to the water tank when it operates.

For the active cooler to be operative, two criteria must be satisfied:

1. The ingoing temperature of the heat exchanger should be close to a setpoint temperature. This is designed in Simulink using a ‘relay’ block.

2. The cooling power of the heat exchanger, which is equal to the cooling demand of the dwelling, should be lower than zero. This means that there is no possibility for the active cooler to operate to only charge the water tank.

When the active cooler is operative, its cooling rate equals the current cooling demand hence the active cooler always operates on its maximum capacity. When non operative, its cooling rate and mass flow equal zero.

The Simulink model, as well an analysis of what each set of components calculates, is described in depth in Appendix B.

7

Simulation output

The simulation in DesignBuilder providesthe heating and cooling load of the case-study dwelling. As expected, the cooling load is significantly higher than the respective heating because of the hot climate of Cyprus.

In order to investigate further the system designed, a number of parameters that could potentially influence the results are identified. Also identified is a base case with a constant set of values for the otherwise variable parameters that gives some initial results of the system and is used to compare results in the sensitivity analysis.

For the sensitivity analysis, several values are investigated for each parameter. Graphs and comments highlight how significant or insignificant is each parameter for the overall efficiency of the system.

Varied analysis investigates a smaller number of parameters and a smaller number of valuesfor each. All the unique combinations are simulated and for each parameter the results are presented individually to illustrate the trends followed when a specific value is used.

7.1. DesignBuilder

As mentioned earlier, the first step in the simulation process is to derive the cooling profile of the case study dwelling, from DesignBuilder. In the simulation only the cooled zones are included, which are the kitchen, the three bedrooms and the living room, and the intervals are set to be annual, monthly, daily, hourly and sub-hourly. The results are normalised by area and the area considered is the occupied area which includes only the floor areas of the cooled zones. It should be noted that the total occupied area for the simulation is 110.2 m^2, which does not equal the total floor area of the cool zones as presented in table 5-1 because the area used here is net, thus does not include the thickness of external and internal walls.

The normalised cooling load, including zone heating, sensible cooling and total cooling, for the four intervals is presented in the figures 7-1 to 7-4. Figure 7-1 provides a very clear idea of the total cooling requirement of the dwelling for the period of the whole year. The total cooling load equals 76232 Wh/m^2 which when multiplied by the occupied area of the cooled zones results in an annual cooling load of 8400 kWh. From the same figure, it is also obvious that the cooling requirement of the dwelling is much higher than its respective heating.

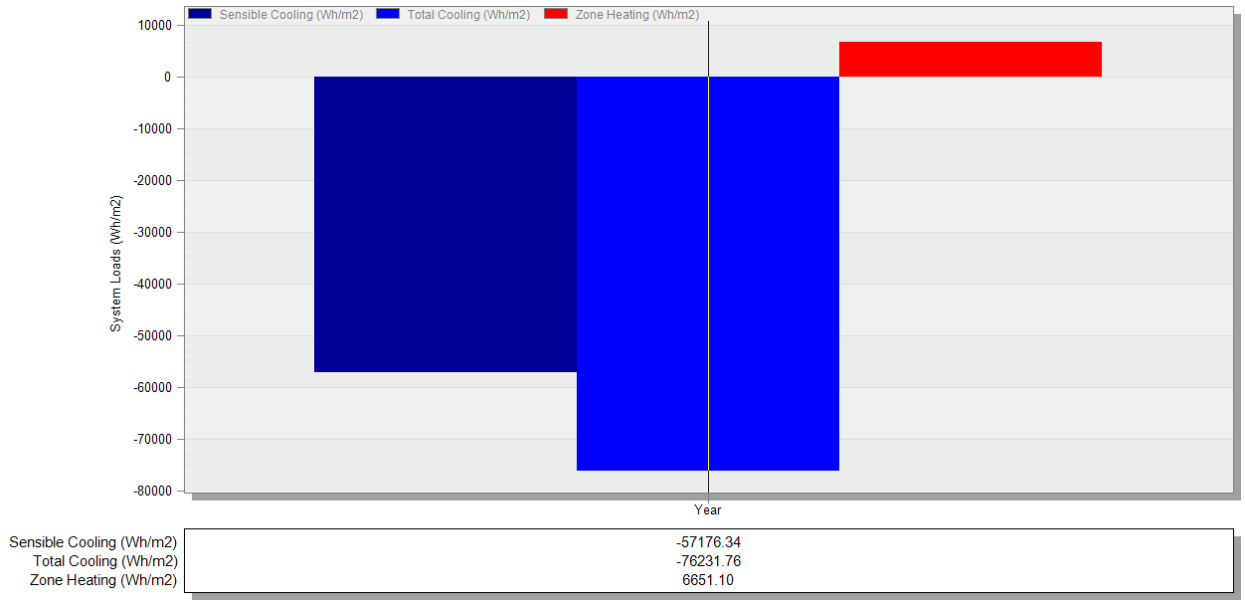

Figure 7-1. Annual system loads of the dwelling, from DesignBuilder.

Interpreting the results of figures 7-2 to 7-4, one can easily understand that there is great fluctuation of the cooling, and heating load, through the duration of year and of the day. The hottest months of the year, which are August and July, experience the largest cooling loads while the need for cooling reduces significantly during nighttime as a result of the absence of solar loads. The latter fact is reinforced by figure 7-5, where a zoomed version of the loads on a typical summer day are presented.

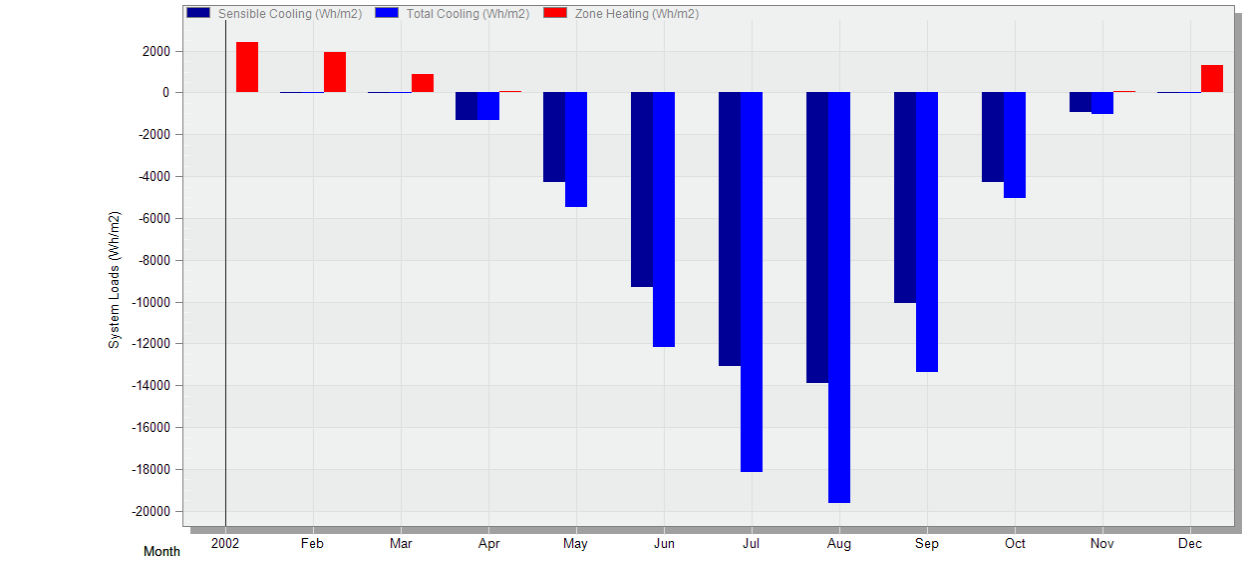

Sensible Cooling (Wh/m2)	0.00	-1.18	-18.58	-1309.17	-4268.49	-9294.64	-13088.82	-13893.54	-10086.89	-4300.40	-913.18	-1.44
Total Cooling (Wh/m2)	0.00	-1.34	-19.36	-1329.94	-5486.71	-12153.09	-18163.31	-19613.53	-13354.34	-5070.65	-1038.05	-1.44
Zone Heating (Wh/m2)	2390.88	1947.84	882.27	52.54	0.00	0.00	0.00	0.00	0.00	0.00	62.50	1315.06

Figure 7-2. Monthly system loads of the dwelling, from DesignBuilder.

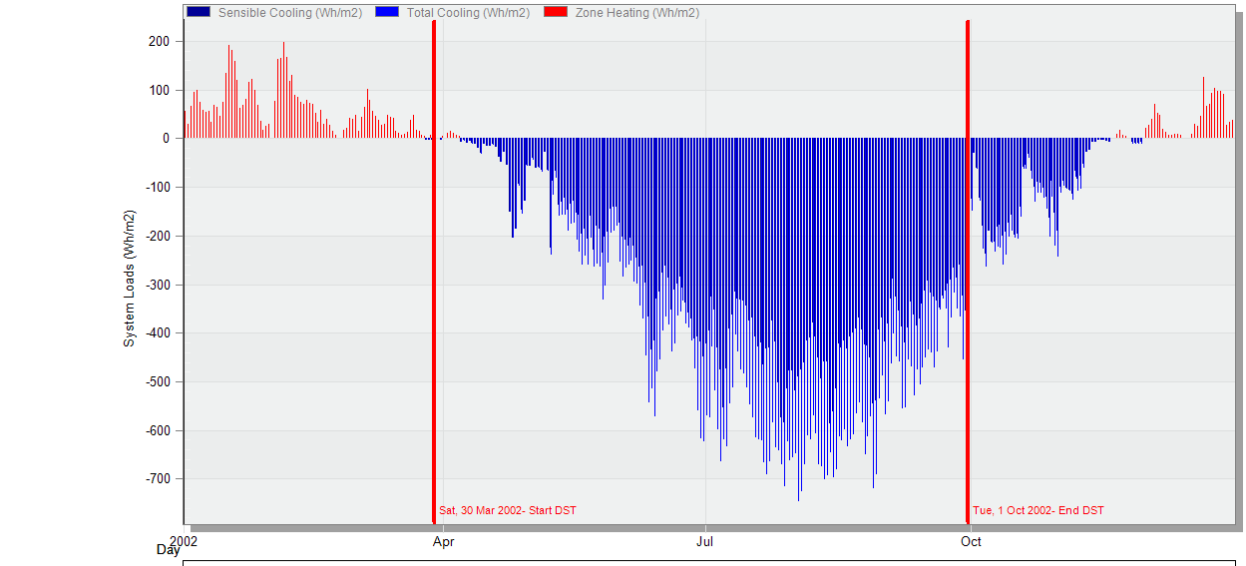

Sensible Cooling (Wh/m2)	0.00	0.00	-9.06	-130.01	-330.47	-369.27	-432.60	-323.59	-90.53	-7.44
Total Cooling (Wh/m2)	0.00	0.00	-9.30	-156.65	-480.21	-573.09	-632.50	-330.30	-112.56	-11.19
Zone Heating (Wh/m2)	163.76	55.46	0.00	0.00	0.00	0.00	0.00	0.00	0.00	0.00

Figure 7-3. Daily system loads of the dwelling, from DesignBuilder.

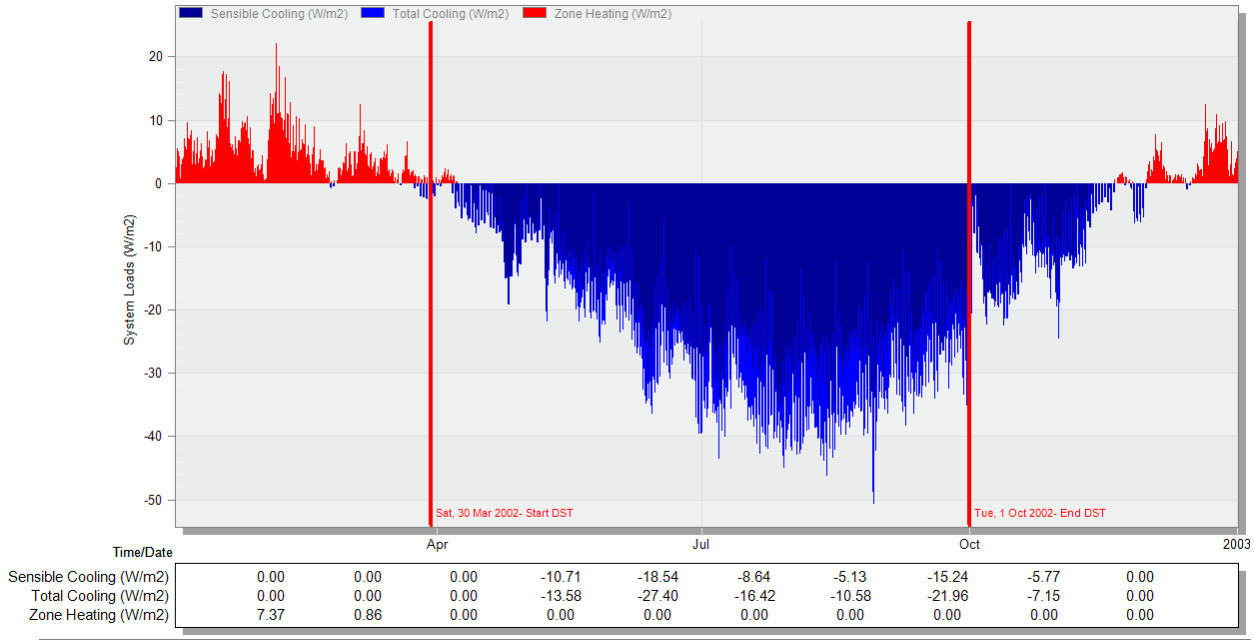

Time/Date	Apr			Jul			Oct			2003
Sensible Cooling (W/m2)	0.00	0.00	0.00	-10.71	-18.54	-8.64	-5.13	-15.24	-5.77	0.00
Total Cooling (W/m2)	0.00	0.00	0.00	-13.58	-27.40	-16.42	-10.58	-21.96	-7.15	0.00
Zone Heating (W/m2)	7.37	0.86	0.00	0.00	0.00	0.00	0.00	0.00	0.00	0.00

Figure 7-4. Hourly system loads of the dwelling, from DesignBuilder.

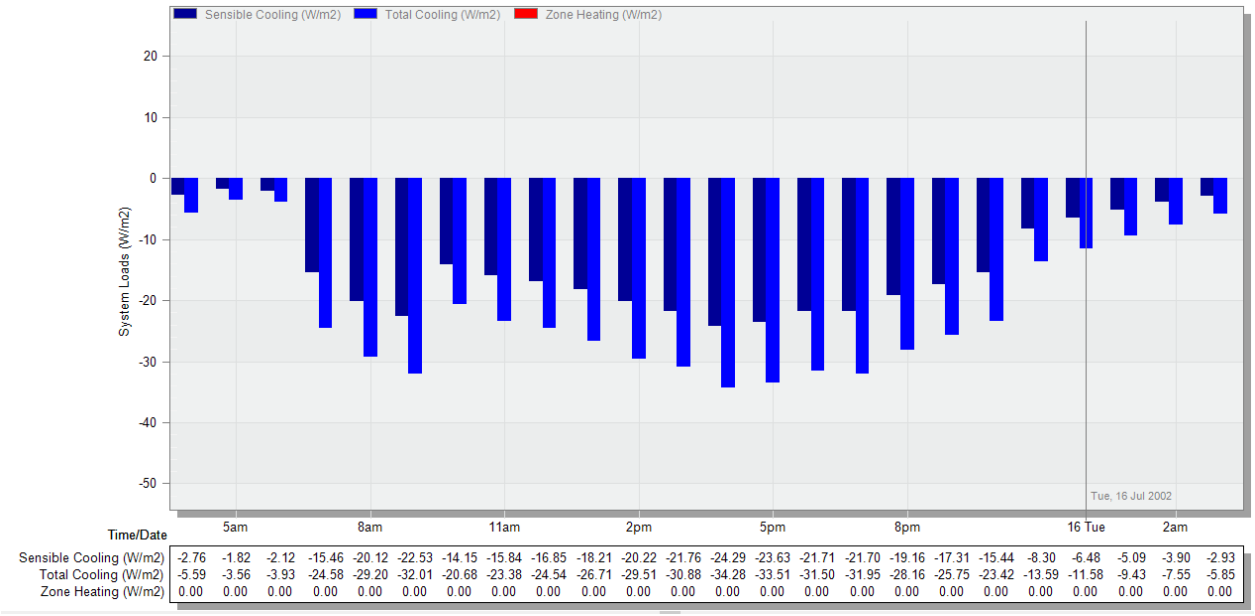

Time/Date	5am			8am			11am			2pm			5pm			8pm			16 Tue			2am	
Sensible Cooling (W/m2)	-2.76	-1.82	-2.12	-15.46	-20.12	-22.53	-14.15	-15.84	-16.85	-18.21	-20.22	-21.76	-24.29	-23.63	-21.71	-21.70	-19.16	-17.31	-15.44	-8.30	-6.48	-5.09	-3.90	-2.93
Total Cooling (W/m2)	-5.59	-3.56	-3.93	-24.58	-29.20	-32.01	-20.68	-23.38	-24.54	-26.71	-29.51	-30.88	-34.28	-33.51	-31.50	-31.95	-28.16	-25.75	-23.42	-13.59	-11.58	-9.43	-7.55	-5.85
Zone Heating (W/m2)	0.00	0.00	0.00	0.00	0.00	0.00	0.00	0.00	0.00	0.00	0.00	0.00	0.00	0.00	0.00	0.00	0.00	0.00	0.00	0.00	0.00	0.00	0.00	0.00

Figure 7-5. System loads of the dwelling on a typical summer day, from DesignBuilder.

Another output of DesignBuilder to be used in the following simulations in Matlab and Simulink is the temperature within the dwelling. In figure 7-6 the plot of the operative temperature against time for the period of the whole year with an hourly interval is presented. This temperature is an average temperature of all the cooled zones of the dwelling, and it is sufficient for the following simulations since the dwelling is simulated as one zone in Matlab and Simulink. The operative temperature reaches around 26.5 °C in the summer months, which is around 1.5 °C higher than the cooling setpoint temperature. In the winter months it is much lower but with notable fluctuations.

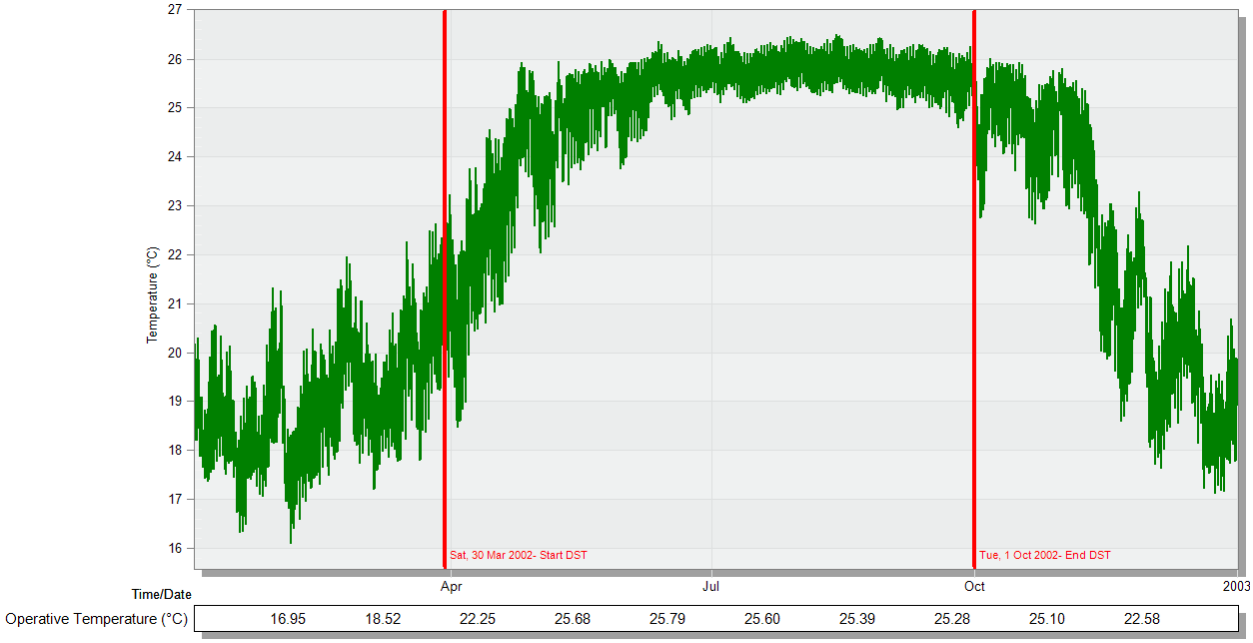

Figure 7-6. Hourly operative temperature of the dwelling, from DesignBuilder.

7.2. System parameters and base case

The results of the simulation are influenced by a number of input variable parameters that should be altered in order for their significance to be investigated. Those variables are related to the several components of the system: the daytime radiative cooler itself, the water buffer tank, the active cooler and the heat exchanger. In addition, variables related to DesignBuilder calculations exist. The list of variables includes:

a. Water buffer tank:
   1. Radius r_{tank}
   2. Height h_{tank}
   3. U-value U_{tank}
   4. Heat conduction coefficient of water λ_w
   5. Effective conduction coefficient for free convective mixing of water $\lambda_{w,mix}$

b. Active cooler:
   6. Water temperature drop in the active cooler ΔT_{act}

c. Heat exchanger:
   7. Efficiency of the heat exchanger eff_{exch}

d. DesignBuilder parameters:
   8. Location (climate data)
   9. Cooling setpoint temperature

e. Daytime radiative cooler:
   10. Surface area A_{dtc}
   11. Effective heat transfer coefficient H_{dtc}
   12. Shortwave radiation transmission coefficient τ_{sw}
   13. Longwave radiation transmission coefficient τ_{lw}

14. Longwave emissivity coefficient ε_{lw}
15. Specific mass flow rate of water $\dot{m}_{dtc,sp}$
16. Minimum required temperature difference between the buffer tank and the daytime cooler ΔT_{dtc}

a. Water buffer tank:

The Matlab Simulink model of the water tank was provided while being already validated. It concerns a cylindrical tank and its original dimensions are 1.5 m height and 0.5 m radius.

Only one geometrical parameter is altered for the analyses and it is the height as it is considered more significant than the radius when it comes to how the stratified water tank works since it influences the height of the water layers. In the original model for the stratified water tank, the height is equal to 1.50 m, which in combination with a radius of 0.5 m gives a tank volume of 1.18 m^3. A number of height values are investigated ranging from 0.50 to 2.50 m. These height values, in combination with a constant radius of 0.50 m, give respectively tank volumes ranging from 0.39 to 1.96 m^3. For reference, Zhang *et. al* (2018) come to the result that the optimised tank volumes for the four US locations they investigate are 0.30, 0.55, 0.75 and 1.30 m^3.

The original U-value of the tank is 0.285 W/m^2K. A number of values ranging from 0.10 to 1.00 W/m^2K are investigated to examine whether the insulating condition of the tank plays a significant role. It is worth noting that the tank is assumed to be located outside so its surface has direct contact with the air dry-bulb temperature.

The heat conduction coefficient of water and the effective conduction coefficient for free convective mixing of water are two parameters that, more or less, have unknown values. In the modelling of the tank values of 0.6 W/mK and 1000 respectively have been assumed. For the former, values between 0.2 and 1.0 W/mK are investigated while for the latter, values between 500 and 1300 W/mK.

b. Active cooler:

Investigating the performance of the active cooler is not the objective of this research. Therefore, investigating the capabilities of the whole system with an altering parameter for the active cooler would not give any valuable result. For this component, it is assumed that equipment with a good performance is used and an active cooler that reduces the temperature of water by 8 °C is used.

c. Heat exchanger:

The performance of the heat exchanger is also not a topic investigated in this research. As in the case of the active cooler, good performance equipment is assumed to be used. The efficiency of the exchanger is considered to be constant at 0.75.

d. DesignBuilder parameters:

The two parameters mentioned before relevant to the DesignBuilder simulations are the cooling setpoint temperature and the location along with its climate data. For the former a setpoint temperature of 25 °C is used for the base case. In addition to that, temperatures ranging from 23 to

27 °C are investigated. Regarding the latter, the original concept behind this thesis project is to investigate the application of this passive cooling method to Cyprus. But since climate data are not available for more than one location in Cyprus, which is Larnaca, simulations are also made for other locations in the Mediterranean that experience similar climates to the one of Cyprus. These locations are Tel Aviv, Athens, Cairo and Rome. In addition, the system is applied to Amsterdam, which has an entirely different climate and cooling load, to get an indication of the capabilities of it in such a location.

e. Daytime radiative cooler:

In order to examine which properties of the daytime cooler are detrimental for the calculation of its total cooling rate, we should look at the formula by which that rate is calculated that is the following:

$$P_{cool,dtc} = A_{dtc}[\, P_{sw} \cdot \tau_{sw} + P_{lw} \cdot \tau_{lw} \cdot \varepsilon_{dtc} - \tau_{lw} \cdot \varepsilon_{dtc} \cdot \sigma \cdot T_{dtc,mean}^{4} + H_{dtc}(\theta_{air} - \theta_{dtc,mean})] \quad (26)$$

This formula consists of the sum of four parts multiplied by the surface area of the cooler. The four parts are:

1. Absorbed shortwave solar power $P_{sw} \cdot \tau_{sw}$
2. Absorbed longwave solar power $P_{lw} \cdot \tau_{lw} \cdot \varepsilon_{dtc}$
3. Power radiated out $\tau_{lw} \cdot \varepsilon_{dtc} \cdot \sigma \cdot T_{dtc,mean}^{4}$
4. Convective and conductive heat losses $H_{dtc}(\theta_{air} - \theta_{dtc,mean})$

Three out of the four parts have a positive sign, hence they increase the total and they reduce the cooling power, as it has a negative sign. It should be noted that the subtraction θ_{air} - $\theta_{dtc,mean}$ also gives a positive sign almost always. The only part that reduces the total and increases the absolute value of the cooling power is the third one which is the power radiated out.

In figure 7-7, the contribution of each part to the total cooling power provided by the DTC is illustrated, for the base case. This case is the one that consists of a set of values kept constant for each parameter with each one altered each time to inspect its significance. Here it is used to show the contribution of each part of the passive cooler power equation. The basic-case values of the parameters are presented thereafter. Some of the parameters are explained in later paragraphs.

- h_{tank} = 1,50 m
- U-Value$_{tank}$ = 0.285 W/m^{2}K
- λ_{water} = 0.6 W/mK
- $\lambda_{water,mixing}$ = 1000
- Setpoint temperature = 25 °C
- Climate = Larnaca
- A_{dtc}=40% (of roof area)
- τ_{sw} = 0.05
- τ_{lw} = 0.95
- ε_{lw} = 1.0
- H_{dtc} = 0,5 W/m^{2}K
- $\dot{m}_{dtc,sp}$ = 0.003 kg/m^{2}s

- $\Delta T_{dtc} = 2$

Observing figure 7-7, in which the unit of power is W/m² as it has not been yet multiplied by the surface of the cooler, makes it obvious that the more important parts, at least for the base-case variables, are the longwave power radiated out and the absorbed longwave power. These are of the same order of magnitude but with a different sign.

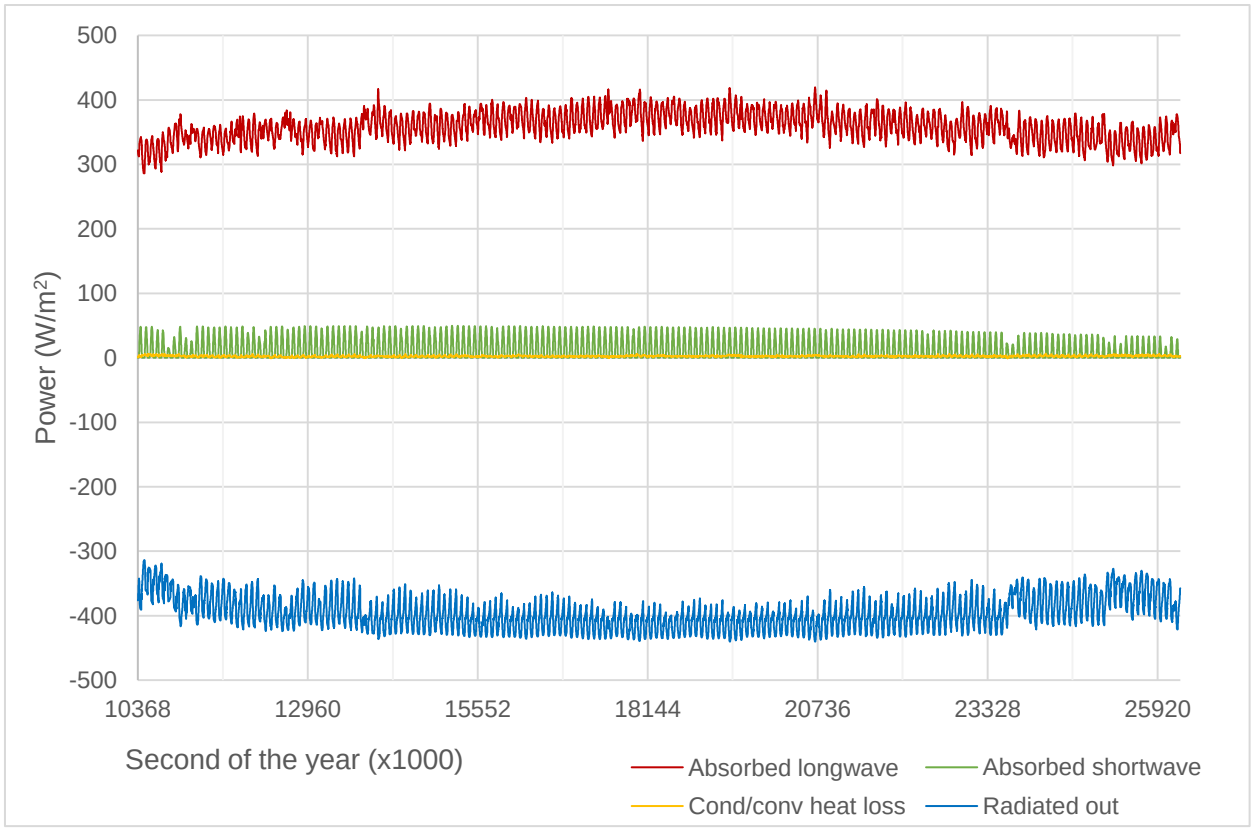

Figure 7-7. Contribution of each part to the total cooling load produced by the daytime cooler at each moment for the base-case scenario.

Figure 7-8 shows the energy produced by the passive and the active coolers in the six months period that the simulation takes place, using the base-case variables. The total cooling from the DTC is higher but the difference between them is small. The ratio of the passive to active cooling power is 1.12.

The surface area of the DTC is obviously detrimental. Values for areas that cover from 10 to 90 % of the surface of the dwelling are considered. The higher percentages are unrealistic as it would be peculiar for such a high percentage of a roof to be covered by radiative cooling apparatus. Their inclusion in the sensitivity study is made to investigate how significantly they can change the simulation results.

The shortwave radiation transmission coefficient appears only at the first part of the equation. This part should have the lowest absolute value possible for the DTC to be more efficient. A value of 0 would be ideal and it is be amongst the values investigated. In addition, the simulation results when the value is changed UP TO 0.40 are examined.

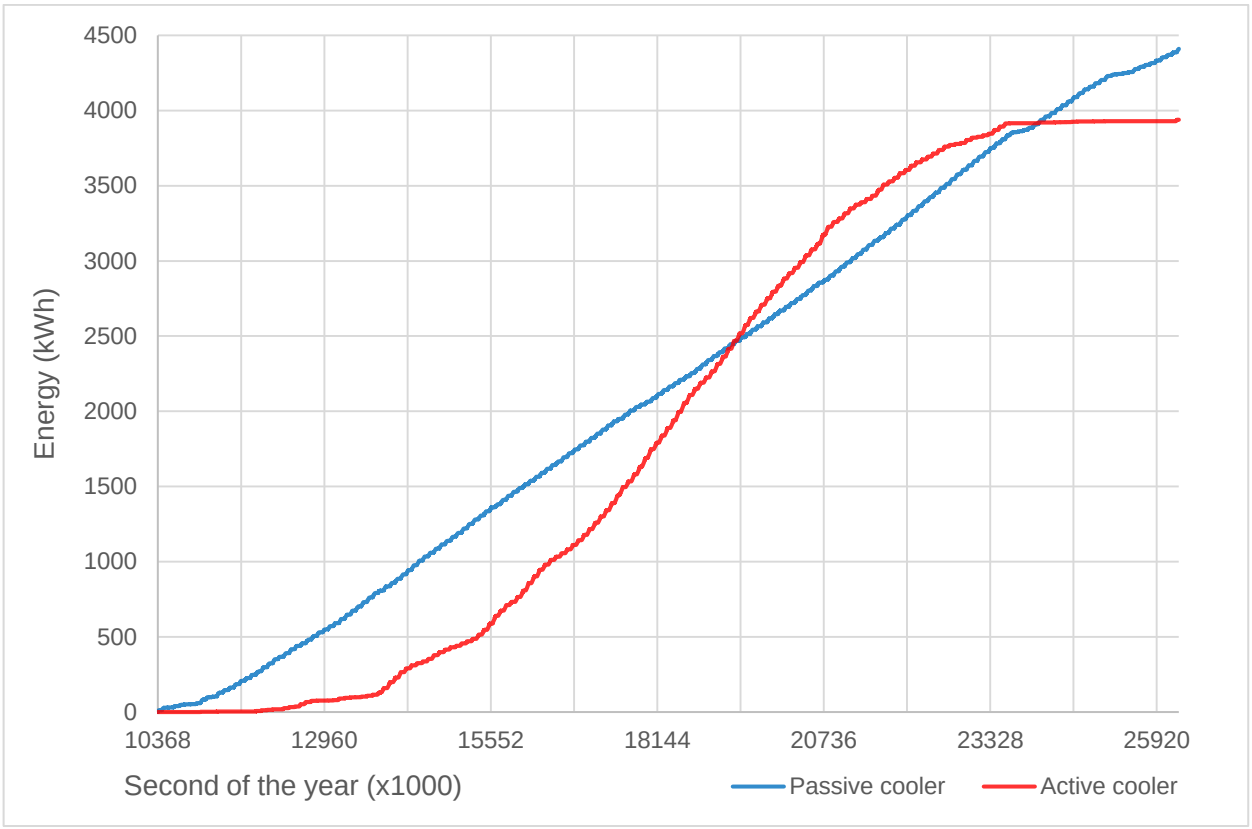

Figure 7-8. Cooling energy provided by the passive cooler and the active cooler for the six-month period for the base case scenario.

The longwave radiation transmission coefficient and the longwave emissivity coefficient appear together as a product in the second and the third part. The second part is of a small order of magnitude and reduces the absolute value of cooling power while the third one is of a large order of magnitude and increases it. This means that the product of these two coefficients should be as close to 1 as possible. In addition, since the two values always appear as a combined product and not as individual coefficients, there is no reason in altering the coefficients individually. Combined coefficient products ranging from 0.50 to 1.00 are investigated.

Regarding the fourth part of the passive cooler equation, the conductive and convective heat losses, it can be concluded from figure 7-7 that it is insignificant. But this is when H_{dtc} has a very small value close to 0. When this parameter increases, the efficiency of the system is endangered. The unrealistic value of 0 W/m^2 is investigated along with values ranging up to 20 W/m^2.

There are two more parameters relevant to the DTC that are not present in its fundamental equation: the specific mass flow rate of water, $\dot{m}_{dtc,sp}$, and the minimum required temperature difference between the buffer tank and it, ΔT_{dt}. For the former, values between 0.0002 and 0.007 are investigated. For the latter, a required temperature difference between 0 and 4 degrees is investigated.

7.3. Sensitivity analysis

Using the base case as identified in the previous section and altering each time only one of the parameters, the sensitivity of the model to each parameter is investigated. Below the simulation results for each variable parameter are presented. For each parameter, the several values examined are shown along with the resulting cooling energy produced by the passive and the active coolers. In addition, the ratio of the produced energy of the two coolers is presented which illustrates clearly how significant each parameter is. A summary of the values investigated for each parameter is shown in the table in Appendix C.

7.3.1. Water tank height

Figure 7-9 illustrates how the change in the value of the height of the water tank influences the ratio between the two coolers. The higher the height is, the greater the energy savings are since the ratio of the cooling energy provided from the DTC to the cooling energy provided from the active cooler increases. Whether this conclusion applies also in combination with changes in the values of the other parameters too is studied in the varied analysis which is the next step.

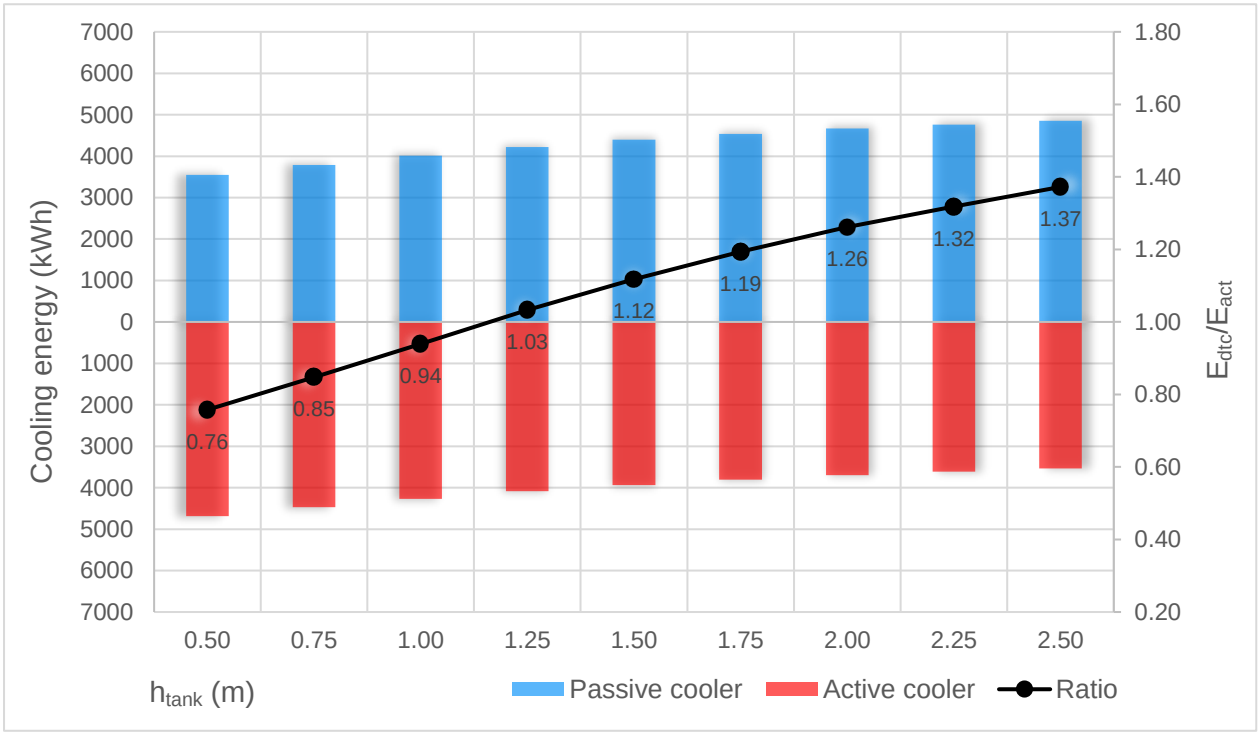

Figure 7-9. The sensitivity of the system to the height of the buffer tank.

7.3.2. Passive cooler surface area

The results shown in figure 7-10 are according to expectations. The area that the passive cooling devices cover on the roof is detrimental for the efficiency of the system and the larger this area is, the greatest the energy savings will be. The E_{dtc}/E_{act} ratio grows significantly from approximately 0.35 to

1.57 when the area that the passive cooler covers on the roof increases from 10 to 90%. It seems that is important to have an area of at least 40% as the slope of the ratio line between 10 and 40% is greater than the one between 40 and 90%.

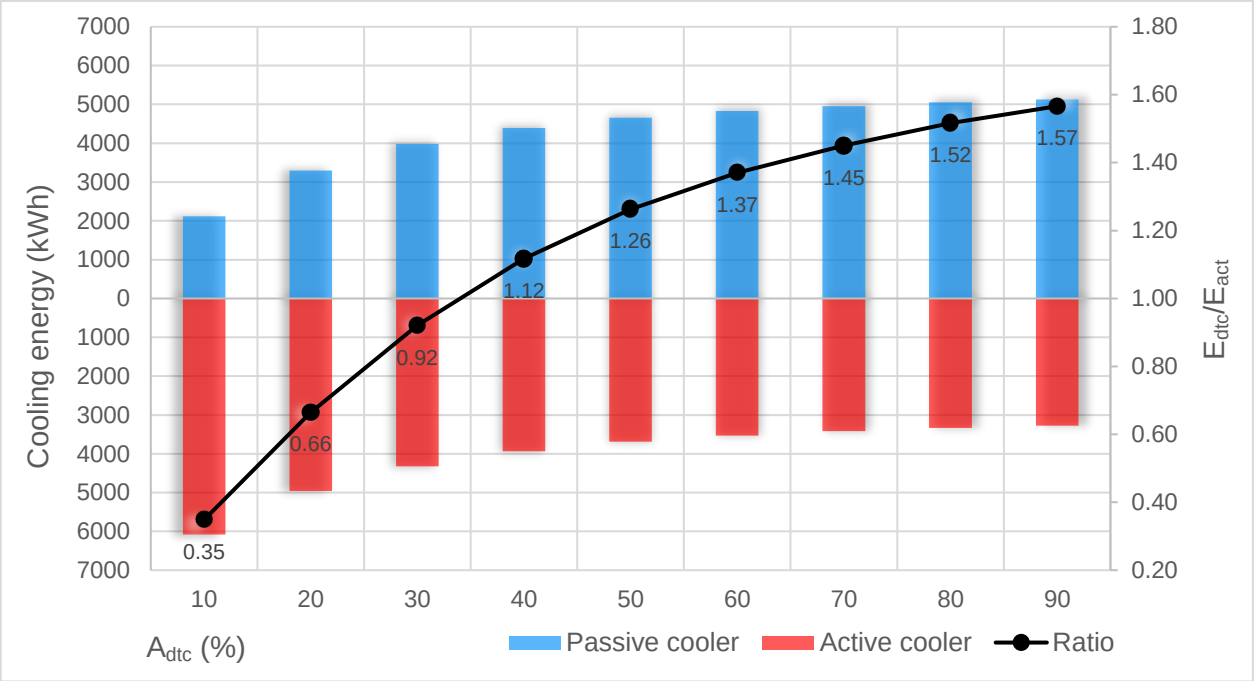

Figure 7-10. The sensitivity of the system to the area (as percentage of the roof area) of the radiative cooler.

7.3.3. Shortwave and longwave coefficients

The data presented in figure 7-11 are also according to expectations. Increasing the shortwave transmission coefficient contributes negatively to the cooling rate of the DTC and a coefficient equal to 0 would be ideal. Having a coefficient of 0 results in a ratio so higher than having a coefficient of 0.05. The ratio for the latter is 1.12, which is the base case, while for the former it reaches the very high value of 1.76. In reality achieving so low shortwave transmission coefficients is very hard.

The increase in the combined product of the longwave transmission and emissivity coefficients, as presented in figure 7-12, contributes positively to the E_{dtc}/E_{act} ratio. This result is, though, not to be trusted as altering other variables of the system could cause complications in which this product could be required to be lower. Judging only from these data, it is very clear that ratio between the two produced energies is directly proportional to the product of the two coefficients.

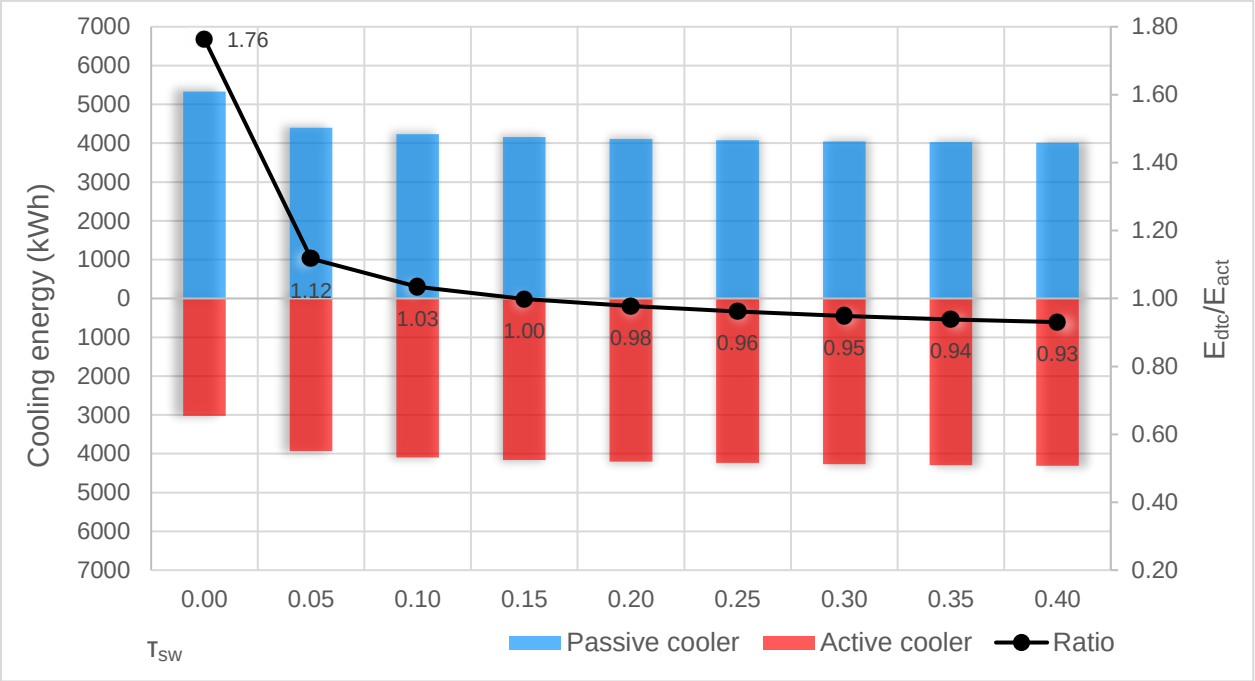

Figure 7-11. The sensitivity of the system to the shortwave transmission coefficient.

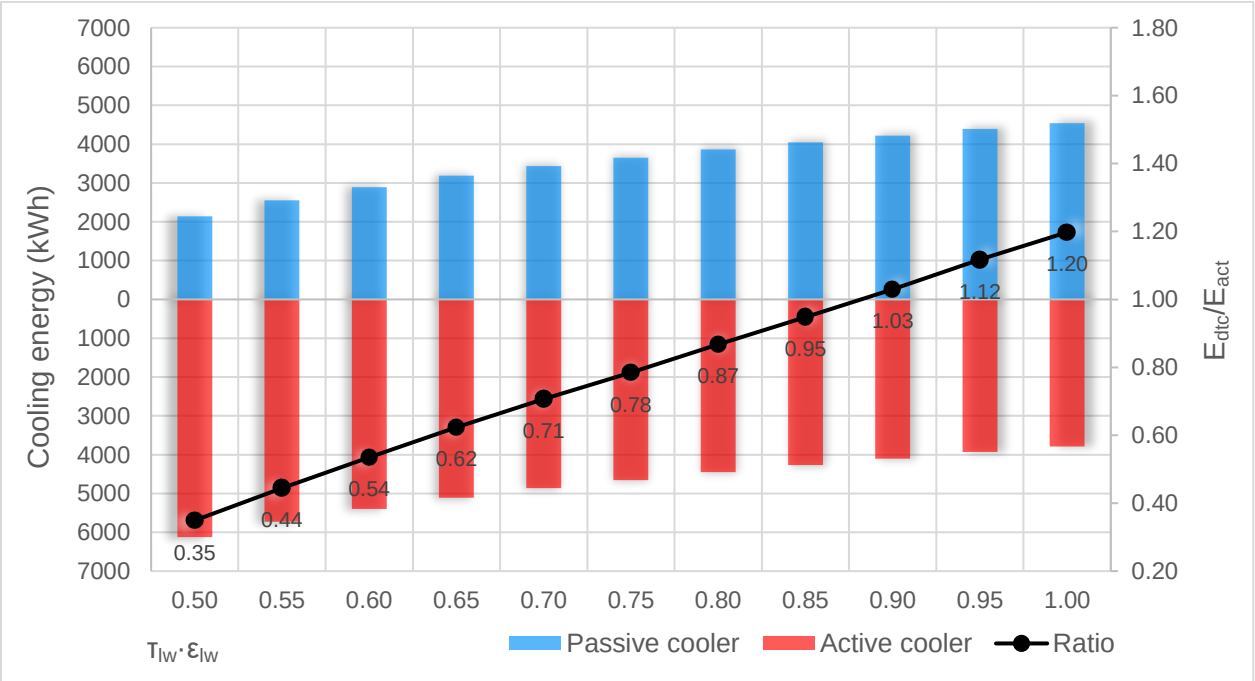

Figure 7-12. The sensitivity of the system to the product of the longwave transmission and emissivity coefficients

7.3.4. Effective heat transfer coefficient

The effective heat transfer coefficient should be as low as possible for the cooling power of the passive cooler to be increased and this is also visible in the data shown in figure 7-13 and 7-14. A coefficient equal to zero would be ideal but this would be almost impossible. The values between 0 and 5 W/m^2,

with a step of 0.5 W/m², are shown in the first figure in order to illustrate how significant are small changes of this variable. For these values the ratio decreases from 1.23 to 0.57. In the second figure the values between 5 and 20 W/m², with a step of 2.5 W/m² are shown. Those values are used so that the behaviour of the system when there is very limited insulation for the passive cooler, can be investigated and are also more realistic. Increasing the effective heat transfer coefficient decreases the passive-to-active ratio with the decrease being less significant for higher values.

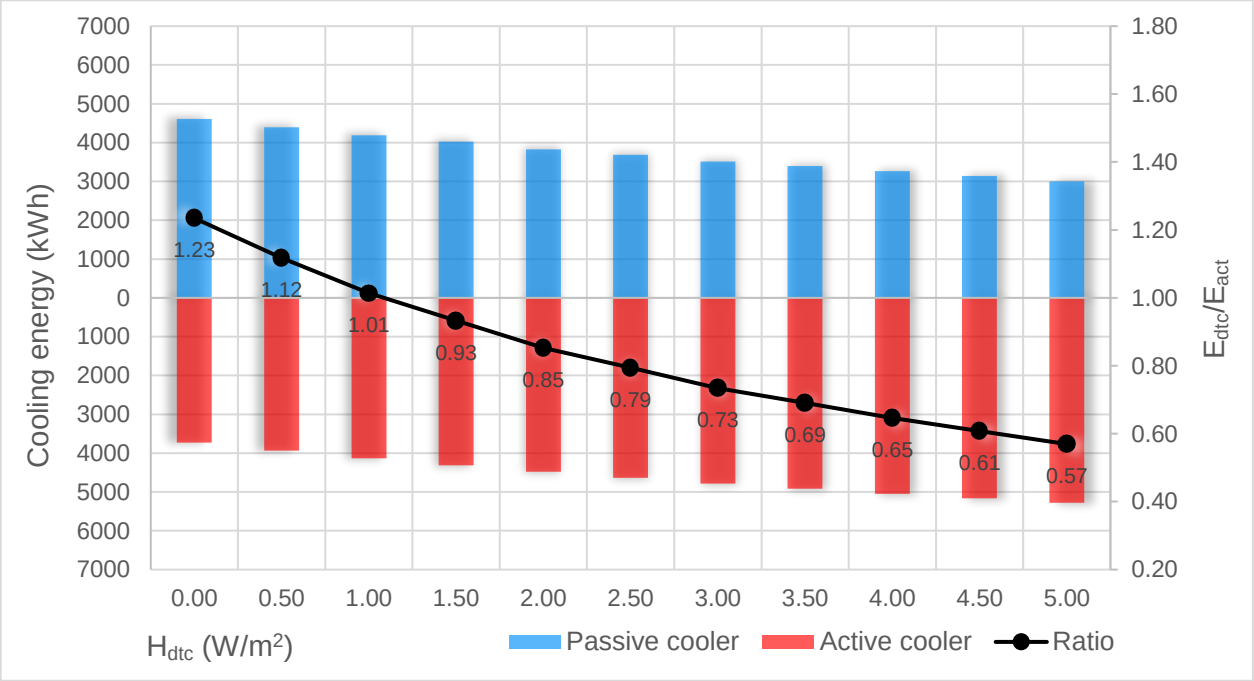

Figure 7-13. The sensitivity of the system to the effective heat transfer coefficient for values between 0 and 5 W/m²

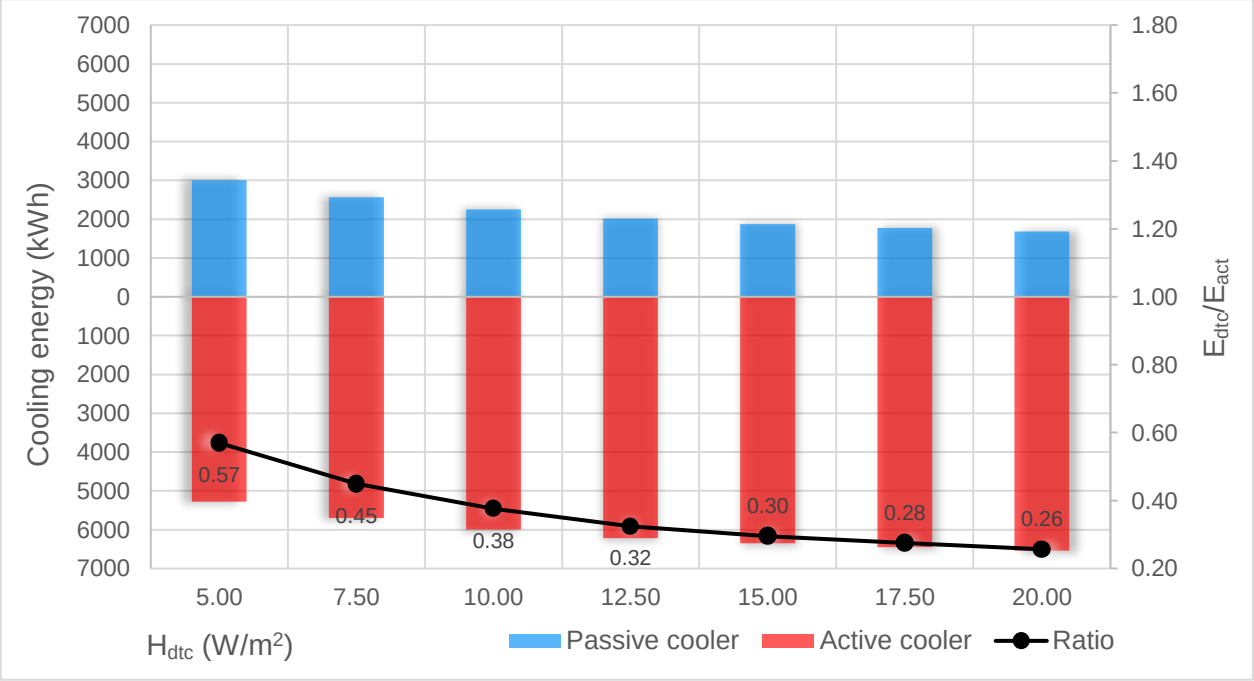

Figure 7-14. The sensitivity of the system to the effective heat transfer coefficient for values between 5 and 20 W/m²

7.3.5. Specific mass flow of water in DTC

Figure 7-15 illustrates that the specific mass flow rate of water through the DTC should be as low as possible for the cooling power of the DTC to be increased. Increasing the flow rate from 0.001 to 0.002 kg/m²s, reduces the ratio by 0.12. After that value, an increasement 0.001 kg/m²s reduces the ratio by 0.25 with the rate at which the ratio decreases being lower for higher values. Figure 7-16, though, shows that decreasing the flow rate to values lower than 0.001 kg/m²s reduces the ratio.

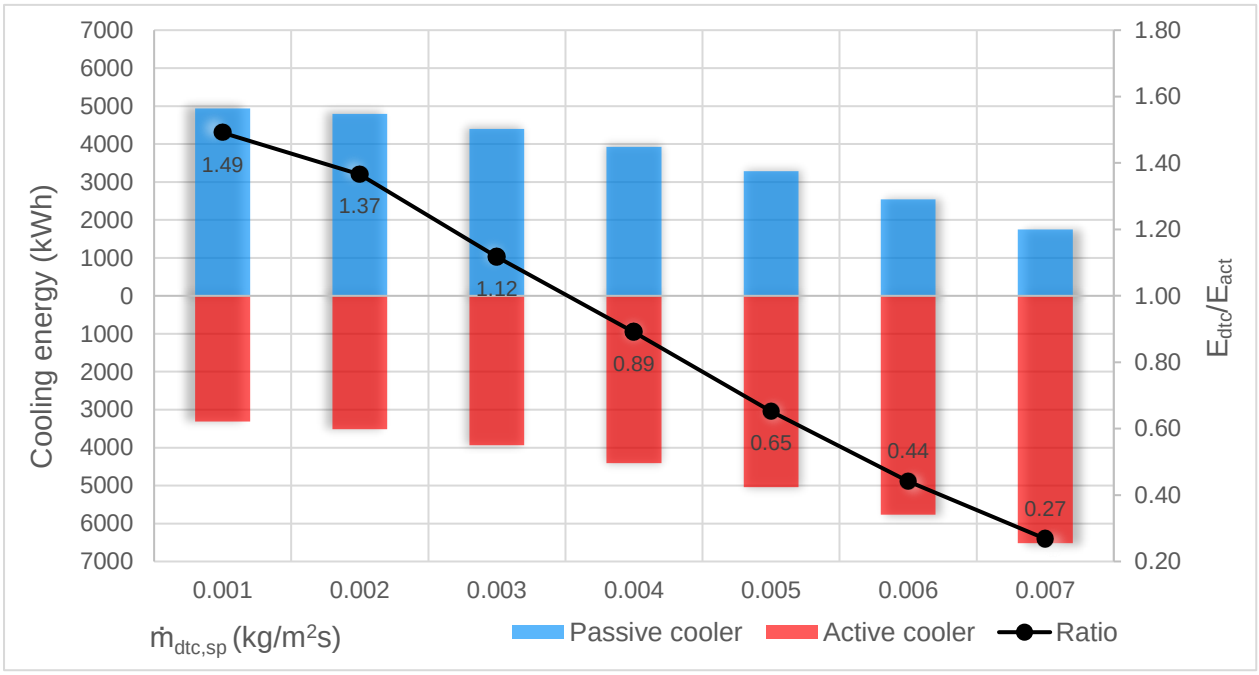

Figure 7-15. The sensitivity of the system to the mass flow rate of water within the passive cooler (> 0.001 kg/m²/s).

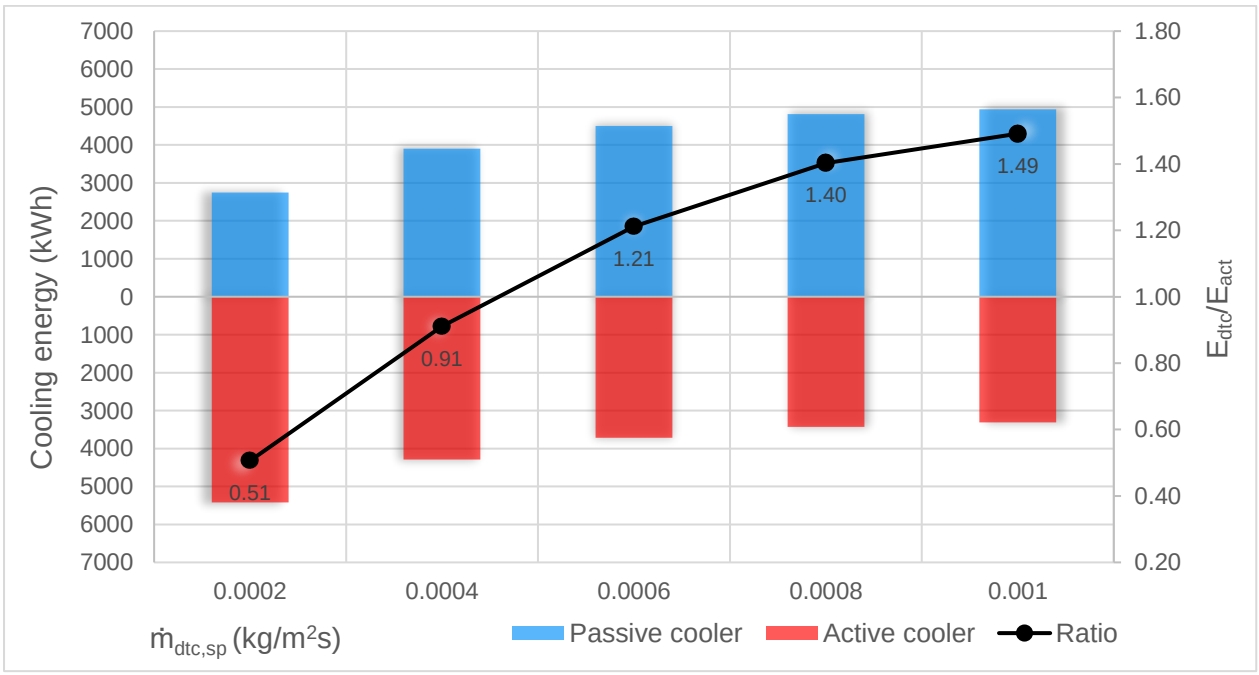

Figure 7-16. The sensitivity of the system to the mass flow rate of water within the passive cooler (< 0.001 kg/m²/s).

7.3.6. DTC-Buffer tank minimum temperature difference

From examining figure 7-17, one can argue that increasing the minimum required temperature difference between the buffer tank and the DTC, decreases the E_{dtc}/E_{act} ratio and thus reduces the efficiency of the system. The only exception is the ratio at exactly 0 °C which is lower than the maximum ratio which appears at 0.5 and 1.0 °C.

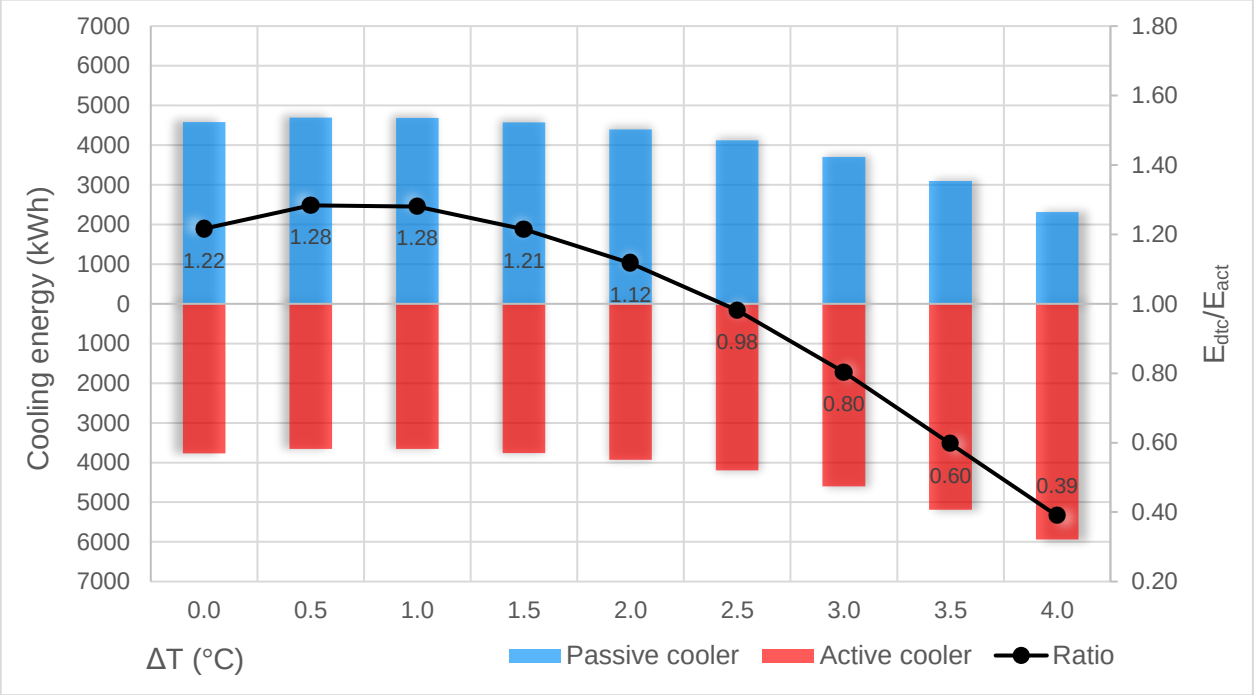

Figure 7-17. The sensitivity of the system to the minimum required temperature difference between the buffer tank and the passive cooler.

7.3.7. Insulation of buffer tank

The U-Value of the storage tank has no influence in the ratio of the produced energies, as shown in figure 7-18. Someone would expect that altering the insulation properties of a tank that is directly exposed to the air temperature would have serious consequences, but this is not the case. On average, the mean daily temperature (ΔT) of water inside the water tank is about 7 K lower than the mean daily temperature. The base-case cylindrical water tank has an external surface (A) of 5.50 m^2 in direct contact with the air temperature. With ta U-value of 1 W/m^2K, at maximum, the heat transfer in the tank (q) can be calculated using the equation:

$$q = U \cdot \Delta T \cdot A = 1.0 \cdot 7 \cdot 5.50 = 18.5\ W \qquad (27)$$

This heat transfer value in W can be transformed into daily energy in kWh by multiplying by the number of seconds in a day and dividing by the number of seconds in an hour times one thousand. This gives a value of 0.92 kWh which is minimal compared to the daily cooling load of the dwelling which justifies why the U-value of the tank is insignificant to the performance of the system, at least for values being lower than 1 W/m^2K

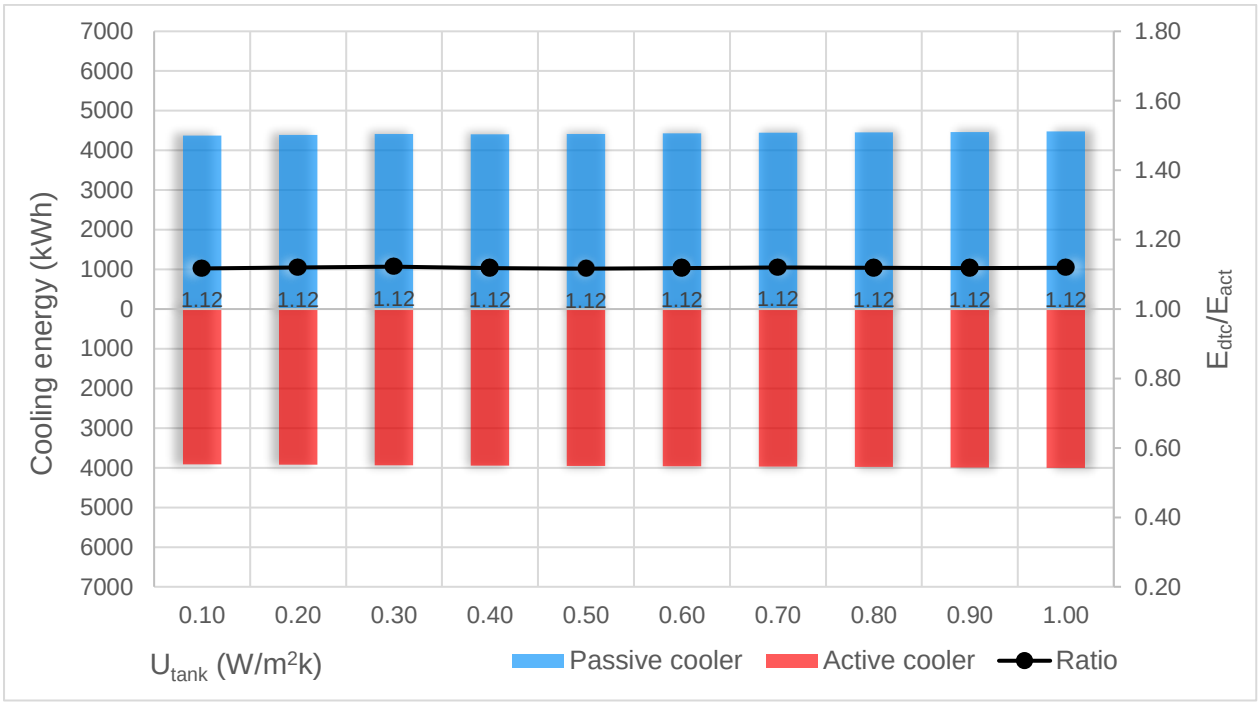

Figure 7-18. The sensitivity of the system to the U-value of the water storage tank.

7.3.8. Heat conduction and mixing coefficients of water

The two parameters relevant to the mixing properties of the water in the buffer tank have no influence in the ratio between the energy produced, as can be seen in figures 7-19 and 7-20.

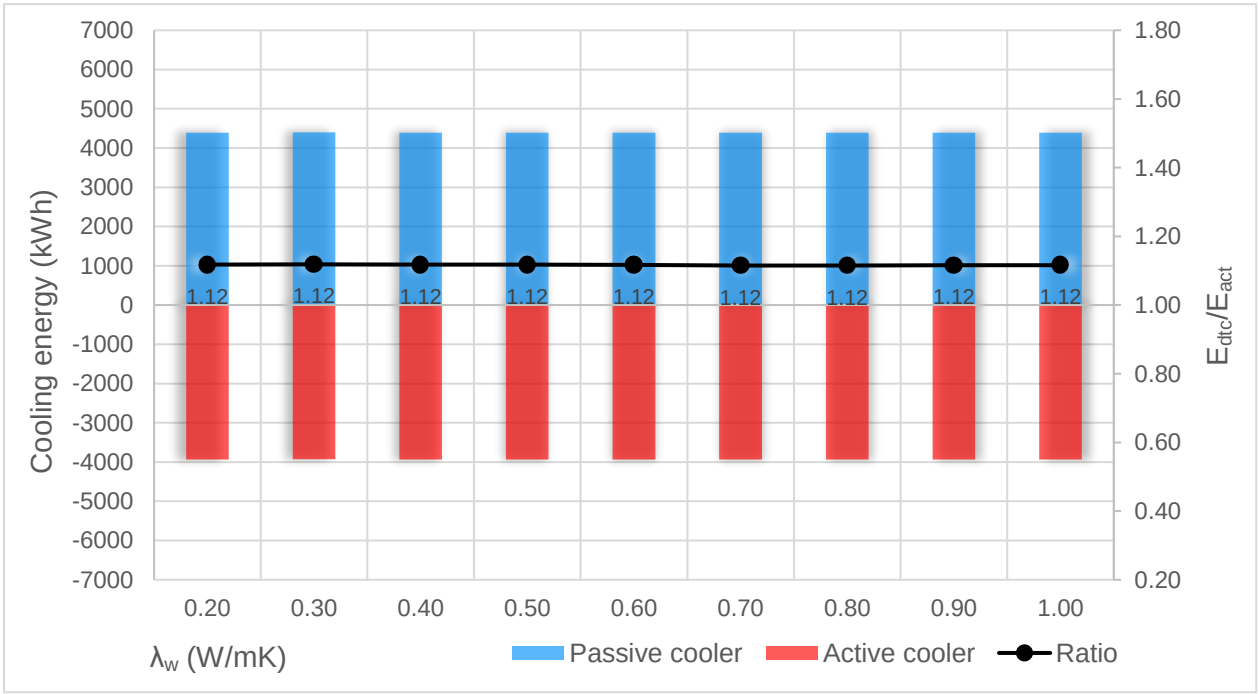

Figure 7-19. The sensitivity of the system to the heat conduction coefficient of water in the tank.

The system is not sensitive to any of the changes in the heat conduction coefficient of water and the effective free conduction coefficient for free convective mixing of water. This is good for the model designed as those values were not precisely known when the model of the water tank was designed so them being insignificant reduces importantly the unreliability of the model.

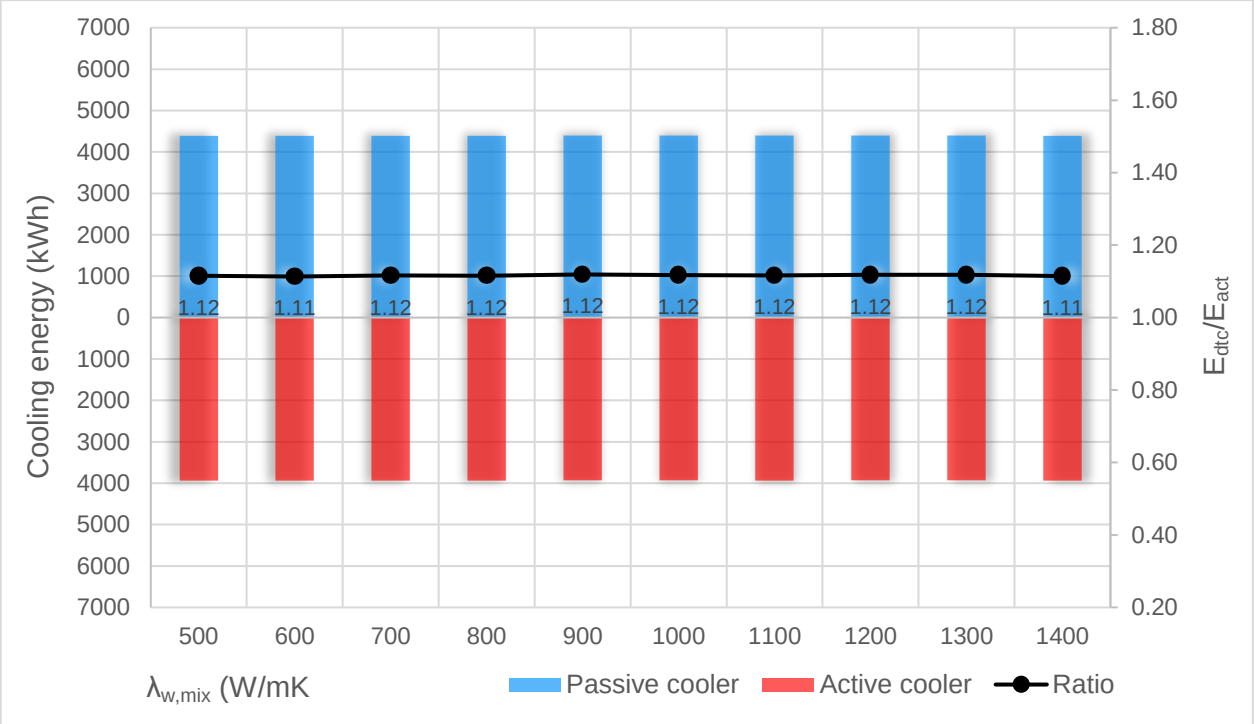

Figure 7-20. The sensitivity of the system to the effective free conduction coefficient for free convective mixing of water.

7.3.9. Cooling setpoint temperature

Altering the cooling setpoint temperature of the dwelling has significant influence on the energy ratio as illustrated in figure 7-21. For lower setpoint temperatures, the passive produced energy has a smaller share in the cooling energy production as expected and since the total cooling load of the dwelling is increased.

Setting a higher cooling temperature reduces the cooling load of the dwelling and subsequently increases the ratio of passive-to-active cooling energy. The cooling load and the ratio remain constant for setpoint temperatures between 24.5 and 26.0 °C.

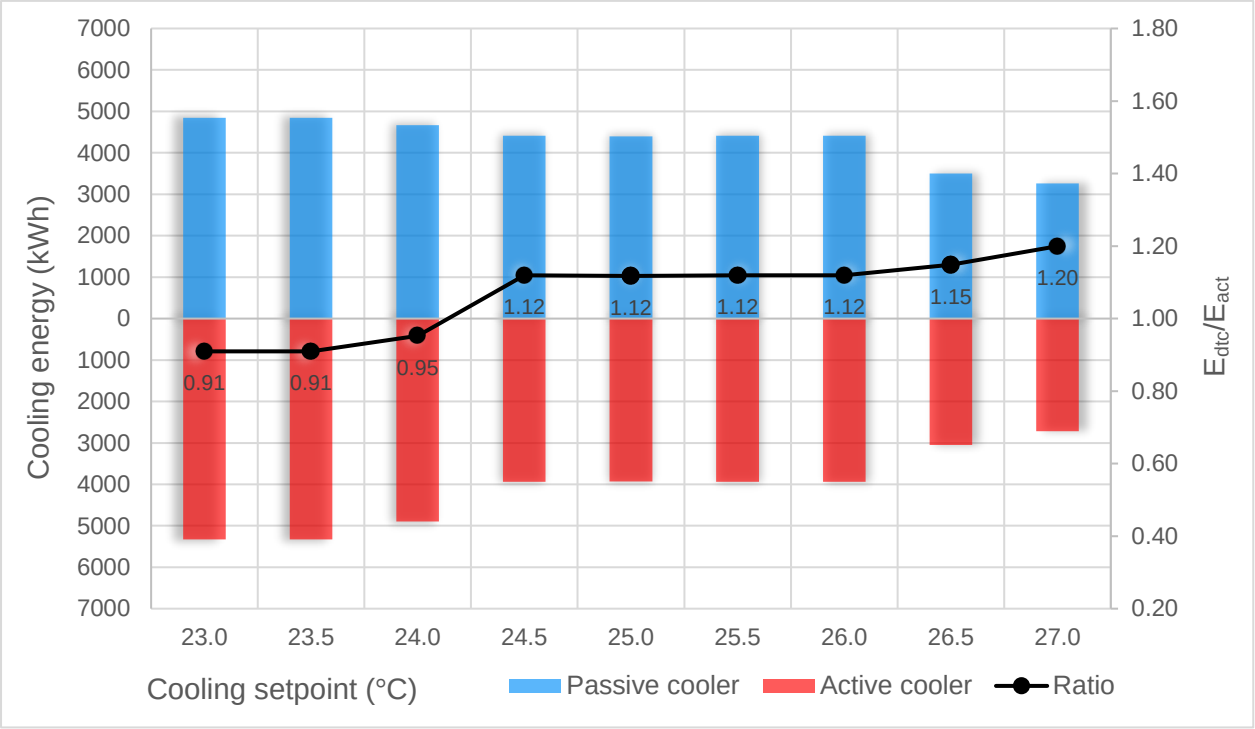

Figure 7-21. The sensitivity of the system to the cooling setpoint temperature of the dwelling.

7.3.10. Location

The sensitivity of the system to the location where the dwelling is, is investigated. As mentioned earlier, besides Larnaca four more Mediterranean cities are investigated; Cairo, Tel Aviv, Athens and Rome. In addition, a simulation is made for Amsterdam. It is worth noting that the same dwelling, representative for Cypriot standards, is used in all the simulations. Figures 7-22 and 7-23 illustrate the average daily dry-bulb temperature and relative humidity for those locations respectively.

As can be seen in the temperature graph, Cairo is the city that experiences generally the highest temperatures. Amongst the Mediterranean cities, the lowest temperature trend is found in Rome.

The humidity graph shows that the lowest relative humidity is shared, for periods of the year, between Cairo and Athens. The Mediterranean location that has the highest relative humidity levels is Rome.

Amongst all the cities, Amsterdam is the one that has the lowest average temperature and the highest average relative humidity for the whole duration of the year, owing to the fact that it has a totally different climate.

Figure 7-24 illustrates the sensitivity of the system to the location of the dwelling. The Mediterranean city in which a higher E_{dtc}/E_{act} ratio is Rome which indicates that the system is more efficient in locations where the environmental temperature is lower, and this makes sense since also the cooling load is lower. The effect of the location's humidity is not clear.

Amsterdam appears to have a very high ratio, and this is a result of its very low cooling load. Also, for that reason the graph on figure 7-24 has a logarithmic vertical scale.

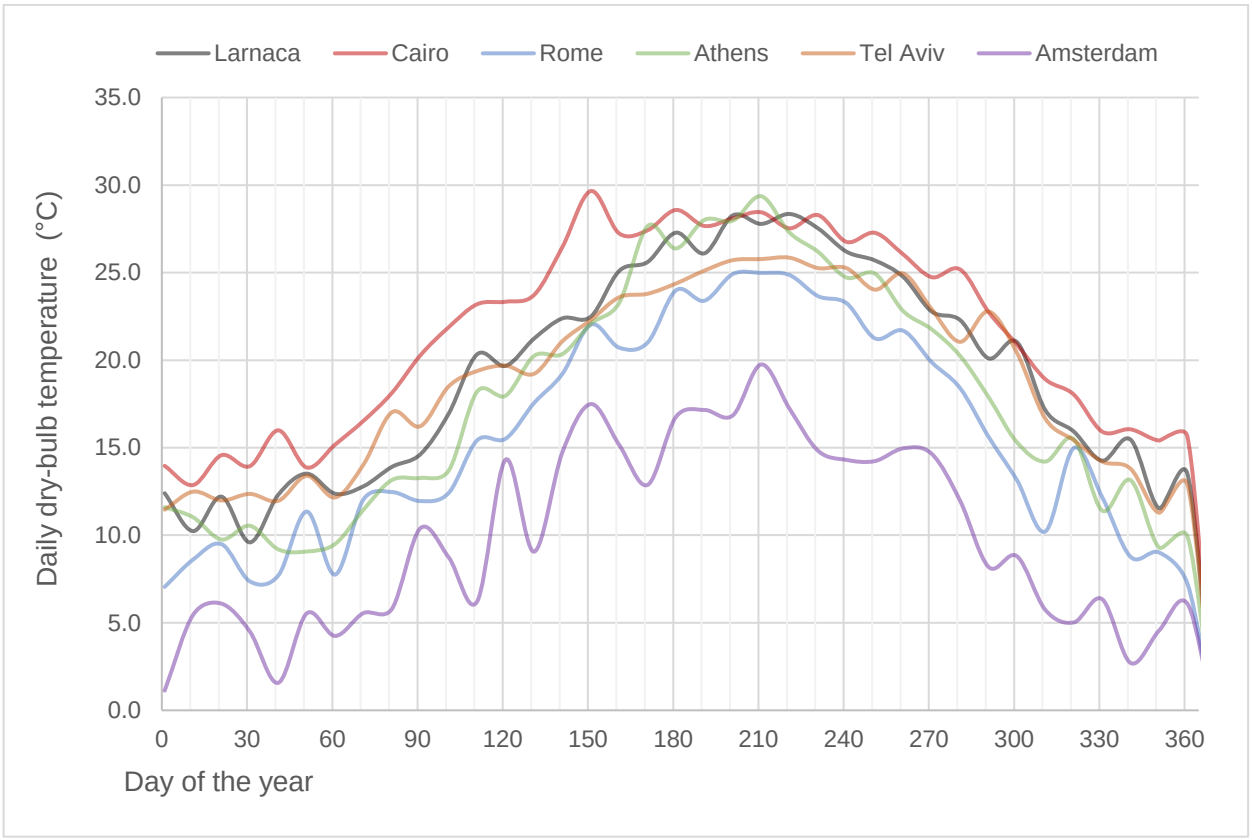

Figure 7-22. Average daily dry-bulb temperature in the cities investigated.

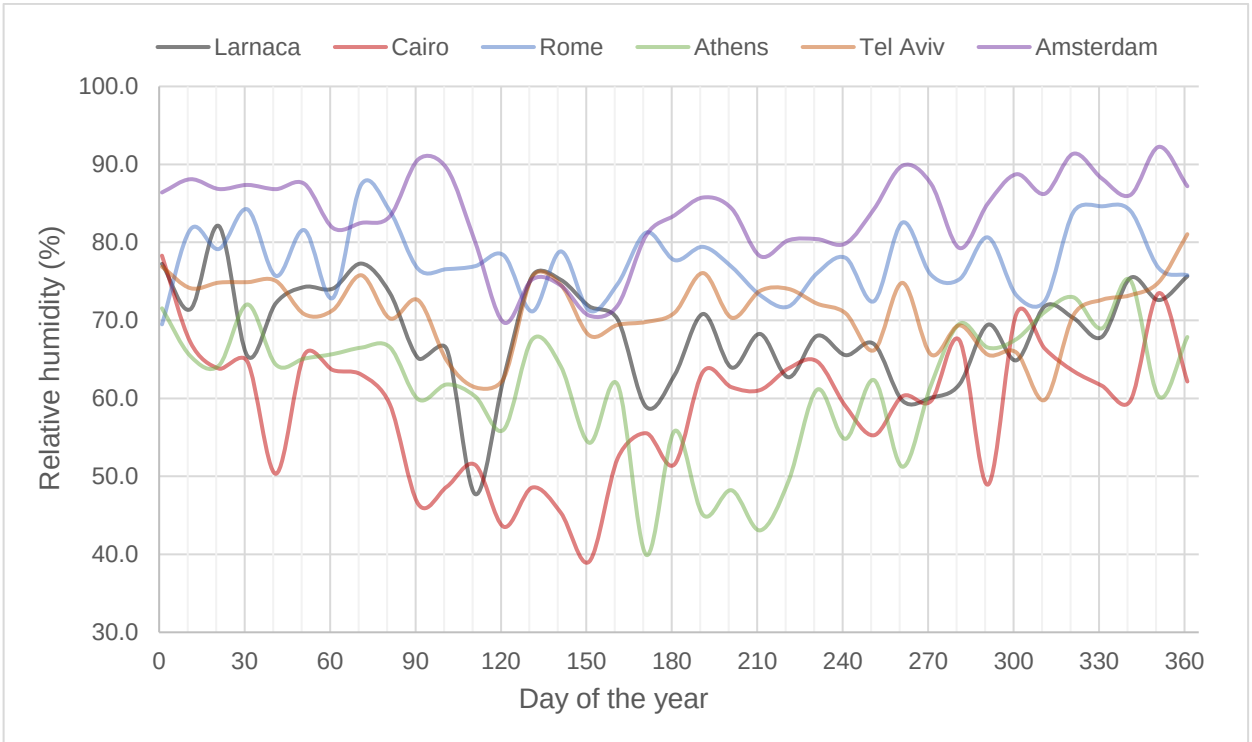

Figure 7-23. Average daily relative humidity in the cities investigated.

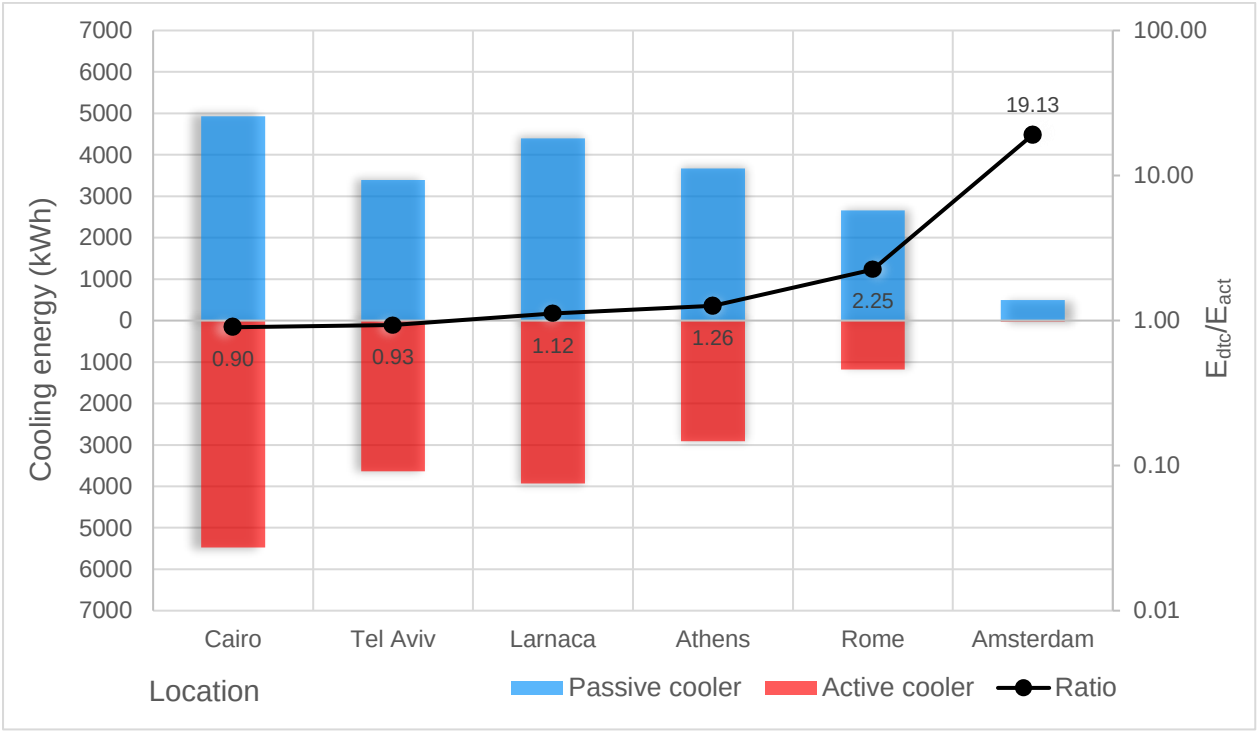

Figure 7-24. The sensitivity of the system to the location of the dwelling.

7.4. Varied analysis

In this section, a group of variables is selected to be investigated further and a smaller number of values for each is considered. This is a complete varied analysis which means that all the combinations resulting from altering the parameters with their corresponding values were simulated. In table 7-1 the values investigated for each variable are listed. The seven investigated parameters are:

- Height of the buffer tank, h_{tank}
- Surface area of daytime cooler, as a percentage of the roof area, $A_{dtc,per}$
- Shortwave radiation transmission coefficient of the daytime cooler, τ_{sw}
- Product of the longwave radiation transmission coefficient and longwave emissivity coefficient of the daytime cooler, $\tau_{lw} \cdot \varepsilon_{lw}$
- Effective heat transfer coefficient of the daytime cooler, H_{dtc}
- Specific mass flow rate of water in the daytime cooler, $\dot{m}_{dtc,sp}$
- Minimum required temperature difference between the buffer tank and the daytime cooler, ΔT_{dtc}

Since, as mentioned earlier, all the combinations of variables values are considered, there are 6144 unique cases for which a simulation was executed. In order to do that a 'master file' is used in Matlab which was able to change a value for a variable each time, conduct the simulation and continue to the next run.

For each simulation, the energy provided by each of the two coolers was collected. The total number of simulations was split into smaller sets so that there is better control. For each set, two arrays were exported consisting of the passive cooling and active cooling energy for each. In addition, seven arrays each consisting the value of each variable were exported. The total simulation time for all 6144 runs was about 77 hours.

Variable	Unit	Nº of values	Values			
h_{tank}	m	4	1.00	1.25	1.50	1.75
A_{dtc_per}	%	4	20	30	40	50
τ_{sw}	-	3	0	0.05	0.10	
$\tau_{lw} \cdot \varepsilon_{lw}$	-	4	0.85	0.90	0.95	1.00
H_{dtc}	W/m^2	4	0.5	1.0	2.0	5.0
$\dot{m}_{dtc,sp}$	kg/m^2s	4	0.001	0.002	0.003	0.004
ΔT_{dtc}	degrees	2	2	3		

Table 7-1. The values of the variable parameters of the system that are investigated during the varied analysis.

After the completion of the simulations, post-processing of the large amount of data was made in Microsoft Excel. The arrays from several sets of simulations were combined together into nine tables which were later transformed into a 6144-row table including all of the data, using the Kutools for Excel add-on that is capable of managing large amounts of data. For each simulation, the passive cooling energy was divided by the respective active for the ratio between the two to occur. Figure 7-25 illustrates the ratio of all 6144 cases plotted against the total cooling energy produced. This is an insignificant value as it sees not important differentiations. It ranges between about 8200 and 8450 kWh, which is very close to the cooling load of the dwelling for the six months period simulated. It is used here as a value of the horizontal axis to help the dots spread more evenly in the plot area.

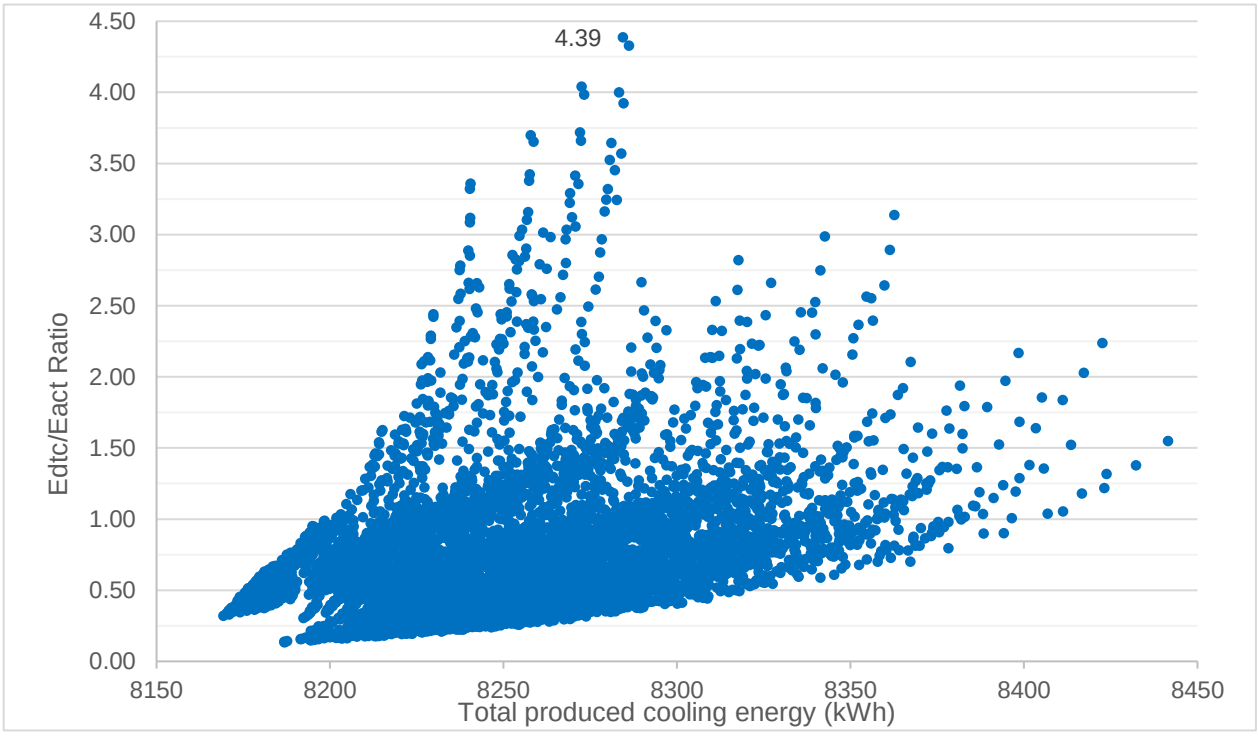

Figure 7-25. The ratio of the 6144 cases investigated plotted against the total cooling energy produced by the two coolers.

As can be seen in Figure 7-25, the greatest ratio occurred amongst the simulations is 4.39 which means that using this specific combination of values, the passive cooler is able to produce more than four times the energy of the active cooler. This would result in significant energy savings. The set of values that leads to this ratio is to be discovered in the following paragraphs where the behaviour of each parameter's value is described separately.

It should be noted that in figures 7-26 to 7-32, the simulation cases are split into set of cases for which a value is used and then sorted from the one having the greatest E_{dtc}/E_{act} ratio to the one having the smallest. The latter is done so that the cases can be distinguished in the graph.

7.4.1. Water tank height

In figure 7-26 the behaviour of the system when the height of the water tank changes is illustrated. Greater ratios are achieved when the water tank is higher, but that increase doesn't appear to be that significant when other variable have favourable values. High enough ratios that would make the system efficient are also achieved when the height has smaller values of 1.00 or even 0.75 m.

The greatest ratios, which include the maximum of 4.39, appear when the tank has its largest height which is 1.5 m. In total, the two highest ratios are achieved when the tank has its maximum value.

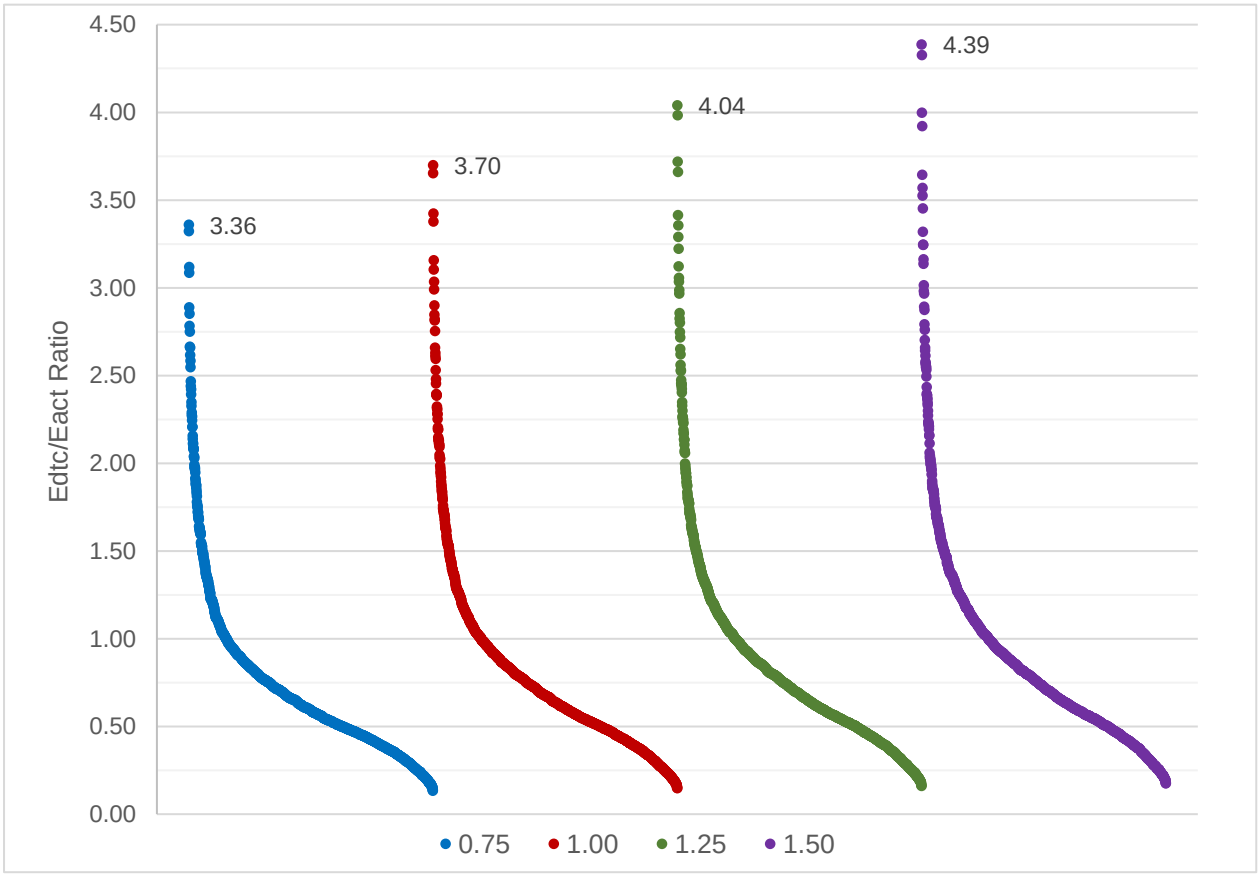

Figure 7-26. The E_{dtc}/E_{act} ratio of the simulations grouped by the value of the height of the water tank (m).

7.4.2. Passive cooler surface area

It is known from earlier stages that the passive cooler surface area is a detrimental factor for the ratio of the energy produced by the two coolers. This is reinforced by the data presented in figure 7-27. There it is very clearly shown that increasing the percentage of the area that the passive cooler occupies on the roof, has enormously beneficial effects to the increasing of the ratio.

The highest ratio achieved is, of course, when the surface area has its larger value, which is 50%. But more interesting is the fact that using an area of 40% gives a ratio equal, at the best case, to 3.01 that is much lower. For surface percentages equal to 30 and 20%, the highest achieved ratio is 2.00 and 1.24. In total, the 35 highest ratios are achieved when the passive cooler covers 50% of the roof.

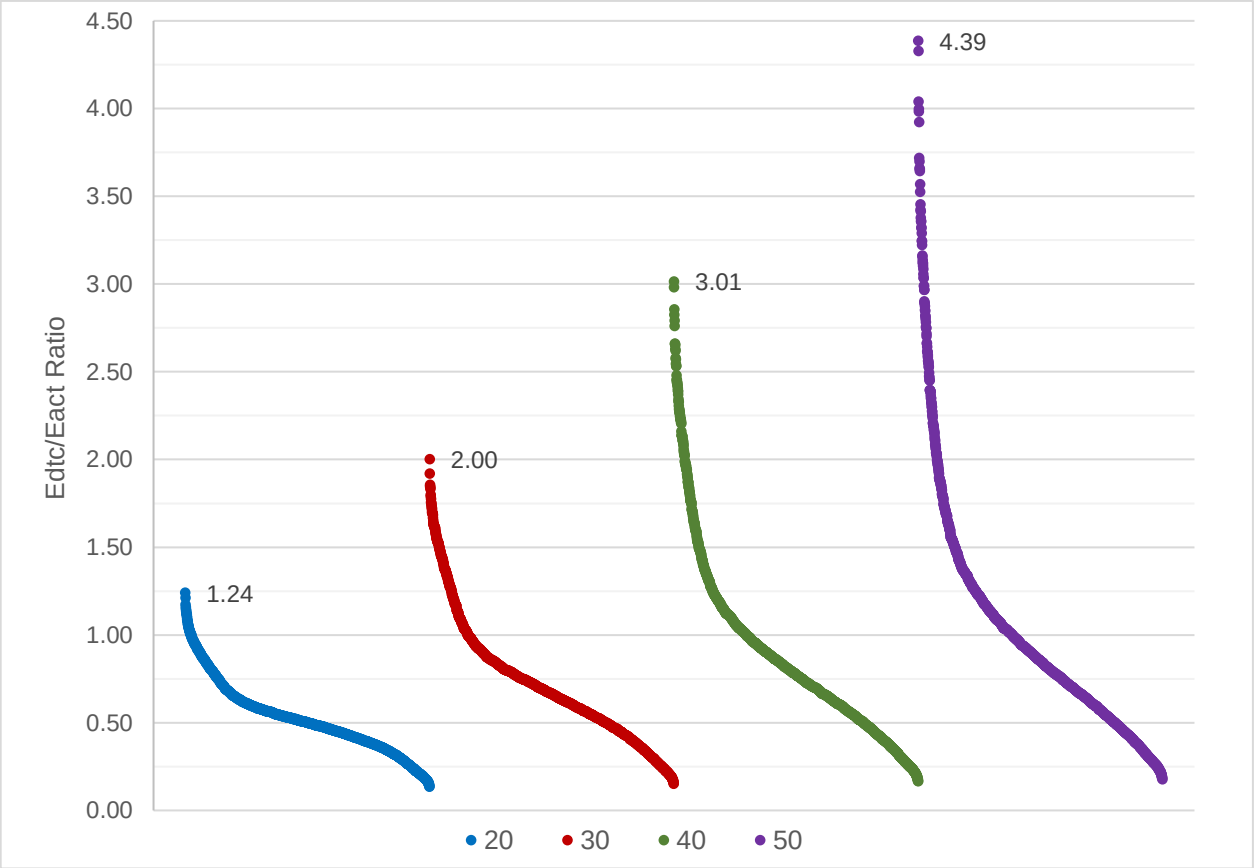

Figure 7-27. The E_{dtc}/E_{act} ratio of the simulations grouped by the value of the surface of the passive cooler (% of the roof area).

7.4.3. Shortwave transmission coefficient

How important it is for the shortwave transmission coefficient to be kept as close to 0 can be seen in figure 7-28. The gap between the highest achieved ratio, which is 4.39, between that group of cases and the rest of cases is huge. When the coefficient is equal to 0.05 the highest possible ratio is only 1.99.

It is clearly underlined, that one of the most important parameters influencing the efficiency of the system is to almost not have any transmission in shortwave frequencies. The 189 highest ratios are achieved when the shortwave transmission coefficient equals 0.

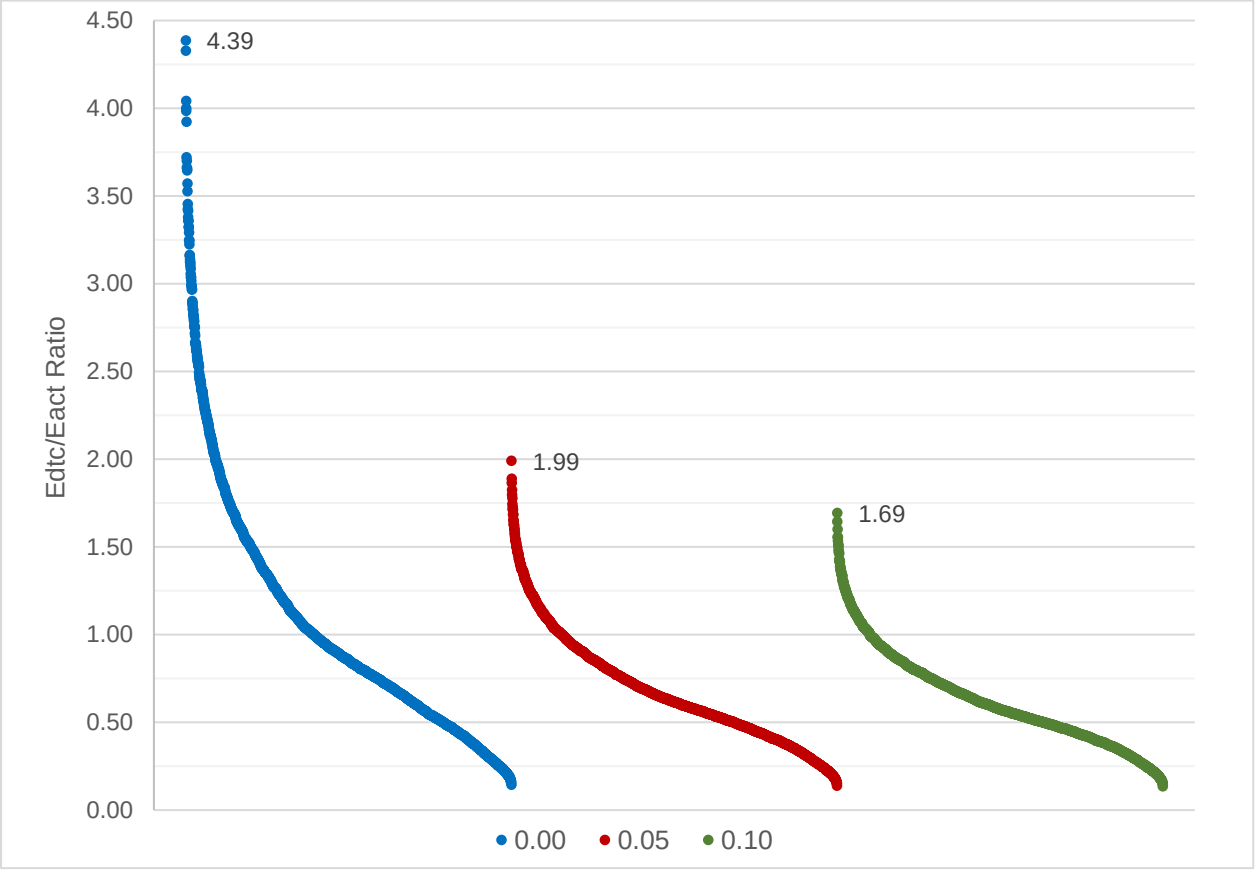

Figure 7-28. The E_{dtc}/E_{act} ratio of the simulations grouped by the value of the shortwave transmission coefficient.

7.4.4. Longwave coefficients

The coefficients related to longwave power are also important for the efficiency of the system as figure 7-29 shows. The higher the product of the longwave radiation transmission coefficient and the longwave emissivity coefficient is, the higher E_{dtc}/E_{act} ratios are achieved.

The three highest possible ratios are achieved when the product equals 1.00 while also significant ratios are achieved with lower values. In detail, when the product is reduced to 0.95, 0.90 and 0.85, the highest achieved ratio equals 4.00, 3.64 and 3.22 respectively. Those are ratios capable of maintaining a very efficient system which leads to the conclusion that lower values of the two coefficients can be tolerated.

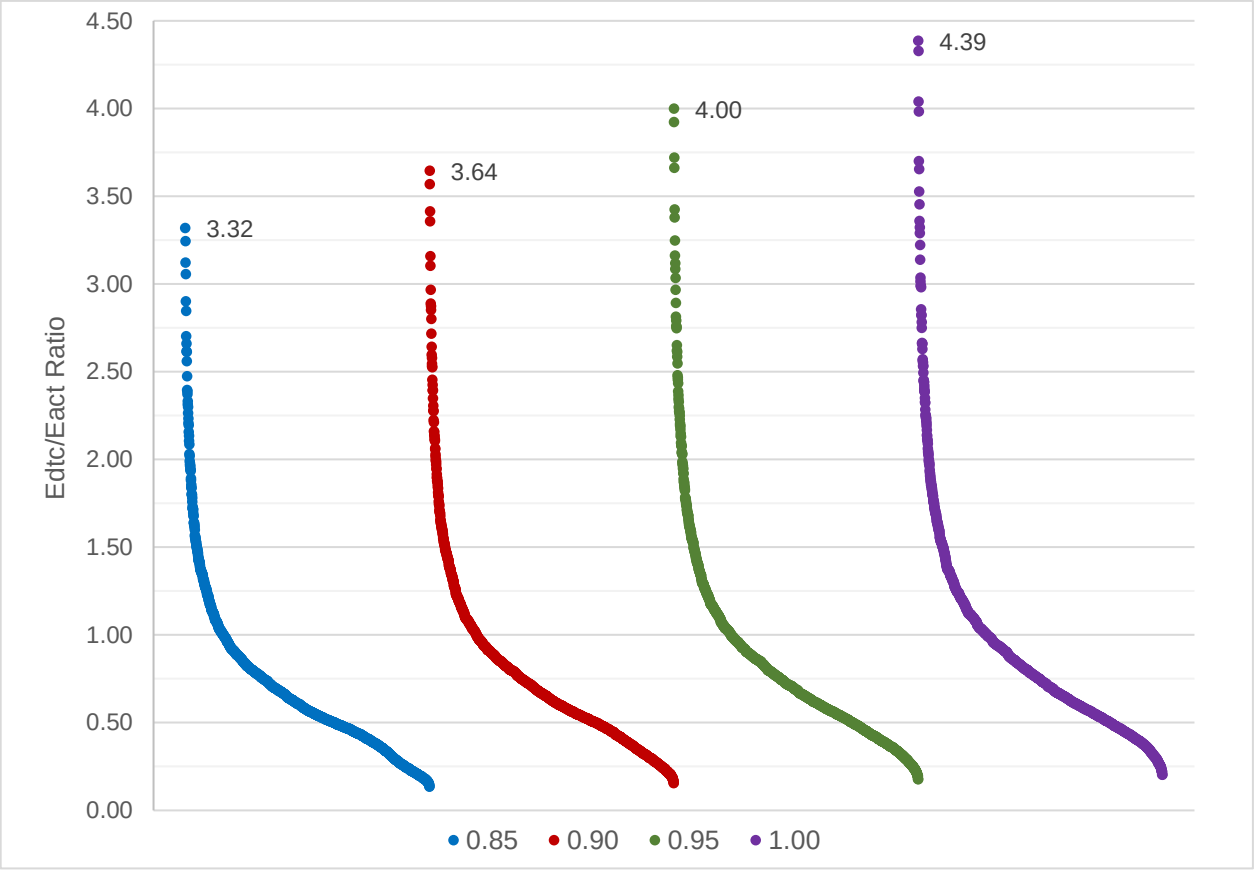

Figure 7-29. The E_{dtc}/E_{act} ratio of the simulations grouped by the value of the product of the longwave radiation transmission coefficient and the longwave emissivity coefficient.

7.4.5. Effective heat transfer coefficient

The effective heat transfer coefficient of the daytime cooler, which is related to the heat losses to the environment should have a value as low as possible and this is depicted in figure 7-30. Having a coefficient as low as 0.5 W/m^2 results in achieving the highest twelve possible E_{dtc}/E_{act} ratios.

Increasing the value of H_{dtc}, reduces the ratio. When it is equal to 1.0 W/m^2, the highest achieved ratio is 3.53 and when it is equal to 2.0 W/m^2 is 12.49. Those values are still high enough and could result in high energy savings. When the coefficient is increased further to 5.0 W/m^2, the ratio reaches a maximum of only 1.26 which is a low value.

Having an effective heat transfer coefficient, at least, lower than 2.0 W/m^2 is fundamental for the system to reach considerable energy savings.

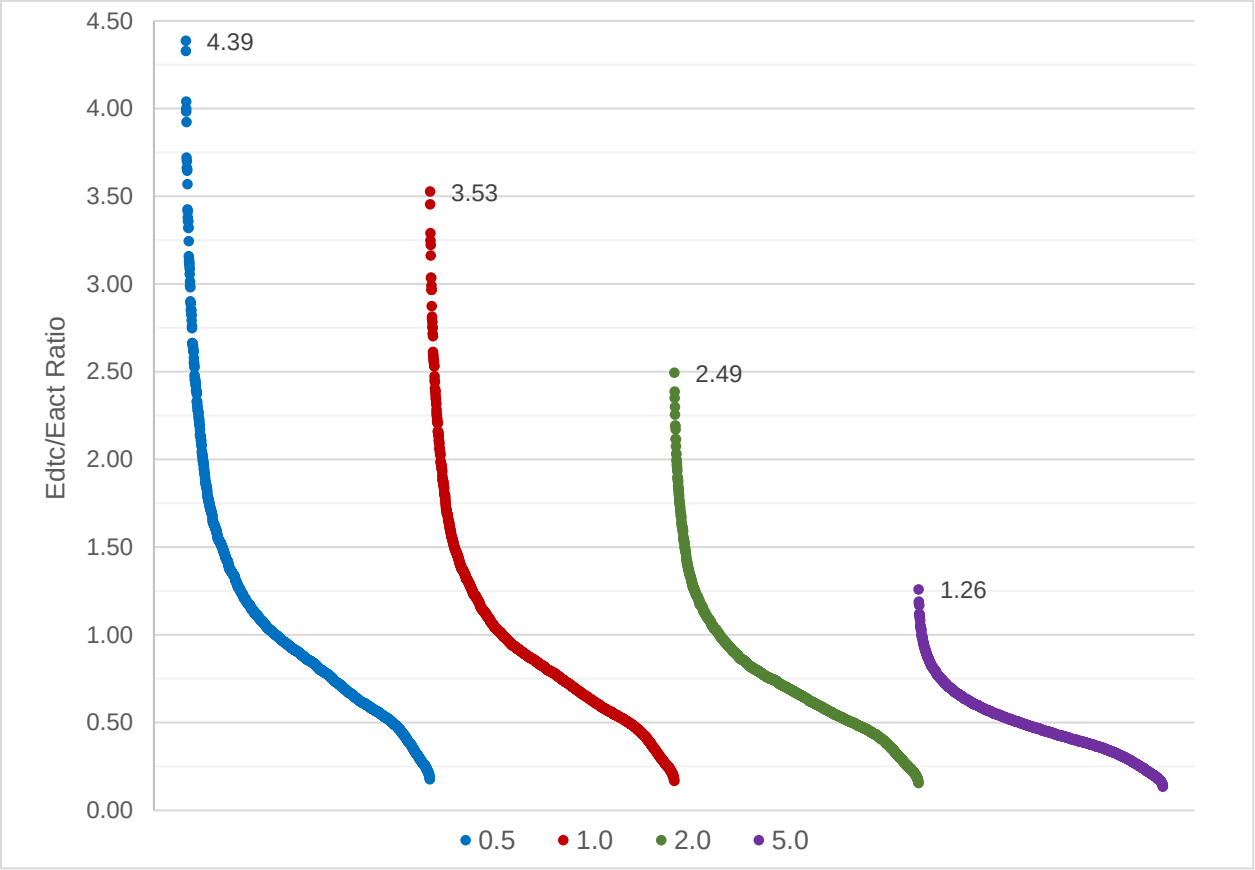

Figure 7-30. The E_{dtc}/E_{act} ratio of the simulations grouped by the value of the effective heat transfer coefficient (W/m²).

7.4.6. Specific mass flow rate of water in DTC

Figure 7.31 illustrates how reducing the value of the specific mass flow rate of water within the passive cooler results in higher passive energy production. The highest 27 possible ratios appear when the rate is equal to 0.001 kg/m²s that is the lowest investigated value in the varied analysis. The group of highest ratios for when this rate is used has significantly greater values than the respective groups for when larger rates are investigated.

Increasing the specific mass flow rate to 0.002, 0.003 and 0.004 kg/m²s gives a maximum ratio of 3.14, 2.24 and 1.55 respectively.

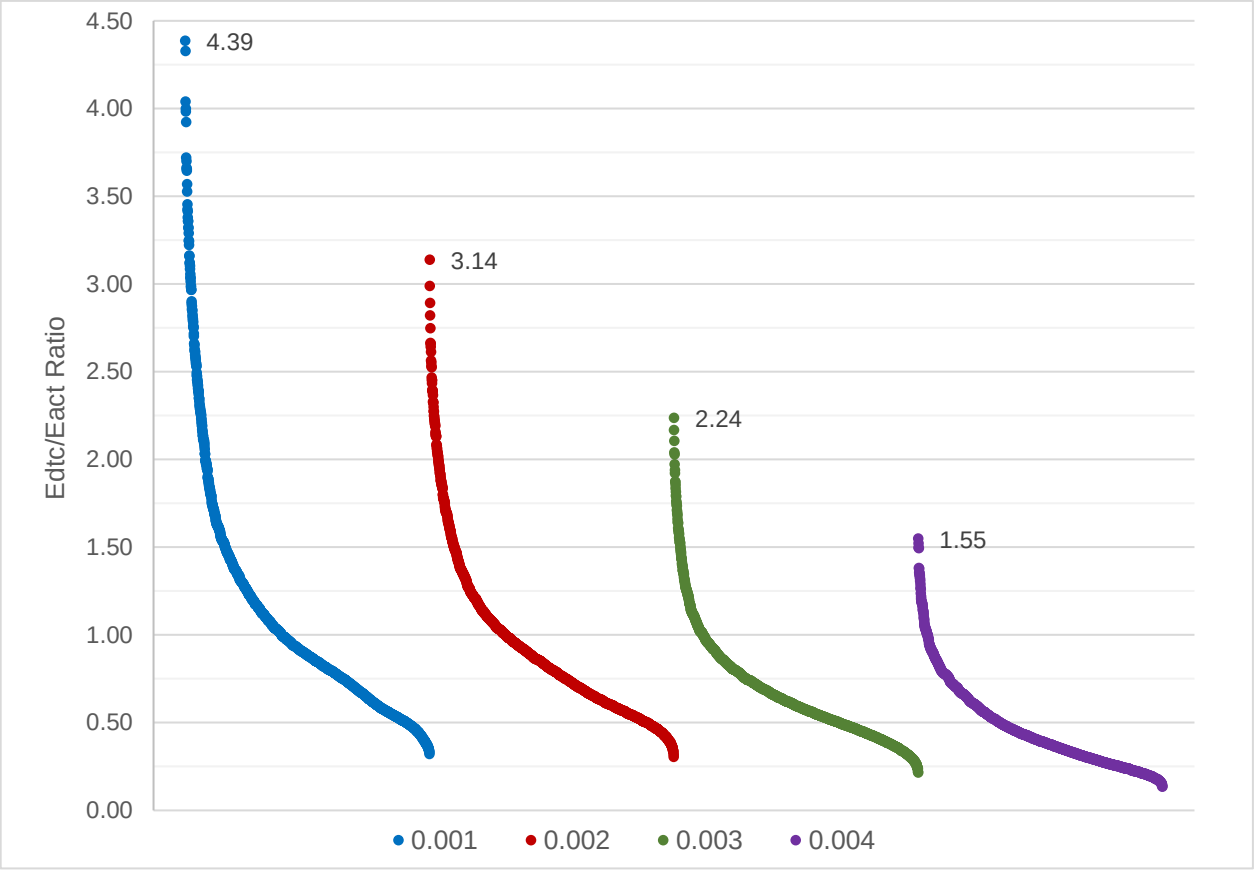

Figure 7-31. The Edtc/Eact ratio of the simulations grouped by the value of the specific mass flow rate within the daytime cooler (kg/m²s).

7.4.1. DTC-Buffer tank minimum temperature difference

The value for the minimum required temperature difference between the buffer tank and the daytime cooler seems to not influence significantly the ratio between the passive and active cooling produced energy. This is illustrated in figure 7-32 where one can see that having the lowest of the values, which is 2 °C, results in having an only slightly higher ratio.

The highest possible ratio of 4.39, occurs when the temperature difference is 2 °C. Increasing that difference to 3 °C results in a highest achieved ratio of 4.33 which is the second highest possible ratio. Both the temperature difference could lead to considerable energy savings.

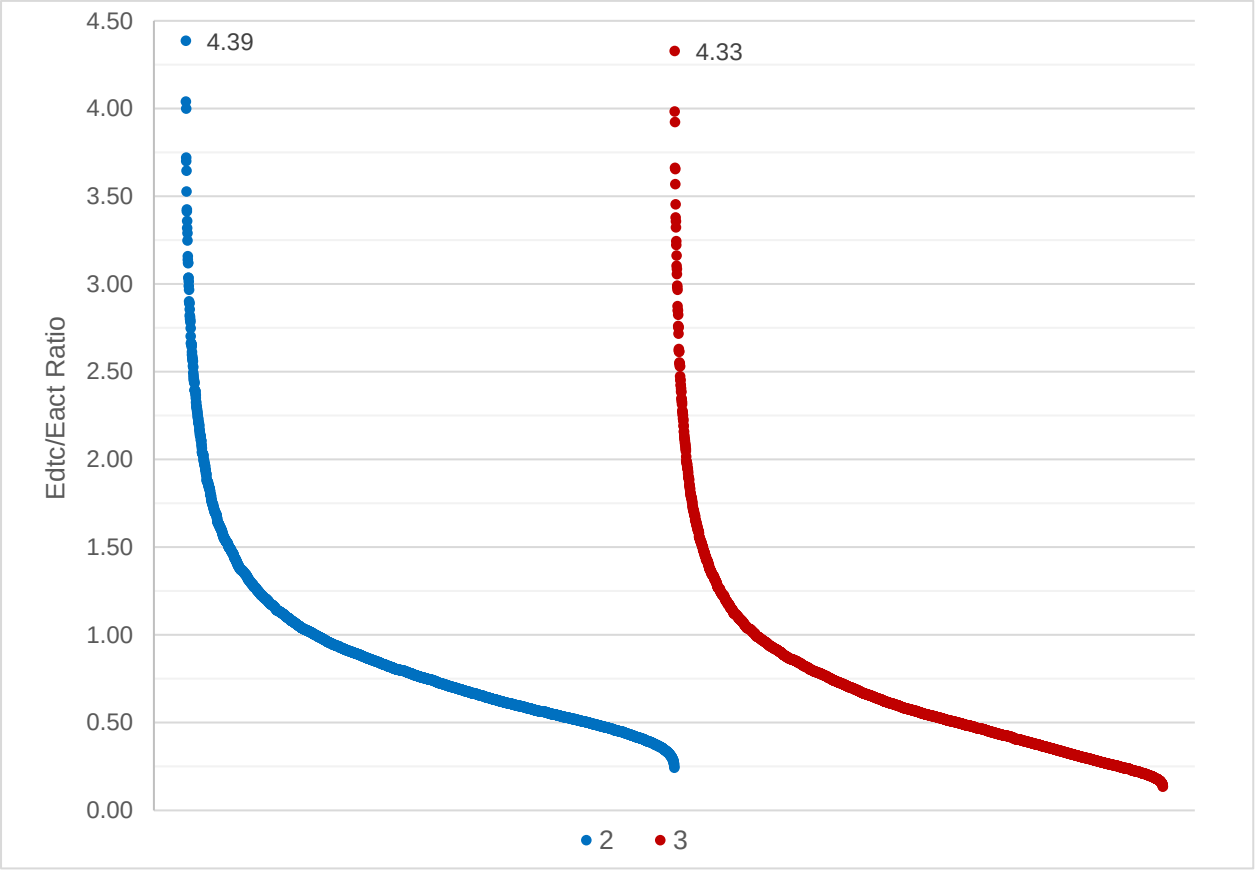

Figure 7-32. The Edtc/Eact ratio of the simulations grouped by the value of the minimum required temperature difference between the buffer tank and the daytime cooler (°C).

7.4.2. Summary

Summing up for the varied analysis, the highest possible ratio between the cooling energy produced by the passive cooler and the cooling energy produced by the active cooler is 4.39 and it occurs when the parameters investigated have the following values:

- h_{tank} = 1.5 m
- $A_{dtc,per}$ = 40%
- τ_{sw} = 0.00
- $\tau_{lw} \cdot \varepsilon_{lw}$ = 1.00
- H_{dtc} = 0.05 W/m²
- $\dot{m}_{dtc,sp}$ = 0.001 kg/m²s
- ΔT_{dtc} = 2 °C

8

Conclusions and recommendations

The sensitivity and varied analyses conducted, made it clear that for daytime radiative cooling to be effective, a number of variable parameters should have specific values. If those requirements are met, then a system as the one proposed could result in significant energy savings.

Cyprus which was chosen as the geographical field of application of this research appears to be ideal. This is a consequence of mostly its specific climate characteristics and average configuration of its dwelling stock. Applying daytime passive cooling cannot be realistic unless it is done in combination with using a supplementary active system.

In practice, applying such a hybrid system would require not only the passive cooler to be specifically designed but also other components of the system, such as the active cooler, the heat exchanger and the storage tank.

Further research in the topic is required to come closer into making daytime passive cooling a reality that would save large amounts of energy. In such a research, a more practical approach could be followed to investigate the engineering aspects of systems like that. In addition, investigating a higher number of parameters and values for them could provide with very useful information.

8.1. Findings

The sensitivity and completed varied analysis executed for this research to investigate the influence of the value of several parameters in the energy cooling results of a combined daytime passive and active cooling system that uses a water tank as a thermal storage medium gave some useful information on the capabilities of such a system, the significance of each parameter and the value that results in the highest energy savings.

Simulating the system in the varied analysis showed that when all the parameters have their favourable values, passive cooling energy that is more than four times the active cooling energy can be produced.

The height of the stratified tank in which the cooled water is stored should be as high as possible. This happens because the more the volume of the tank is, the more cooled energy can be stored that can be used when passive supply is not available.

The surface that the daytime radiative apparatus covers on the roof of the dwelling should also be as high as possible since the passive cooling energy production is directly proportional to it.

The shortwave transmission coefficient of the daytime cooler should have a value as close to 0 as possible in order to not transmit shortwave power at all. This value is unrealistic, even when considering recent technological advance. Keeping the coefficient close to 0.05 still results in significant energy savings.

The coefficients related to longwave power, which are the longwave radiation transmission coefficient and the longwave emissivity coefficient, should be as high as possible. Ideally, they should both be equal to 1 so that their product also equals 1. Values that give a product as low as 0.85 can still result in considerable passive energy production, when in combination with favourable values for other parameters.

The heat losses of the daytime cooler to the environment should be as low as possible for high energy savings to achieved. The effective heat transfer coefficient should ideally have a value of 0 W/m^2. Since this requires a perfectly insulated apparatus, which is hardly possible, keeping the value of the coefficient lower than 2.0 W/m^2 should be the realistic goal in such a design.

The specific mass flow rate of water inside the daytime cooler should be low. Values between 0.001 and 0.002 kg/m^2s would give the highest passive energy production.

The minimum required temperature between the water tank and the passive cooler that must be satisfied for the passive cooler to operate should be in the range of 0.5 to 2.0 °C. The value is not clear and according to the sensitivity analysis, values of 0.5 and 1.0 °C are ideal.

8.2. Conclusions

The system designed, simulated and investigated has very high application potential since it can result in very significant energy savings. The ratio of 4.39 between the energy produced by the daytime cooler and the energy produced by the active cooler, which is the highest occurred in the

simulations, means that in such a system, it is possible to cover more than 80% of the cooling load with passive produced energy.

Cyprus is an ideal field of application for such a system that takes advantage of the recent technological advance in wavelength selective-emittance material research mainly because of the long periods of clear skies it experiences. Serious energy savings can be achieved when a combination of design requirements is met.

Daytime radiative cooling cannot be successfully used without also the parallel use of an active cooling system. This could be possible only if a very large percentage of the roof area is utilised, very large storage tanks are used and daytime cooling equipment with excellent physical properties is realised. Still, the daily weather unpredictability would require an active system to exist as back-up.

The Mediterranean climate seems is ideal for applying such a system. The high average summer temperatures of the Mediterranean cities result in high cooling loads that can be covered, to a large extent, by daytime passive cooling. The influence of humidity is unclear.

8.3. Practical recommendations

A successful application of a cooling energy system that includes a daytime radiative cooler requires this cooler to have almost excellent physical properties related to its minimum transmission of shortwave power, maximum transmission of longwave power and minimum heat losses to the environment. In this research utilisation of such a cooler is made in combination with other elements.

Having a flat roof is detrimental for producing daytime cooling energy. Installing the apparatus in a sloped roof comes with a number of implications and limits importantly the capabilities of the system. Also, the system works much better when the roof-to-cooled-area ratio is high. This means that applying this cooling technique to buildings consisting of more than one floor would not lead to significant energy savings.

The equipment, besides the passive cooler per se, needed for the system to operate is a water tank, heat exchangers, an active cooler and piping between the several components. The water tank should be stratified and have a large enough volume, to the magnitude of 1 m^3 to be able to store sufficient amounts of cooled water for when there is not passive cooled energy supply; that is during nighttime and when there is not clear sky access. The heat exchangers that provide the spaces with cooled air must have high efficiency; in this research efficiency is set to be equal to 0.75. The active cooler that provides with supplementary cooling can be in the form of a split-air-conditioner and be centralised. It should also be efficient; here it is assumed that the temperature drop within the active cooler is 8 °C.

8.4. Further research recommendation

This research followed a theoretical approach which was reinforced by the use of Matlab Simulink as the main simulation tool. In further research on this topic, more practical approaches can be followed so that an ideal design of the daytime cooler itself, and of the whole system, can be determined. It

would be interesting to know how a cooler that meets all the physical requirements identified in this research is like and how difficult it is to realise it. Also combining all the elements of the system in an energy calculating software, such as EnergyPlus, to investigate their efficiency would also be a nice topic for further research.

A similar research as the one made, could be conducted using a wider range of values for the variable parameters and also investigating the significance of more parameters such as the ones related not only to the passive cooler, but also to the other elements of the system. This would be, of course, more time-consuming simulation-wise and would require more post-processing time and probably the use of more appropriate tools able to manage large amounts of data.

In addition, translating the passive and active energy production ratios, as identified in this research, into real electricity savings, when taking into consideration elements of the system as pumping, is a topic to be further researched.

References

Aowabin, R., Smith, A., & Fumo, N. (2015). Simplified modeling of thermal storage tank for distributed energy heat recovery applications.

Department of Meteorology. (2018). *The climate of Cyprus*. Retrieved 2018, from Department of Meterology: http://www.moa.gov.cy/moa/ms/ms.nsf/DMLcyclimate_en/DMLcyclimate_en?OpenDocument

Dincer, I., & Rosen, A. M. (2011). *Thermal energy storage: System and applications.* Wiley.

Economidou, M., Zangheri, P., & Paci, D. (2017). *Long-term strategy for mobilizing investments for renovating Cyprus national building stock.* Joint Research Center of the European Commission.

Ekechukwu, V., & Onyegegbu, S. (2014). Analysis of stratified thermal storage systems: An overview. *Heat and mass transfer*.

Ezekwe, C. I. (1990). Performance of a heat pipe assisted night sky radiative cooler. *Energy corners, 30*(4), 403-408.

Hossain, M., Jia, B., & Gu, M. (2015). A metamaterial emitter for highly efficient radiagive cooling. *Advanced optical materials, 3*, 1047-1051.

Kecebas, A. M., Menguc, M. P., Kosar, A., & Sendur, K. (2017). Passive radiative cooling design with broadband optical thin-film filters. *Journal of quantitative spectroscopy & Ratiative transfer, 198*, 179-186.

Kou, J.-l., Jurado, Z., Chen, Z., Fan, S., & Minnich, A. J. (2017). Daytime Radiative Cooling Using Near-Black Infrared Emitters. *ACS Photonics, 4*, 626-630.

Lee, H., Kim, T., Tolessa, M. F., & Cho, H. H. (2017). Enhancing radiative cooling performance using metal-dielectric-metal metamaterials. *Journal of mechanical science and technology, 31*(11), 5107-5112.

MCIT (Ministry of Energy, Commerce, Industry and Tourism). (2013). *Calculation for Setting the Minimum Energy Performance Requirements at Cost Optimal Levels According to Article 5 of the Directive 2010/31/EE for the Energy Performance of Buildings (recast).*

Menicou, M., Exizidou, P., Vassiliou, V., & Christou, P. (2015). An economic analysis of Cyprus' residential. *International Journal of Sustainable Energy*, 166-187.

Michael, A., Demosthenous, D., & Philokyprou, M. (n.d.). Natural ventilation for cooling in mediterranean climate: A case studyin vernacular architecture of Cyprus. *Energy and Buildings, 144*, 333-345.

Panayiotou, G., Kalogirou, A. S., Maxoulis, N. C., & Florides, A. G. (2010). Cyprus building energy performance methodology: A comparison of the calculated and measured energy consumption results.

Raman, A. P., Anoma, M. A., Zhu, L., Rephaeli, E., & Fan, S. (2014). Passive radiative cooling below ambient air temperature under direct sunlight. *Nature, 515*, 540-544.

Rephaeli, E., Raman, A., & Fan, S. (2013). Ultraboradband photonic structures to achieve high-performance daytime radiative cooling. *Nano letters, 13*, 1457-1461.

Suichi, T., Ishikawa, A., Hayashi, Y., & Tsuruta, K. (2019). Performance limit of daytime radiative cooling in warm humid environment. *AIP Advances, 8*.

Vall, S., & Castell, A. (2017). Radiative cooling as low-grade energy source: A literature review. *Renewable and Sustainable Energy Reviews, 17*, 203-820.

Van der Linden, A. C., Erdtsieck, P., Kuijpers, V. G., & Zeegers, A. (2017). *Buiding physics.* ThiemeMeulnhoff.

WIlson, G., Zunica, I., Fairen, V., & Otto, D. (2012). Module 1: Introduction to climate change in the context of sustainable development TEXTBOOK T869 Climate Change: from science to lived experience.

Wu, D., Liu, C., Xu, Z., Liu, Y., Yu, Z., Yu, L., . . . Li, R. (2018). The design of ultra-broadband selective near-perfect absorber based on. *Materials and Design, 139*, 104-111.

Yang, P., Chen, C., & Zhang, Z. M. (2018). A dual-layer structure with record-high solar reflectance for daytime. *Solar Energy, 169*, 316-324.

Zeyghami, M., Goswami, D. Y., & Stefanakos, E. (2018). A review of clear sky radiative cooling developments and applications in. *Solar Energy Materials and Solar Cells, 178*, 115-128.

Zhai, Y., Ma, Y., David, S. N., Zhao, D., Lou, R., Tan, G., . . . Yin, X. (2017). Scalable-manufactured randomized glass-polymer hybrid metamaterial for daytime radiative cooling. *Science*.

Zhang, K., Zhao, D., Yin, X., Yang, R., & Tan, G. (2018). Energy saving and economic analysis of a new hybrid radiative cooling. *Applied Energy, 224*, 371-381.

Appendix A: Matlab script

Water properties:

The first thing given as input to the script is the characteristics of water, in which density, specific heat capacity and heat conduction coefficient is included, as follows:

```
% Characteristics of the water
water.rho = 1000;           % density, kg/m3
water.c   = 4280;           % spec. heat capacity, J/kgK
water.la  = 0.6;            % heat conduction coefficient, W/mk
```

Water tank:

Next, the properties related to the water buffer tank are given. They include geometrical parameters as well as the U-value of the tank, an effective conduction coefficient for free convective mixing, the number of water layers or nodes in the tank and the initial temperature in all free nodes.

```
% Geometry
water.r = 0.5;              % radius water column in tank (diameter = 2*r)
water.h = 1.5;              % height water column in tank
water.A = pi*water.r^2;     % surface area horizontal cross-section of tank
                            % (water), m2 (v=water.A*water.h)

tank.U  = 0.285;            % U-value of tank insulation (bottom, top and side)
                            % with respect to tank inside surface area

% For unstable temperature stratification, the mixing due to free convective
% flows is modelled as conductive transfer.
% the effective 'conduction' coefficient for free convective mixing is given
% here:
water.la_mixing = 1000;

T_tank_init = 18;    % Start temperature in all free nodes

nodes_tank = 10;     % Number of water layers (nodes) in the tank
```

Dwelling:

Regarding the dwelling, the Matlab input includes the area of its cooled spaces, the area of the roof which is the area available for the installation of the DTC equipment and its maximum cooling load. The latter is used later in the script in relevance to the active cooler properties. The script is as follows:

```
% Specifications for dwelling
A_room = 83.5;                  % Cooled area of the dwelling, m2
A_roof = 152.6;                 % Area of the roof, m2
P_cool_room_max = xlsread('input.xlsx','max_cool_load','A1'); % Maximum
                                % (negative value) cooling load of room, W/m2
```

Daytime radiative cooler:

The input for the passive daytime cooler in the Matlab script includes the area of the DTC, the transmission, emissivity and heat transfer coefficients, the mass flow rate of water through the cooler and the minimum required temperature between the buffer and the DTC. The input is as follows:

```
% Specifications for the daytime cooler
A_dtc_per    = 0.4;              % surface area of daytime cooler as a
                                 % percentage of the roof area
A_dtc = A_dtc_per*A_roof;        % surface area of daytime cooler, m2
H_dtc        = 0.5;              % effective heat transfer coefficient from
                                 % liquid in cooler to outside, W/m2K
tau_sw       = 0.05;             % transmission coefficient foil for shortwave
                                 % radiation
tau_lw       = 0.95;             % transmission coefficient foil for longwave
                                 % radiation
eps_lw       = 1;                % longwave emissivity coefficient of cooled
                                 % surface in daytime cooler
mdot_dtc_sp = 0.003;             % specific mass flow rate of water through
                                 % daytime cooler, kg/m2/s
mdot_dtc = A_dtc*mdot_dtc_sp;    % mass flow rate of water through daytime
                                 % cooler, kg/s
deltaT_dtc   = 2;                % minimum required temperature difference
                                 % between the top temperature of the buffer
                                 % tank and the outgoing dtc temperature
                                 % charging the buffer with cold water from
                                 % the daytime cooler
holdtime_dtc = 1800;             % once the condition for water flow between
                                 % the daytime cooler and the buffer tank is
                                 % met, this water flow is at least held for
                                 % this amount of time
```

Active cooler:

For the active cooler the script input is shown below. Here, the water temperature drop inside the cooler is given as input.

```
% Specifications for active cooler
deltaT_act = 8;                                  % Water temperature drop in
                                                 % the active cooler
```

Heat exchanger:

Regarding the heat exchanger, its only parameter given as input is its efficiency, as follows:

```
% Specifications for heat exchanger
eff_exch = 0.75;      % Efficiency of the heat exchanger
```

Simulation times:

Last part of the input is the simulation times. Here the simulation start and stop times are given as input. The total simulation time corresponds to the period from the start of April until the end of October that is approximately the cooling period of the season. The simulation doesn't take place for the whole year as this is, firstly, unnecessary and it will, secondly, increase the simulation times.

```
% Simulation times
start_time = 10.368e6;          % Start of April
stop_time  = 26.265e6;          % End of October
```

Water tank modelling:

Last in the Matlab model, are the definitions related to the modelling of the stratified energy storage tank. Those start by defining the number of nodes related to the tank:

```
nkl_tank = nodes_tank;         % number of free nodes room
nkv_tank = 3;                  % number of fixed nodes (environmental
                               % temperature and incoming water temperatures)
nk_tank  = nkl_tank+nkv_tank; % total number of nodes in water column

nnr_bot     = 1;               % node number bottom node water column
nnr_top     = nkl_tank;        % node number top node water column
nnr_env     = nkl_tank+1;      % node number environmental temperature
nnr_in_bot  = nkl_tank+2;      % node number incoming water temperature at
                               % the bottom
nnr_in_top  = nkl_tank+3;      % node number incoming water temperature at
                               % the top
```

Then the mass matrix is defined as follows:

```
%definition of mass matrix
M_tank=zeros(nkl_tank);
for k=1:nkl_tank
    M_tank(k,k)= water.rho*water.c*water.A*water.h/nkl_tank;
    % mass is rho*c*volume [J/K]
end
```

The conductivity values between the several nodes are defined using the following script:

```
% define the 'conductivity' values between the nodes
% matrix Y(i,j) contains de conductivity between node i and j where i<j
% use an imaginary number for a direction-dependent flow element
% for example flow from 1 to 3: Y(1,3)=20i
% use a negative number for a reversed flow
% for example flow from 3 to 1: Y(1,3)=-20i
h_node = (water.h/(nkl_tank-1));
Y_tank=zeros(nk_tank);
for k=1:nnr_top-1
    Y_tank(k,k+1) = water.la*water.A/h_node;
end
Y_tank(nnr_bot,nnr_env)  = tank.U*water.A + tank.U*2*pi*water.r*h_node;
for k=nnr_bot+1:nnr_top-1
    Y_tank(k,nnr_env)    = tank.U*2*pi*water.r*h_node;
end
Y_tank(nnr_top,nnr_env)  = tank.U*water.A + tank.U*2*pi*water.r*h_node;
```

Next, an empty initial stiffness matrix is defined using a subroutine from another Matlab model, called 'fillS'. This model is presented later.

```
% create empty initial stiffness matrix with nk_tank rows and columns
Si_tank = zeros(nk_tank);
% fill initial stiffness matrix with values
```

```
% first row is node 1
% second row is node 2
% etc
for i=1:nk_tank-1
   for j=i+1:nk_tank
      Si_tank=fillS(Si_tank,Y_tank,i,j);  %subroutine is in fillS.m
   end
end
% definition of stiffness matrix to be used in the Simulink model
% part of Si that reflects the free nodes only
S_tank = Si_tank(1:nkl_tank,1:nkl_tank);
% the part Si(1:nkl_tank,nkl_tank+1:nk_hall) relates to the fixed nodes and
% is used separately in the Simulink model
S_tank_fixed = Si_tank(1:nkl_tank,nkl_tank+1:nk_tank);
```

The next step includes the definition of the time-depended adjective flows. This is done in two parts. The first part is relevant to the upward water flow in the tank while the second part to the downward water flow:

```
% Definition of (time-dependent) advective flows

% pre-input for stiffness matrix part 1, upward water flow in tank,
% in Simulilnk multiplied with Q_bottom_in
Y_tank_c1=zeros(nk_tank);
Y_tank_c1(nnr_bot,nnr_in_bot) = water.c*(-1i);
for k=nnr_bot:nnr_top-1
    Y_tank_c1(k,k+1)          = water.c*(1i);
end
% fill initial stiffness matrix for non-linear part 1 with values
% constants in the variable part of the stiffness matrix
Si_tank_c1_var = zeros(nk_tank);
for i=1:nk_tank-1
   for j=i+1:nk_tank
      Si_tank_c1_var=fillS(Si_tank_c1_var,Y_tank_c1,i,j);
      %subroutine in fillS.m
   end
end
% definition of stiffness matrix for non-linear part 1, to be used in the
% Simulink model
% only the first nkl_tank rows of Si_tank_c1_var are used, all columns are
% maintained
S_tank_c1_var = Si_tank_c1_var(1:nkl_tank,:);


% pre-input for stiffness matrix part 2, downward water flow in tank, in
% Simulilnk multiplied with Q_top_in
Y_tank_c2=zeros(nk_tank);
Y_tank_c2(nnr_top,nnr_in_top) = water.c*(-1i);
for k=nnr_bot:nnr_top-1
    Y_tank_c2(k,k+1)          = water.c*(-1i);
end
% fill initial stiffness matrix for non-linear part 2 with values
% constants in the variable part of the stiffness matrix
Si_tank_c2_var = zeros(nk_tank);
for i=1:nk_tank-1
   for j=i+1:nk_tank
      Si_tank_c2_var=fillS(Si_tank_c2_var,Y_tank_c2,i,j);
```

```
      %subroutine in fillS.m
   end
end
% definition of stiffness matrix for non-linear part 2, to be used in the
% Simulink model
% only the first nkl_tank rows of Si_tank_c2_var are used, all columns are
% maintained
S_tank_c2_var = Si_tank_c2_var(1:nkl_tank,:);
```

Last part of the Matlab script, includes a pre-input for free convective mixing and the creation of a help matrix as follows:

```
% pre-input for free convective mixing
S_tank_c3_var = zeros(nkl_tank,nkl_tank,nkl_tank);
for k=1:nkl_tank-1
    S_tank_c3_var(k,k,k)     =  water.la_mixing*water.A/h_node;
    S_tank_c3_var(k,k+1,k)   = -water.la_mixing*water.A/h_node;
    S_tank_c3_var(k+1,k,k)   = -water.la_mixing*water.A/h_node;
    S_tank_c3_var(k+1,k+1,k) =  water.la_mixing*water.A/h_node;
end
% Create a help matrix the select elements from vector T_free
K_help = zeros(nkl_tank);
for i=1:nkl_tank-1
    K_help(i,i+1) = 1;
end
```

The script of the subroutine of the separate file 'fillS', mentioned earlier, is as follows:

```
function filled=fillS(S,Y,i,j)
if imag(Y(i,j))==0 % 'conduction' element
    S(i,i)=S(i,i)+Y(i,j);
    S(i,j)=S(i,j)-Y(i,j);
    S(j,i)=S(j,i)-Y(i,j);
    S(j,j)=S(j,j)+Y(i,j);
elseif imag(Y(i,j))> 0 % flow from i to j
    S(j,i)=S(j,i)-imag(Y(i,j));
    S(j,j)=S(j,j)+imag(Y(i,j));
elseif imag(Y(i,j))< 0 % flow from j to i
  S(i,i)=S(i,i)-imag(Y(i,j));
  S(i,j)=S(i,j)+imag(Y(i,j));
end
if Y(i,j) < 0
   error('Negative admittance not allowed')
end
filled=S;
```

Appendix B: Simulink model

Data input:

In figures B-1 and B-2 the blocks related to the five inputs from the Excel file are presented. Three of the inputs come directly from the climate data provided by EnergyPlus while the rest two come from the DesignBuilder simulation. All five of them are values per time step, for the whole year. The five inputs are:

- From EnergyPlus (time step = 1 hour):
  - Incoming longwave radiation, W/m^2
  - Incoming shortwave radiation, W/m^2
  - Outside dry-bulb air temperature, °C
- From DesignBuilder (time step = 10 min):
  - Dwelling cooling load, W/m^2
  - Dwelling temperature, °C

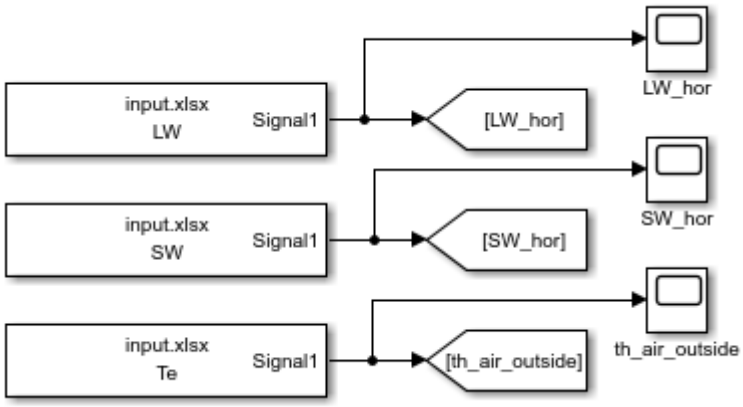

Figure B-8-1. Input of EnergyPlus hourly weather data from Excel file.

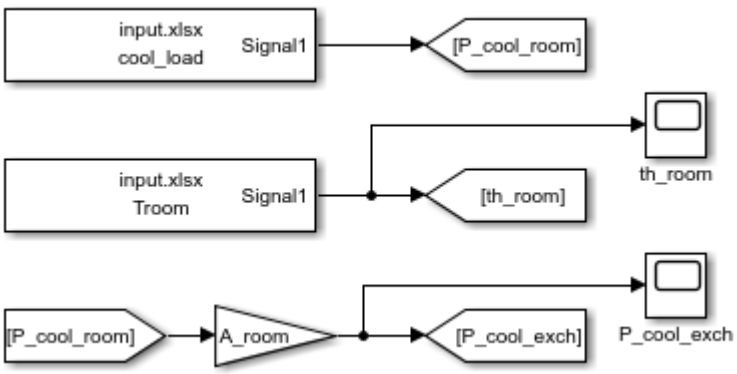

Figure B-8-2. Input of DesignBuilder simulation data from Excel file.

The cooling load of the dwelling is given in W/m^2 so it is multiplied by the cooled area of the dwelling in order for the load unit to be watts.

Mass flow rate and temperature of flows:

The next set of blocks of the Simulink model are related to the mass flow rate of water into the buffer tank and to the temperature of flows towards the passive and active coolers, the heat exchanger and the buffer tank.

In figure B-3, the set relevant to the volumetric flows towards the tank are shown. Here, the mass flow to the bottom of the water tank equals the sum of the flows of the two coolers while the mass flow to the top of the tank equals the flow of the heat exchanger.

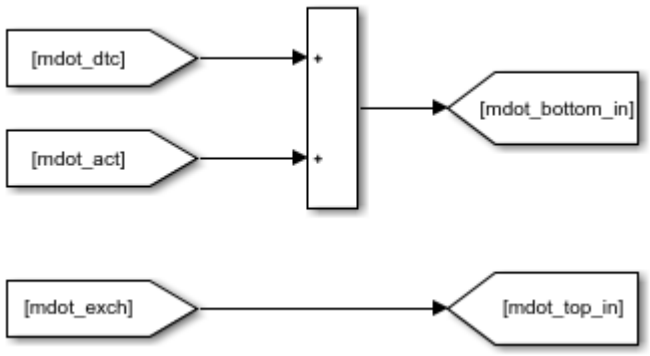

Figure B-8-3. Mass flow rates into the buffer tank.

The set of blocks related to the temperature of water flows into the passive and active coolers and into the heat exchanger are shown in figure B-4. The incoming temperature of water to the two coolers equals the temperature at the top of the water tank while the respective temperature of the heat exchanger equals the temperature at the top of the water tank.

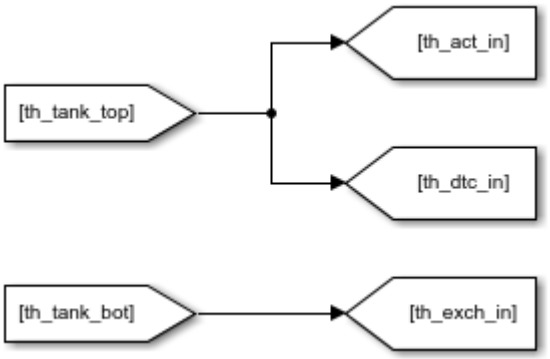

Figure B-8-4. Temperature of water flows towards the two coolers and the heat exchanger.

The blocks in figure B-5 describe the incoming temperature of water flows at the bottom and at the top of the water tank. If there is no incoming water flow at the bottom of the water tank, then its

respective temperature equals zero. If there is a flow, its temperature is calculated with the following equation:

$$\theta_{bot,in} = \frac{\dot{m}_{dtc} \cdot \theta_{dtc,out} + \dot{m}_{act} \cdot \theta_{act,out}}{\dot{m}_{bot,in}} \quad (28)$$

Where: $\theta_{bot,in}$ = Temperature of ingoing water to the buffer tank, °C

$\dot{m}_{bot,in}$ = Mass flow of water to the bottom of the buffet tank, kg/s

The temperature of ingoing water to the top of the tank equals the temperature of the outgoing water from the heat exchanger.

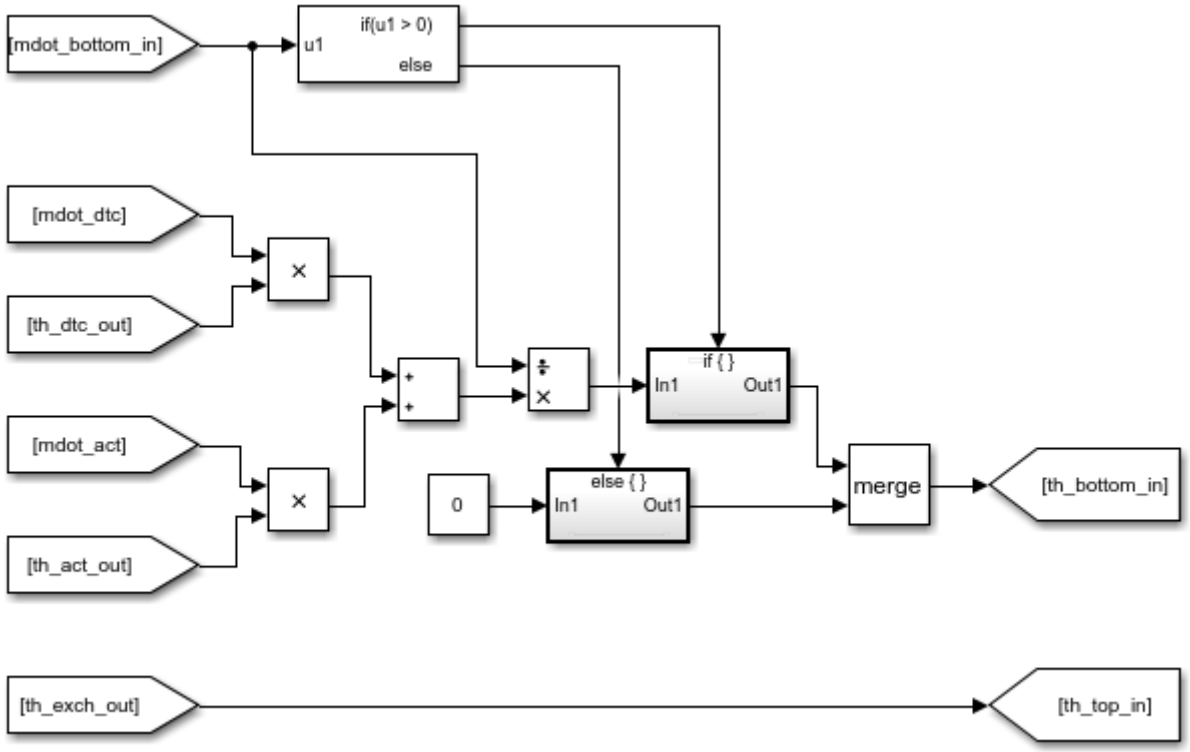

Figure B-8-5. Temperature of flows towards the buffer tank.

Daytime radiative cooler:

The set of blocks related to the DTC physics can be seen in the following figures. Figure B-6 shows the calculation of the cooling rate of the DTC and of its outgoing water temperature using the equations 13 to 16 presented in section 6.2.2. The two lines extending at the top of this figure lead to the lines of figure B-7, where the control of flow rate from the DTC to the buffer tank takes place. Here the DTC provides water to the tank only if its outgoing temperature of water is lower by a certain amount of degrees from the temperature at the top of the water tank. There is a changed signal held for a certain period, for simulation purposes, presented in figure B-8.

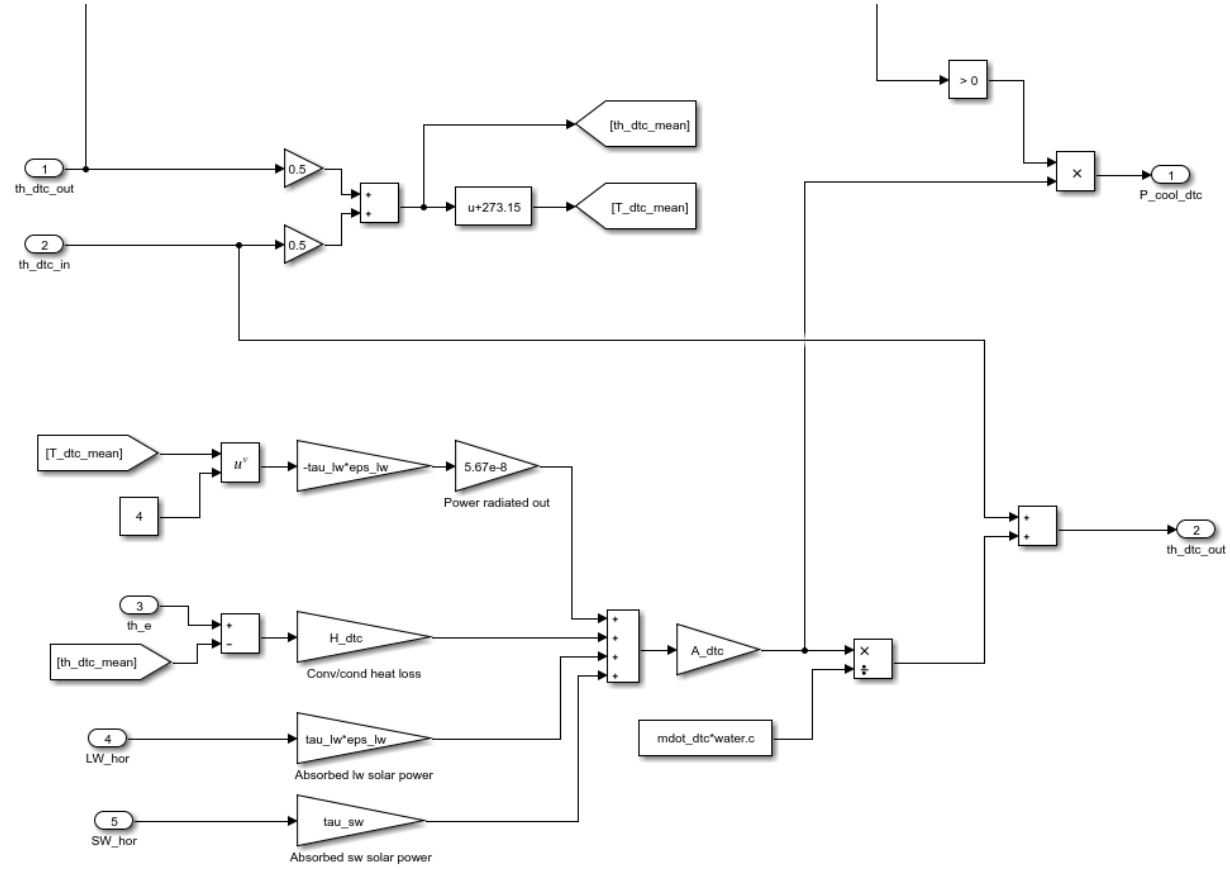

Figure B-8-6. Heat balance of the daytime radiative cooler.

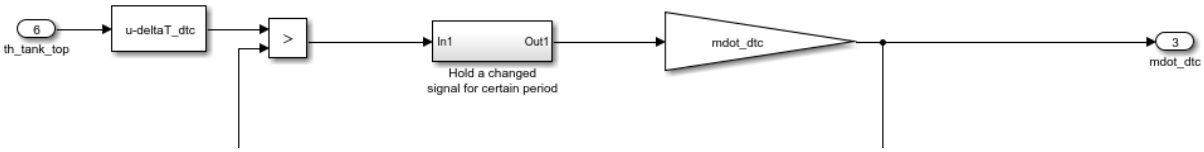

Figure B-8-7. Control of flow of water from the DTC to the buffer tank.

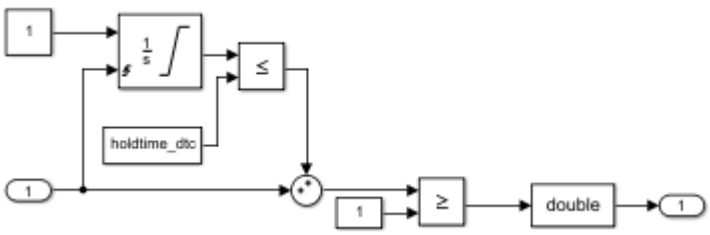

Figure B-8-8. Changed signal held for a certain period.

Active cooler:

The outgoing temperature of the active cooler and the mass flow rate within it are calculated using the blocks shown in figure B-9. Equations 19 and 20 are used for the respective calculations. The line extending at the top of this figure leads to the line starting at the bottom of figure B-10, where the blocks related to the control mechanism of the active cooler are shown. Here two situations should be satisfied for the active cooler to be operative:

1 The ingoing temperature of the heat exchanger should be close to a setpoint temperature. This is possible using the 'relay' block which gives an output of 1 when the temperature is between 18.5 and 19.5°C. This corresponds to a setpoint temperature of 19°C with a bandwidth of 1°C. An output of 0 is given elsewise.

2 The cooling power of the heat exchanger, which is the cooling demand of the dwelling, should be lower than zero. This means that there should be a cooing demand at the moment.

When the active cooler is operative, its cooling rate equals the current cooling demand hence the active cooler always operates on its maximum capacity. When non operative, its cooling rate and mass flow equal zero.

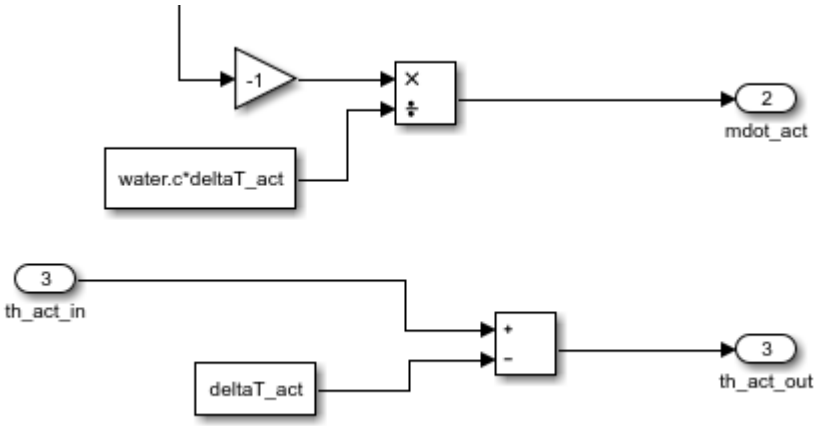

Figure B-8-9. Calculation of mass flow and outgoing water temperature of the active cooler.

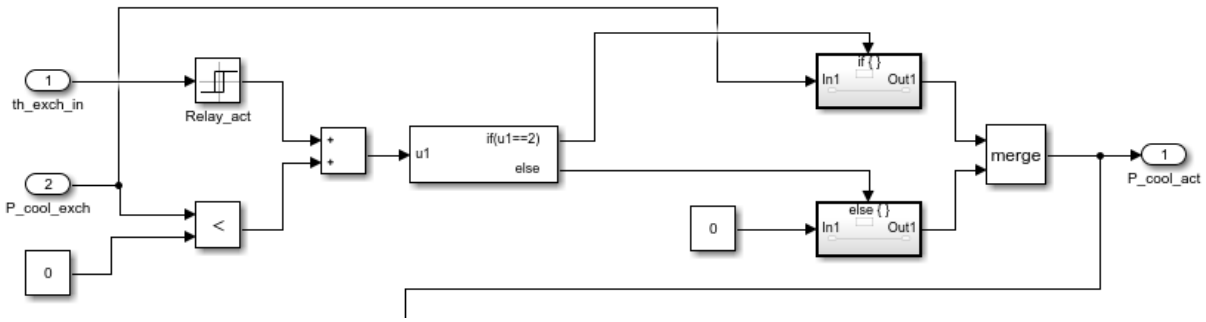

Figure B-8-10. Control mechanism of the active cooler.

Heat exchanger:

Regarding the heat exchanger, its mass flow rate and outgoing water temperature are calculated using the set of blocks presented in figure B-11. Equations 17 and 18 are used for these calculations.

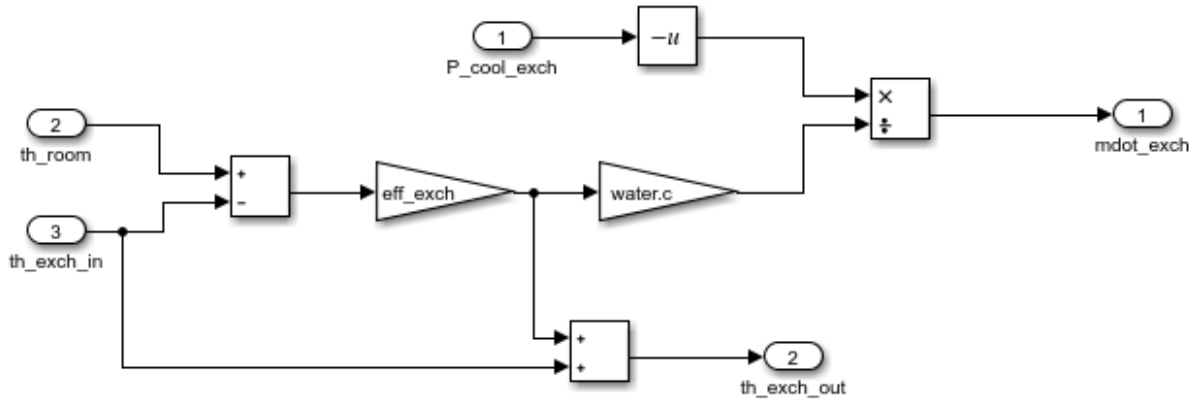

Figure B-8-11. Simulink blocks related to the heat exchanger.

Water tank:

The set of blocks used to calculate the temperature ate the top and at the bottom of the water tank can be seen in figure B-12. The tank is modelled as a stratified energy storage water tank and the time-depended signals used as input are the outside dry-bulb air temperature and the incoming temperatures at the bottom and at the top of the tank. The last two temperatures, as mentioned earlier are the temperatures of the flows from the two coolers and from the heat exchanger respectively. The subsystem in which the advective flows are calculated is shown in figure B-13 while the subsystem related to the free convective mixing is shown in figure B-14.

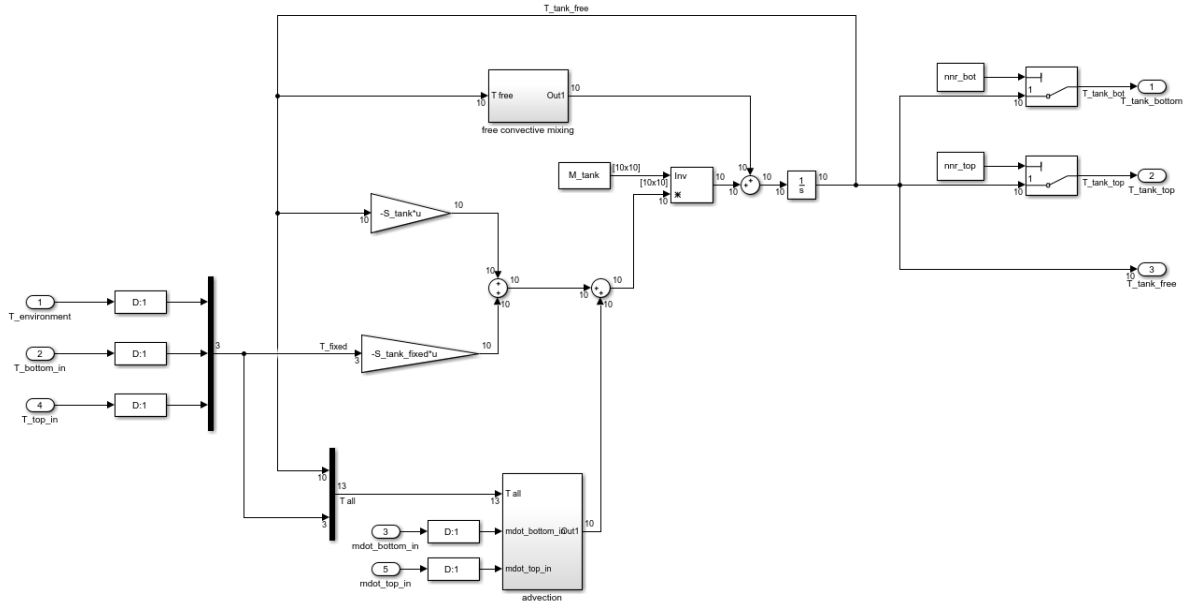

Figure B-8-12. Subsystem calculating the temperature at the top and bottom of the water tank

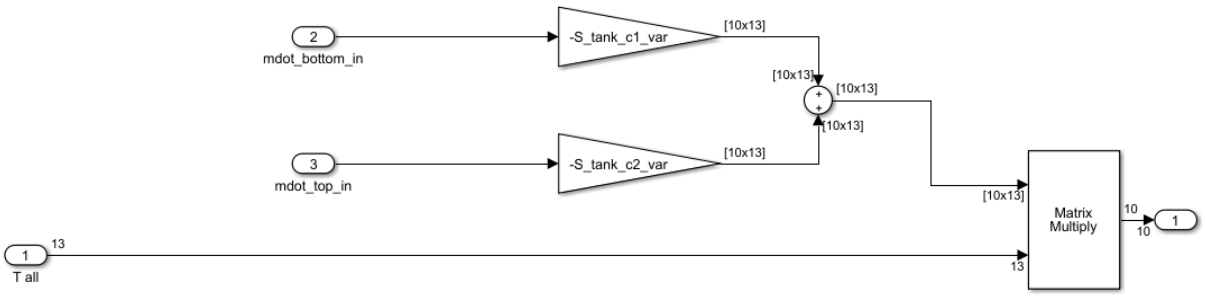

Figure B-8-13. Subsystem calculating the advective flows in the water tank.

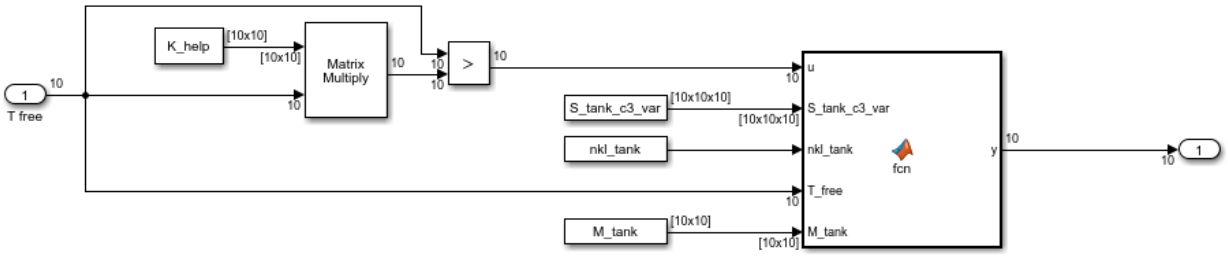

Figure B-8-14. Free convective flows subsystem of the water tank.

The convective mixing subsystem contains a Matlab function, the script of which is the following:

```
function y = fcn(u, S_tank_c3_var, nkl_tank,T_free,M_tank)

m = zeros(nkl_tank);
for i=1:nkl_tank-1
    m = m + u(i)*S_tank_c3_var(:,:,i);
end
y = -M_tank\(m*T_free);
```

Appendix C: Sensitivity analysis values

The following table shows the values that are investigates for each variable parameter for the sensitivity analysis.

Variable	Unit	Values															
h_{tank}	m	0.50	0.75	1.00	1.25	1.50	1.75	2.00	2.25	2.50							
A_{dtc}	%	10	20	30	40	50	60	70	80	90							
τ_{sw}	-	0	0.05	0.10	0.15	0.20	0.25	0.30	0.35	0.40							
$\tau_{lw} \cdot \varepsilon_{lw}$	-	0.50	0.55	0.60	0.65	0.70	0.75	0.80	0.85	0.90	0.95	1.00					
H_{dtc}	W/m^2	0	0.5	1.0	1.5	2.0	3.0	3.5	4.0	4.5	5.0	7.5	10.0	12.5	15.0	17.5	20.0
$\dot{m}_{dtc,sp}$	kg/m^2s	0.0002	0.0004	0.0006	0.0008	0.001	0.002	0.003	0.004	0.005	0.006	0.007					
ΔT_{dtc}	°C	0	0.5	1.0	1.5	2.0	2.5	3.0	3.5	4.0							
U_{tank}	W/m^2K	0.10	0.20	0.30	0.40	0.50	0.60	0.70	0.80	0.90	1.00						
λ_w	W/mK	0.20	0.30	0.40	0.50	0.60	0.70	0.80	0.90	1.00							
$\lambda_{w,mix}$	W/mK	500	600	700	800	900	1000	1100	1200	1300	1400						
θ_{set}	°C	23.0	23.5	24.0	24.5	25.0	25.5	26.0	26.5	27.0							
Loc.	-	CAI	TLV	LCA	AHN	RME	AMS										

Table C-1. The values investigated for each parameter during the sensitivity analysis.